Journal of Infrared, Millimeter, and Terahertz Waves (2026) 47:27
https://doi.org/10.1007/s10762-026-01131-6

REVIEW

Terahertz and mm-Wave Research in Latin America

Enrique Castro-Camus[1] · Daniel Ferrusca[2] · John Carpenter[3] · David Hughes[2] · Naser Qureshi[4] · Raul O. Freitas[5] · Elodie Strupiechonski[6] · Jimy Oblitas[7] · Mariana Alfaro-Gomez[8] · Alma Montserrat Gomez-Sepulveda[9] · Felix G. G. Hernandez[10] · Federico Sanjuan[11] · Monica Ortiz-Martinez[1,12]

Received: 11 December 2025 / Accepted: 23 March 2026

Abstract
In this review article, a broad overview of multiple terahertz- and mm-wave-related activities in Latin America is presented. Latin America houses two of the largest radio-telescopes in the world, a synchrotron terahertz beam line, and multiple activities related to sources, detectors, and instrumentation are underway throughout the region. Furthermore, we describe applications of terahertz spectroscopy and imaging in materials inspection, biomedical, industrial, agronomical, and cultural heritage fields, among others. While we try to include a diverse collection of topics and research groups, this review is not exhaustive, and there are additional activities that we could not include.

Keywords Terahertz · Thz · mm-Waves · Latin America

1 Introduction

Soon after the invention of ultrafast lasers in the 1980s [1], the technique of terahertz (THz) time-domain spectroscopy (TDS) was introduced [2], opening the possibility of exploring the electromagnetic spectral band with frequencies between 0.1 and 10 THz, or wavelengths between 30 μm and 3 mm. In parallel, electronic detectors and sources began increasing their operational frequencies, and quasi-optical devices such as quantum cascade lasers [3] started lowering their operation frequency, providing a variety of technologies to access this region of the spectrum [4]. Depending on the specific application, this region is known as the far infrared, millimeter and submillimeter waves, or the terahertz band. The 1990s saw the early development of both electronic

Extended author information available on the last page of the article

Published online: 14 April 2026

and optical technologies that began filling the void of devices for this band. Since then, electromagnetic waves in this region have found numerous applications ranging from the observation of astronomical objects to the study of fundamental interactions in solids and biological and biochemical systems.

Latin America, the geographical region that spans from the northern border of Mexico to the southernmost point of Chile, including many of the Caribbean islands, is composed of 33 independent countries. It is a region of middle economic income and includes three of the 20 largest economies in the world [5]. These countries are rich in culture and possess extraordinary natural resources. In terms of education, the region has evolved dramatically over the last three decades. While investment in science and technology has marginally improved, the region is still behind in economic importance, with Brazil being the only country in the region investing above 1% of its GDP in research and development [6].

Terahertz and millimeter-wave research in the region is perhaps not fully appreciated. Three major research facilities can be easily identified in Latin America, some of which are funded and supported by broad international collaborations that also involve institutions outside this geographical region. First, the Atacama Large Millimeter/submillimeter Array (ALMA), along with several other important radio telescopes installed in the northern region of Chile, makes this area one of the largest research hubs in the field worldwide. Second, the Large Millimeter Telescope (LMT), situated in central Mexico, stands as a cornerstone of the national scientific infrastructure and remains the world's largest single-dish facility specifically optimized for observations at millimeter wavelengths. Alongside ALMA, these observatories constitute two of the most significant research infrastructures in the millimeter and submillimeter bands globally. Their strategic importance is underscored by their roles as primary anchors in the Event Horizon Telescope (EHT) collaboration. By leveraging the LMT's unique 50-m collecting area and ALMA's unprecedented interferometric sensitivity, this global network produced the first-ever images of supermassive black hole shadows in the M87 galaxy, and at the Galactic Center, Sagittarius A* [7, 8]. This landmark scientific achievement was internationally recognized with the 2020 Breakthrough Prize in Fundamental Physics [9–11], awarded to the EHT collaboration in acknowledgment of its transformative impact on astrophysics. Third, the SIRIUS synchrotron light source in Campinas, São Paulo, Brazil, includes a dedicated terahertz beamline. Additionally, the Laboratorio Nacional de Ciencia y Tecnología de Terahertz in Mexico, composed of three campuses, offers excellent device-fabrication laboratories as well as state-of-the-art terahertz spectroscopy and imaging capabilities. These services, along with terahertz training and event organization, are intended to support the broader terahertz community in Mexico and the region.

In the following sections, we present topical reviews of some of the most significant contributions from the region, divided by the research topics with the largest number of publications. Of course, this review is not exhaustive, and we encourage authors from different countries in the region to contact us for future topical reviews or regional events on the subject.

2 Advancements in Millimeter Wavelength and Terahertz Astronomy: Single-Dish and Interferometric Telescopes

by *Daniel Ferrusca*[1], *John Carpenter*[2] *and David H. Hughes*[3]

[1]dferrus@inaoep.mx
[2]john.carpenter@alma.cl
[3]dhughes@inaoep.mx

For over five decades, millimeter and submillimeter (0.1–10 THz) observations have opened a unique window onto the universe. The isotropic Cosmic Microwave Background (CMB), with a temperature of 2.73 Kelvin, dominates the energy density of the cosmos as relic millimeter-wavelength blackbody radiation from the Big Bang, encoding the initial conditions of structure formation. Meanwhile, roughly half of the energy produced by nucleosynthesis in stars throughout cosmic history is absorbed by dust in interstellar clouds and re-emitted as thermal radiation at terahertz frequencies. These clouds, which contain significant amounts of cold dust mixed with molecular and atomic gas, provide a direct probe of obscured star formation and the physical conditions in galaxies at all epochs across cosmic time. Observations at (sub-)millimeter wavelengths thus enable studies of the formation and evolution of structure ranging from the primordial universe to the birth of stars and planets within our own Galaxy.

Detecting these faint cosmic signals from the ground is challenging due to atmospheric absorption and the difficulty of measuring high-frequency radio photons. Addressing these challenges has driven continuous innovation in detector technologies, improving both sensitivity and mapping capabilities of heterodyne and continuum instruments. Equally important has been the construction of large single-dish telescopes and interferometric arrays, making it possible to map the CMB and the complex distributions of dust and gas in the interstellar medium of galaxies with unprecedented detail.

Latin America has played a central role in these developments. High-altitude sites ($\sim$ 5000 m) on Volcán Sierra Negra in Mexico and the Chajnantor Plateau in Chile host world-class facilities, including the Large Millimeter Telescope (LMT), the Atacama Large Millimeter/submillimeter Array (ALMA), and a suite of telescopes and experiments targeting the CMB and its anisotropies. These sites provide the necessary dry, stable conditions essential for observing faint millimeter and submillimeter signals across the sky.

Regional academic institutions have also contributed directly to telescope and instrument design, providing technical expertise that has helped establish some of the most sensitive and capable astronomical research facilities in the field. This section reviews these developments at terahertz frequencies, highlighting the detector technologies that underpin modern instruments, the major telescope observatories that operate in the region, and other future astronomy projects that will further strengthen the scientific and technological impact of Latin America. Table 1 shows a summary of the major THz/mm-wavelength instrumentation projects with Latin American involvement described in this section. While every effort has been made to cover key developments and groundbreaking technologies, this review is not exhaustive, and the

Table 1 Summary of major THz/mm-wave astronomical projects and instruments with involvement of the Latin American scientific community

Project	Location	Technology	Key scientific achievement/objective
AzTEC [12]	LMT (Mexico)	Bolometers	Surveys of obscured star formation at 1.1 mm; achieved background-limited sensitivity.
RSR [13]	LMT (Mexico)	Heterodyne	Blind searches for molecular/atomic lines; 36 GHz bandwidth at 3 mm
APEX-SZ [14]	APEX (Chile)	TES	High-sensitivity Sunyaev-Zel'dovich effect measurements in galaxy clusters
MUSCAT [15–17]	LMT (Mexico)	LEKIDs	First large KID camera at LMT; high-speed 1.1 mm mapping
TolTEC [18]	LMT (Mexico)	LEKIDs	Simultaneous 3-band (1.1, 1.4, 2.0 mm) imaging with polarization sensitivity
ALMA Band 1 [19]	ALMA (Chile)	Heterodyne	Chilean-produced optics; operation in 35–50 GHz range
ALMA Band 2 [20]	ALMA (Chile)	Heterodyne	Deployment phase; near quantum-limited performance (67–116 GHz)
ALMA Band 3 [21]	ALMA (Chile)	Heterodyne	Commissioned; imaging of molecular gas and star formation (84–116 GHz)
LLAMA [22, 23]	Argentina	Heterodyne	Regional ALMA-standard receivers for VLBI and single-dish observations
ACT/Simons [24, 25]	Chile	TES/KIDs	Groundbreaking CMB mapping, gravitational lensing, and inflation signatures
ngVLA [26]	USA, Mex, Can	Receivers	Planned 244-antenna array for black holes and protoplanetary disks studies

omission of any specific instrument or telescope is not intentional. The field continues to advance at a rapid pace, with new projects and technologies constantly emerging to push the boundaries of our understanding of the cosmos.

2.1 Detector Technologies in the THz Band

The detection of faint cosmic signals in the THz and millimeter bands is fundamentally constrained by the low energy of submillimeter photons and the overwhelming thermal background from the atmosphere and telescope optics. Achieving the sensitivity required to resolve high-redshift star formation and CMB anisotropies requires instrumentation that operates in a background-limited regime, where the detector's internal noise is lower than the statistical fluctuations of the incident photon flux. This requirement has driven the transition from traditional semiconductor-based bolometers [27] to advanced superconducting architectures, such as transition-edge sensors (TES) [28, 29] and kinetic inductance detectors (KIDs) [30, 31], which offer superior scalability, sensitivity, and stability.

These technologies have dramatically improved sensitivity, bandwidth, and dynamic range, enabling precise measurements of faint signals from a wide range of

astrophysical phenomena, including star and planet formation in our Galaxy, the structure and evolution of the interstellar medium, dust-obscured star formation and active galactic nuclei in nearby and distant galaxies, and the cosmic microwave background. A significant and growing share of the development, integration, and deployment of these sophisticated instruments for large-aperture single-dish telescopes and interferometric platforms comes from the Latin American scientific community. In this section, we highlight the pivotal involvement of Mexico and Chile as key participants in advancing next-generation astronomical instrumentation and detector technology.

Advancements in Millimeter-Wavelength Detector Technology in Mexico The Millimeter Wavelength Astronomical Instrumentation Laboratory (Laboratorio de Instrumentación Astronómica de Ondas Milimétricas -*LIAOM* in Spanish) at the National Institute of Astrophysics, Optics and Electronics (INAOE) in Mexico has undergone a significant evolution, establishing a robust foundation for cutting-edge astronomical research. This journey began with the foundational expertise gained from the deployment of early-generation instruments, such as the AzTEC camera, which utilized semiconductor bolometers and operated at the LMT from 2011 to 2018. This period was critical for the development of local expertise in millimeter-wave detectors and cryogenic instrumentation. Building upon this experience and the broader advancements in technologies like TES, the laboratory has consolidated its capabilities by moving toward next-generation devices. The current state of this advanced instrumentation is exemplified by the Mexico-UK Submillimeter Camera for Astronomy (MUSCAT), a collaborative effort featuring a large array of KIDs. This section briefly describes the laboratory's role in these detector technologies and other strategic collaborative efforts.

Semiconductor Bolometers Early large-format millimeter-wave cameras, such as the AzTEC [12] camera developed by the University of Massachusetts, utilized a 144-pixel array of semiconductor bolometers as a primary solution for high-sensitivity continuum imaging at 1.1 mm ($\sim$ 273 GHz). The central challenge at these frequencies is that the energy of an individual photon is extremely small, requiring detectors capable of converting this energy into a measurable temperature change. To solve this, bolometers were fabricated on low-stress silicon nitride membranes, an architecture specifically chosen to minimize heat capacity and provide strong thermal isolation from the substrate.

Each bolometer included a thermally isolated absorber with a dedicated neutron transmutation doped (NTD) germanium thermistor, where the thermal link to the substrate was defined by a thin-film gold conductor patterned onto one of the micromesh support legs. This configuration enabled precise control of the thermal conductance (G), a critical factor governing time constant and sensitivity. The bolometers operated at a base temperature of 300 mK, achieved via a three-stage, closed-cycle helium-3 adsorption refrigerator integrated into a 4 K cryogenic environment maintained by a liquid helium-cooled cryostat. By defining the thermal link via thin-film gold conductors on micromesh support legs, the system achieved a noise equivalent power (NEP) of $5–7\times10^{-17}$ W/Hz$^{1/2}$ [12], effectively reaching the background-limited performance threshold required for deep-field surveys

AzTEC was first deployed in 2005–2006 at the James Clerk Maxwell Telescope (JCMT) in Hawaii, later in 2007–2008 at the Atacama Submillimeter Telescope Experiment (ASTE) in Chile, and finally in 2011–2018 at the LMT in Mexico. This early deployment of AzTEC on various telescopes, culminating in its installation with the LMT, established a foundational framework for the development and advancement of local expertise in millimeter-wave detectors and cryogenic instrumentation at LIAOM at INAOE in Mexico.

Transition-Edge Sensors To overcome the limitations of semiconductor bolometers in terms of linearity and stability, TES technology was implemented in instruments such as SCUBA 2 [32], MBAC [33], and SPT-3G [34], demonstrating the value of this technology. The TES architecture, featuring an aluminum-titanium (Al-Ti) bilayer, utilizes electro-thermal feedback to maintain the detector within its sharp superconducting transition, providing a self-regulating linearity that is optimal for stable THz observations. Furthermore, the integration of a spiderweb-shaped gold absorber on a 1 μm-thick membrane acts as a specialized solution for THz coupling: it maximizes the cross-section for millimeter-wave absorption while minimizing phonon noise and the cross-section for cosmic ray interference.

A very successful instrument which used this technology was the APEX-SZ [14] led by the University of California - Berkeley, that was installed on the 12-m Atacama Pathfinder Experiment (APEX) telescope located on the Llano de Chajnantor plateau ($\sim$ 5000 m) in the Atacama Desert of northern Chile. This instrument was specifically designed to perform high-sensitivity measurements of the Sunyaev-Zel'dovich (SZ) effect in galaxy clusters. The measurement of SZ effect requires high-precision detection of spectral distortions in the CMB, which demands sensors with high dynamic range and minimal susceptibility to non-optical noise.

The TES detectors operated at an optimized base temperature of 280 mK and were tuned for observations centered at 150 GHz, corresponding to the peak spectral distortion of the cosmic microwave background due to inverse Compton scattering by hot intracluster gas. The bolometers were fabricated using lithographic processes conducive to large-scale production, and the readout was implemented via a frequency-domain multiplexed (FDM) superconducting quantum interference device (SQUID) system [35, 36]. The architecture was designed to be fully compatible with cryogen-free cooling systems, utilizing low-vibration pulse-tube coolers to achieve the required sub-Kelvin temperatures. Compared to earlier semiconductor-based bolometer technologies, the TES array exhibited superior sensitivity, linearity, and stability under photon-limited observing conditions.

The detector architecture (Fig. 1) comprised three primary components: a broadband electromagnetic absorber, a TES, and superconducting bias leads, all integrated onto a 1-μm-thick low-stress silicon nitride spiderweb membrane to reduce heat capacity, and it maximizes the cross-section for millimeter-wave absorption while minimizing phonon noise and the cross-section for cosmic ray interference. The absorber was based on a 3-mm-diameter gold spiderweb structure, optimized to provide efficient coupling to incoming millimeter-wavelength radiation while minimizing heat conduction paths. The TES was fabricated at the center of the absorber and consisted of an aluminum-titanium (Al-Ti) bilayer, with individual layer thicknesses

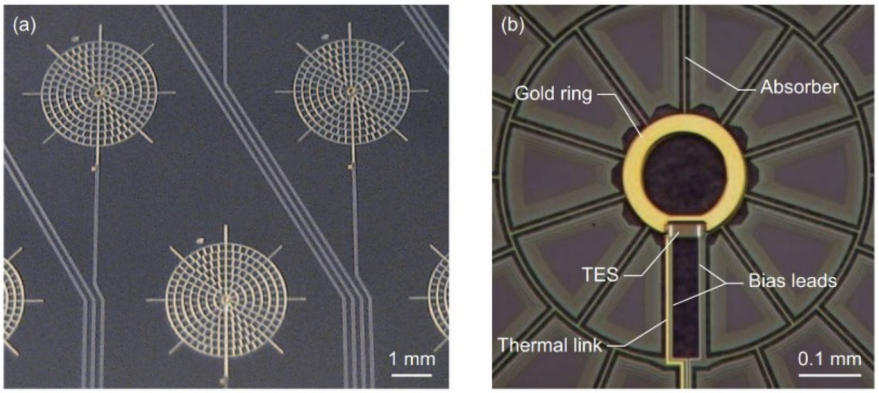

Fig. 1 APEX-SZ transition-edge sensor. **a** Three spiderweb bolometers on a 55-element sub-array. **b** A close-up of the center of the spiderweb shows the elements of the bolometer. The dark areas along the absorber legs and inside the gold ring are regions in which the silicon has been etched away from the spiderweb. Reproduced under the CC-BY-NC-ND 4.0 license from [14] Copyright ©The Authors

finely tuned to yield a superconducting transition temperature (Tc) of 465 mK. This architecture utilizes electro-thermal feedback to maintain the detector within its sharp superconducting transition, providing a self-regulating linearity that is optimal for stable THz observations. The detectors exhibited a NEP of 8.7×10^{-17} W/Hz$^{1/2}$ [14], indicating a photon noise-limited sensitivity suitable for high-resolution cosmological and astrophysical measurements.

Much like AzTEC, the APEX-SZ project significantly advanced regional scientific capacity. It ensured the active participation of scientists from LIAOM and the Latin American community, simultaneously enabling the transfer of knowledge and expertise in advanced THz technologies to local institutions.

Kinetic Inductance Detectors The current frontier in millimeter and submillimeter astronomy is represented by instruments using KIDs which use large-format focal plane arrays to increase mapping speeds. This technology is currently employed in several cutting-edge telescopes across Latin America.

While previous technologies were limited by the complexity of cryogenic wiring and heat dissipation, KIDs provide a transformative solution to the multiplexing challenge by leveraging the unique electromagnetic properties of superconducting materials to form high-Q inductor-capacitor (LC) resonant circuits. KIDs allow hundreds—and eventually thousands—of pixels to be read out through a single microwave transmission line. Each resonator is engineered to operate at a distinct resonance frequency, primarily defined by its fixed capacitance and the kinetic inductance contribution of its superconducting inductor.

Upon absorption of incident photons—typically in the millimeter or submillimeter-wavelength range—Cooper pairs within the superconducting film are broken, leading to an increase in quasiparticle density. This perturbation results in a measurable shift in the kinetic inductance, thereby altering the resonant frequency of the LC circuit. The

frequency shift is monitored using a cryogenic microwave readout system, enabling real-time detection of photon events with exceptional sensitivity.

Representative examples of recent advancements in millimeter-wave instrumentation using KIDs include NIKA-2 [37], BLAST-TNG [38], and TOLTEC [18]. The fabrication of these compact, low-cost, and less complex detectors, compared to technologies like TES, has made KIDs a promising option for the current and next generation of large-scale astronomical cameras. A notable example of the participation of the Latin American scientific community in KIDs technology is the MUSCAT instrument [15]. Designed for observations within the 1.1-mm atmospheric transmission window ($\sim$ 270 GHz), this instrument resulted from a collaboration between LIAOM and Cardiff University. The initiative engaged Mexican researchers, fostered a Ph.D. dissertation [16], and ultimately enabled the laboratory's upgrade to support KIDs technology. The MUSCAT instrument features a 1458-pixel horn-coupled back-illuminated lumped-element kinetic inductance detector (LEKID) array in which millimeter photons are absorbed through a high-resistivity silicon substrate to maximize optical coupling efficiency. The superconducting detector layer—fabricated via thin-film deposition techniques—integrates an interdigitated capacitor (IDC) and a lithographically patterned meandered inductor, which acts simultaneously as the photon absorber and inductive element. The inductive meander is optically coupled to a feedhorn that supports single-mode propagation, providing well-defined beam patterns and polarization selectivity. A superconducting coplanar waveguide (CPW) feedline facilitates the readout of multiple detectors via frequency-division multiplexing, which ultimately dramatically enhances their scalability for large-format focal plane arrays. This architecture significantly reduces the thermal load on the cryogenic system, enabling the deployment of arrays with up to thousands of pixels without compromising the ultra-low-noise performance required for star formation and cosmological studies (Fig. 2).

The MUSCAT array operates within a cryogenic environment, cooled to an ultra-low base temperature of 100 mK using a dilution refrigerator to minimize thermal noise and preserve superconducting behavior [17]. The MUSCAT sensitivity is fundamentally limited by photon shot-noise and quasiparticle generation-recombination (G-R) noise, with a demonstrated NEP reaching 4×10^{-17} W/Hz$^{1/2}$ [17] under background-

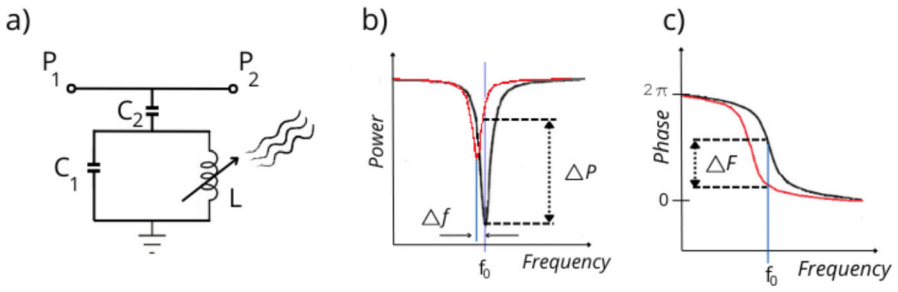

Fig. 2 Microwave kinetic inductance detector. **a** Incident photons are absorbed in a superconducting film, breaking Cooper pairs that generate quasi-particles and causing an inductance increase. This change is measured in a LC resonant circuit. **b** This effect will change the amplitude, resonance frequency, and **c** the phase, which are proportional to the photon energy

limited performance conditions. These characteristics highlight the suitability for MUSCAT to conduct next-generation millimeter-wave cosmology and star formation studies.

Radio Astronomy Instrumentation in Chile Radio astronomy in Chile has a long tradition of instrumentation and scientific development. Beginning in 1959, the MaipúRadio Observatory served as the hub for local radio astronomical activities. Early collaborations with the University of Florida produced decametric band instruments, including the pioneering Maipú-Kentucky trans-hemispheric Very Long Baseline Interferometry (VLBI) experiment [39]. A major achievement of the 1970s was the construction of a large metric band radio telescope, used to conduct a 45 MHz continuum all-sky survey in partnership with Hyogo University [40]. These efforts not only yielded important scientific results but also trained a generation of electrical engineers.

The focus shifted to higher frequencies in the 1980s with the operation of the 1.2-m Southern Millimeter Wave Telescope (SMWT) at Cerro Tololo in collaboration with Columbia University. The SMWT enabled the first CO (1-0) maps of the southern Galaxy and the Magellanic Clouds [41–44]. Since 2004, the Millimeter Wave Laboratory (MWL) at the University of Chile in Santiago has been the center of these activities. The MWL has carried out significant upgrades to the SMWT's instrumentation, including enhancements to the local oscillator, atmospheric opacity measurement systems, and low-noise amplifiers [45–47]. Relocated to Cerro Calán in 2011 [48, 49], the SMWT continues to serve as a training platform for students in astronomy and electrical engineering

Building upon this foundation, the MWL embarked on developing cutting-edge instrumentation for ALMA. Motivated by the opportunity to extend the receiver capabilities of the newly operating Atacama Large Millimeter/submillimeter Array (ALMA), the MWL successfully developed a functional prototype of a state-of-the-art millimeter-wave receiver between 2008 and 2014 [50, 51]. This achievement led to the MWL's inclusion in the international ALMA Band 1 consortium, where it was entrusted with designing and fabricating the entire optics work package. The successful integration of these Chilean-produced components—specifically the horn antenna and precision lenses—into ALMA by the end of 2020 marked a significant technological milestone, demonstrating Chile's capacity to contribute highly sophisticated components to world-class observatories.

Concurrently, the MWL leveraged this experience for the Large Latin American Millimeter Array (LLAMA) [22, 23], a joint Argentine-Chilean project. For LLAMA, the laboratory developed a wide-bandwidth receiver for the 67–116 GHz band, designed to the ALMA cartridge standard and integrating custom Chilean optical components with commercial amplification stages. This project, which underwent extensive electromagnetic modeling and cryogenic testing, further validated the MWL's ability to produce front-line technology [52]. In a continuation of this work, many of the components developed for LLAMA are now being integrated into a new receiver for the SMWT.

In parallel, the MWL has pursued a diverse range of developments, including digital backends [53–56], frequency multipliers [57], dichroics [58], antenna design [59, 60],

holography [61], and downconverters [62, 63]. More recently, a new research line has emerged at lower frequencies to study Fast Radio Bursts and other variable phenomena [64–67].

2.2 Large Millimeter Telescope (LMT)

Over the last 50 years, the field of submillimeter and millimeter astronomy has seen the construction of increasingly larger single-dish and interferometric telescopes, as well as the significant contemporary development of more sensitive background-limited multi-pixel instruments with both spectroscopic and multichromatic imaging capabilities. In addition to the improvements in angular resolution and the introduction of digital spectrometers offering a wider range of available spectral resolutions, the technological gains at THz frequencies have also provided many orders of magnitude increase in telescope mapping speeds, transforming the opportunities for astronomical observations of our local and distant universe.

In Latin America, the LMT or Gran Telescopio Milimétrico (GTM) represents an important example of combining these advantages to construct and operate a large single-dish telescope on a high-altitude site together with the development of larger-format broadband continuum imaging arrays and multi-beam heterodyne spectral-line receivers that operate at THz frequencies [13, 68].

The LMT is a long-term binational collaboration between Mexico and the USA, led by the INAOE and the University of Massachusetts Amherst, respectively. The operation, maintenance, and development of the LMT have been dominated by federal funding from the Mexican Secretaria de Ciencia, Humanidades, Tecnología e Innovacción (SECIHTI), and the US National Science Foundation (NSF). In Mexico, the LMT represents one of the most ambitious, major scientific projects.

The LMT is the world's largest single-dish radio-telescope designed to operate at millimeter wavelengths between 4 and 1 mm (70 to 300 GHz). Located on the summit of volcán Sierra Negra in the Mexican state of Puebla, at an altitude of 4600 m, the 50-m diameter primary reflector of the LMT offers the opportunity to make extremely sensitive observations with competitive intermediate angular resolutions (5–18 arcseconds FWHM at 1–4 mm) that are better than those of other single-dish ground-based facilities operating at similar wavelengths, and equal to or exceeding the angular resolution of space-borne mid-IR and FIR telescopes (e.g., Spitzer, Herschel) that operated at 0.6 to 1.2 THz. Given the high atmospheric transparency at the LMT, with 225 GHz opacities $\tau < 0.06$ during the driest winter months, submillimeter observations (350 GHz) with the LMT are also expected in the future.

The technological development of superconducting detectors based on lumped-element kinetic induction devices (LEKIDS), and their application in current large-format millimeter/wavelength continuum arrays, has been described earlier, including the 1500-pixel MUSCAT camera that operates at 1.1 mm. However, the LMT is currently commissioning the TolTEC camera [18] with even greater capabilities that include a total of 7000 polarization-sensitive LEKIDS detectors that can observe simultaneously in three bands (1.1, 1.4, and 2.0 mm).

Both instruments are able to conduct targeted deep (confusion-limited) imaging observations of known individual Galactic and extragalactic sources, or to map small fields of interest over a few tens of square arcminutes up to areas of 1 sq. degree. Such observations enable studies of asteroids, comets, planets, known star-formation regions in the spiral arms of the Milky Way, local and distant galaxies, clusters of galaxies, active galactic nuclei, and cosmological fields.

Similarly, shallower but much wider-area multi-wavelength continuum surveys with the LMT, covering tens to hundreds of square degrees, can map star-formation (across a wide range of protostellar masses) over a significant fraction of the observable Galactic plane and also create large unbiased cosmological surveys of the high-redshift universe using dusty star-forming galaxies detected at millimeter wavelengths as tracers of the early formation of large-scale structure described by filaments, overdensities, and voids within the cosmic web.

Historically, images and mapping surveys have been the first steps towards new discoveries in astronomy. However, much of the critical astrophysical information related to the dynamical properties, physical conditions, and chemical composition of (proto)planetary and star-formation systems, interstellar clouds, and galaxies is generated by high spectral-resolution (≤ 1 km/s) observations of multiple atomic and molecular species, and their isotopes, of these objects and their surroundings.

In order to provide spectroscopic observations in the available atmospheric windows, the LMT has developed both single-pixel and multiple-beam heterodyne receivers [13]. The majority of these instruments, SEQUOIA, B4R, 1 mm Rx, including OMAYA to be delivered in 2026, provide the necessary range of high spectral resolutions (≤ 1 km/s). In contrast, the Redshift Search Receiver (RSR) offers the unique capability to conduct low spectral-resolution (> 100 km/s) observations instantaneously over an ultra-wide bandwidth (~ 36 GHz) in the 3 mm window. Accordingly, the RSR can make efficient blind searches for molecular and atomic lines, principally transitions from carbon monoxide, as well as from neutral and ionized carbon, oxygen, and nitrogen, that are emitted by dusty, optically-obscured, star-forming galaxies in the early universe. These lines are redshifted to lower observational frequencies as the universe expands before detection by the RSR.

A significant future improvement in undertaking blind spectroscopic observations of high-redshift galaxies, with no prior redshift information, will be offered with the conclusion of the development of FINER, a dual-polarization sideband-separating superconductor-insulator-superconductor (SIS) heterodyne receiver system which comprises two frequency bands covering 120–360 GHz and delivers an instantaneous on-sky frequency coverage of > 30 GHz with 50 km/s resolution [69].

Finally, the recent opportunity for on-chip spectrometers, again using KIDS technologies, to make wide-band, moderate-resolution multi-object spectroscopic observations will play an increasingly important role in the detection of faint, optically obscured high-redshift galaxies and line-intensity mapping of large-scale structure in the universe. The LMT is currently commissioning prototype detectors of SuperSpec [70] which provides moderate resolution ($R\sim 270-290$) in the 1 mm atmospheric window (200–300 GHz) with a lithographically patterned filterbank on a 3.5 cm $\times$ 5.5 cm chip. The filterbank is implemented in niobium, fed by a lensed antenna, and using extremely low-volume ($2.6\mu m^3$) titanium nitride LEKIDs as the sensors.

Fig. 3 Large millimeter telescope on volcán Sierra Negra at 4600 m with Pico de Orizaba in the background. Credit: Francisco Guasco

The northern equatorial latitude (+19° N) of the LMT provides significant coverage of both the northern and southern hemispheres, important extragalactic targets and cosmological fields, a significant fraction of the galactic plane of the Milky Way, and the Galactic center. The LMT also provides 70% overlap with the sky as seen by ALMA, ensuring exciting possibilities for the Latin America research communities to conduct collaborative and complementary projects with both of these world/class observatories (Fig. 3).

2.3 Atacama Large Millimeter/Submillimeter Array (ALMA)

While single-dish facilities such as the LMT are uniquely powerful for wide-field mapping and spectroscopic surveys, they lack the angular resolution required to resolve the detailed structure of individual sources. Interferometric arrays overcome this limitation by combining the signals from many antennas distributed over long baselines, achieving orders of magnitude higher resolution. This capability, together with advances in detector technology, enables sensitive, high-fidelity imaging on the smallest physical scales.

The premier interferometric facility in Latin America and the world is ALMA (Fig. 4). ALMA is operated as a partnership among the European Organisation for Astronomical Research in the Southern Hemisphere (ESO), the US NSF, and the National Institutes of Natural Sciences (NINS) of Japan, in cooperation with the Republic of Chile. Funding is provided by ESO on behalf of its Member States, by NSF in cooperation with the National Research Council of Canada (NRC) and the National Science and Technology Council (NSTC) in Taiwan, and by NINS in cooperation with the Academia Sinica (AS) in Taiwan and the Korea Astronomy and Space Science Institute (KASI).

Fig. 4 Aerial view of the ALMA array on the Chajnantor Plateau, Chile. Credit: Sergio Otárola – ALMA (ESO/NAOJ/NRAO)

ALMA's location on the 5000-m elevation Chajnantor Plateau in northern Chile is essential to its success: the extremely dry atmosphere and high altitude minimize absorption by atmospheric water vapor, allowing efficient observations at wavelengths otherwise inaccessible from the ground. With state-of-the-art receivers, a large collecting area, and an exceptional observing site, ALMA achieves sensitivities that far surpass those of earlier interferometers.

The array comprises 66 high-precision antennas: 50 12 m dishes form the main array, 12 7 m dishes constitute the Atacama Compact Array (ACA), and four 12 m antennas are dedicated to total-power measurements. Depending on configuration, baselines extend up to 16 km, yielding angular resolutions as fine as 5 milliarcseconds at the highest frequencies. ALMA covers 35–950 GHz with ten dual-polarization receiver bands that achieve near quantum-limited performance. Bands 3–10 (84–950 GHz) are fully commissioned, Band 1 (35–50 GHz) recently entered operations, and Band 2 (67–116 GHz) is in deployment.

ALMA is an extremely flexible instrument with a variety of observing modes to support a wide range of science. It can obtain continuum observations with up to 8 GHz of bandwidth per polarization, as well as spectral resolution as fine as 31 kHz (over narrower bandwidths). Additional modes include full polarization, solar observing, and a phasing mode that allows the array to operate as a single, ultra-sensitive aperture for VLBI and pulsar observations.

ALMA has transformed millimeter and submillimeter astronomy by delivering images of unprecedented sensitivity and resolution across the full range of astrophysical environments. Among the most distant galaxies, ALMA has detected galaxies at $z \sim 14.2$ [71, 72], just 300 million years after the Big Bang, providing a direct view into the earliest stages of cosmic structure. Studies of nearby galaxies have mapped the physical and chemical conditions of molecular gas across diverse environments, revealing how star formation proceeds under different galactic conditions [73].

Within the Milky Way, ALMA has exposed the intricate filamentary structure of molecular clouds [74] and traced the formation of stars within their densest regions [75]. In nearby star-forming regions, it has revealed concentric rings and fine substructures in protoplanetary disks [76], tracing the earliest stages of planet formation, while observations of evolved stars have uncovered complex mass-loss patterns that shape their eventual fates [77]. It has also advanced astrochemistry by detecting complex organic molecules in star-forming regions and disks that may represent the precursors of life [78, 79].

ALMA also enables studies of rapidly evolving phenomena. The array has observed transients such as gamma-ray bursts [80], supernovae [81], and tidal disruption events [82] and has traced the variability of relativistic jets on timescales of days to weeks.

On Solar System scales, ALMA has mapped the atmospheres, surfaces, and thermal emission of planets, moons, asteroids, and comets, providing unique insights into their chemical and physical properties [83–86]. Finally, ALMA has enabled unprecedented observations of the Sun at millimeter wavelengths, revealing chromospheric heating and dynamic processes with high spatial and temporal resolution [87].

Beyond its standalone capabilities, ALMA is indispensable to global VLBI efforts. By coherently phasing its 12 m array into a single element, ALMA provides a critical anchor for worldwide VLBI networks operating at millimeter and submillimeter wavelengths. Along with the LMT and APEX, ALMA's inclusion in the Event Horizon Telescope (EHT) was essential to producing the first images of black hole shadows in M87 [7] and Sgr A* [8]. ALMA and LMT also play leading roles in the Global mm-VLBI Array (GMVA), enabling detailed studies of relativistic jets, masers, and the Galactic Center.

Together, these discoveries illustrate the extraordinary breadth of ALMA's scientific reach, from the first galaxies to the Sun, and highlight the central role of high-frequency interferometry in modern astronomy. ALMA is available to the worldwide astronomical community through regular open proposal calls. All data become publicly available after the proprietary period via the ALMA Science Archive, fostering broad international participation and extensive use of archival observations for new investigations.

ALMA continues to evolve through the *Wideband Sensitivity Upgrade* (WSU), a comprehensive program that will initially double and eventually quadruple the instantaneous bandwidth while reducing receiver noise. A new correlator and spectrometer will process this expanded bandwidth at high spectral resolution ($\sim$0.1 km/s), enabling much faster spectral surveys and improved continuum sensitivity. These developments will accelerate discovery in areas ranging from complex chemistry in protoplanetary disks to wide-band cosmological redshift searches.

2.4 Cosmic Microwave Background (CMB) Experiments

The high, dry plateaus of northern Chile have become a premier site for CMB observations. Pioneering work began with the Cosmic Background Imager (CBI; 1999–2008) [88], a 13-element interferometer that produced the first detailed measurements of the small-scale CMB power spectrum and helped establish the Chajnantor plateau as an exceptional site for precision cosmology. Other early efforts included the Mobile Anisotropy Telescope (MAT/TOCO) [89], which mapped anisotropies in the late 1990s, and the Atacama B-mode Search (ABS; 2012–2014) [90], which targeted the polarized CMB signature of inflation. Subsequent experiments have expanded both sensitivity and sky coverage. POLARBEAR [91], deployed on Cerro Toco in 2012, demonstrated arcminute-scale polarization measurements, while the Cosmology Large Angular Scale Surveyor (CLASS) [92], operating since 2016, has targeted large-scale polarization to probe inflation and reionization.

Another major CMB experiment operating in northern Chile is the Atacama Cosmology Telescope (ACT) [24], located on Cerro Toco. ACT surveyed thousands of square degrees of sky at arcminute resolution, producing some of the most detailed maps of CMB temperature and polarization to date and providing precise constraints on cosmological parameters. The experiment also delivered the first high-significance measurements of CMB gravitational lensing by large-scale structure. A key technological advance enabling these results was the adoption of highly sensitive transition-edge sensor (TES) bolometer arrays, which allowed ACT to measure the tiny temperature fluctuations of the CMB with unprecedented precision.

The Atacama Pathfinder Experiment (APEX) [93], a 12-m submillimeter telescope located on the Chajnantor plateau, has also contributed to cosmological studies, particularly through observations of the Sunyaev-Zel'dovich (SZ) effect in galaxy clusters. These measurements probe the interaction of CMB photons with hot intracluster gas and provide valuable information on the distribution of matter in the universe. Although APEX is primarily designed for submillimeter astrophysics, its instrumentation and surveys have supported complementary studies relevant to cosmology. The successful detection of such faint signals relies on advanced detector technologies, including TES bolometers and kinetic inductance detectors (KIDs).

2.5 Future Facilities

The future of millimeter and submillimeter-wavelength astronomy is very promising, with several next-generation instruments and telescopes that will revolutionize our understanding of the cosmos. A few notable examples where the Latin American community is involved are outlined below.

Engineering and performance upgrades to the LMT will provide increased technical and scientific capabilities, together with the anticipated opportunities and cost-effectiveness provided by the technological scalability of KIDs arrays and their readout systems to develop even larger-format cameras and imaging on-chip spectroscopy (e.g., SuperSpec and FINER), as well as very sensitive heterodyne instruments such as OMAYA to be delivered in 2026.

The Simons Observatory (SO) [25] is a major next-generation CMB experiment located in the Atacama Desert, with the goal of making unprecedentedly sensitive and precise measurements of the CMB. The observatory consists of multiple telescopes, including a large-aperture telescope and several smaller ones, which began scientific observations in 2024. The Simons Observatory's instrumentation and technologies are of paramount importance because they are designed to address some of the most fundamental questions in modern cosmology such as probing Cosmic Inflation, mapping Dark Matter and Dark Energy, understanding neutrinos, extragalactic astronomy to study galaxy clusters through the Sunyaev-Zel'dovich effect, the evolution of distant galaxies, and the study of transient events in the millimeter-wave sky.

The LLAMA project is a joint initiative between Argentina and Brazil, located in the Puna de Atacama, in the Province of Salta, Argentina. LLAMA will be a single-dish 12-m telescope capable of performing observations at millimeter and submillimeter wavelengths, and it is also intended to be part of the VLBI network and integrated with

ALMA or APEX, which will allow for a substantial increase in angular resolution, enabling a new level of detail in observing compact, bright sources. The LLAMA project is an important step in astronomy in South America, providing new opportunities for regional and international collaborations.

An international consortium led by Cornell University is constructing the 6-m Fred Young Submillimeter Telescope (FYST) of the Cerro Chajnantor Atacama Telescope (CCAT) Observatory on Cerro Chajnantor at an altitude of 5600 m. Designed for wide-field submillimeter surveys, the telescope will support studies of cosmic origins, cosmology, and the interstellar medium, complementing other major observatories in the region such as ALMA.

The next-generation Very Large Array (ngVLA) [26] will be an array of 244 antennas operating over the frequency ranges 1.2–50.5 GHz and 70–116 GHz, with participation from Mexico through the National Autonomous University of Mexico (UNAM) and INAOE. In parallel, upgrades to the EHT involving the Latin American community are expanding the capabilities of millimeter and submillimeter VLBI. These facilities will provide unprecedented angular resolution and sensitivity for imaging black hole environments, protoplanetary disks, and distant galaxies.

Exciting possibilities also lie with a current development project (AtLAST [94, 95]) to build a new 50 m single-dish millimeter and submillimeter telescope in Chile at a high-site above 5000 m close to ALMA. A primary design goal of AtLAST is to provide a significantly larger telescope field-of-view ($>$ 1 degree diameter) that can exploit continued detector development at terahertz frequencies over the next decade. It is expected that AtLAST will accommodate future mega-pixel multi-band cameras and kilo-pixel imaging high-resolution spectral-line arrays, delivering new insights into the structure and evolution of the Universe.

The progressive development of millimeter-wave instrumentation in Latin America, particularly in Mexico and Chile, has been profoundly influenced by sustained international collaborations and strategic technological initiatives. Over the years, this evolution has encompassed a wide range of innovations, from early bolometric detectors to the implementation of advanced KIDs and the integration of increasingly sophisticated cryogenic systems. This technological growth has mirrored the advancement of observational platforms, with telescopes evolving from initial CMB experiments to the largest millimeter-wavelength telescopes and interferometers on Earth, many of which are now located in the region. These efforts have not only strengthened local scientific and engineering capabilities but have also positioned regional institutions as active contributors to the global landscape of experimental astrophysics. The cumulative impact of these developments underscores the importance of long-term partnerships and knowledge exchange in fostering technological self-reliance and scientific excellence in emerging research communities.

3 Development of Terahertz Sources

by *Naser Qureshi*[1], *Raul O. Freitas*[2], *and Elodie Strupiechonski*[3]

[1] naser.qureshi@icat.unam.mx

[2] raul.freitas@lnls.br
[3] elodie.claire@cidesi.edu.mx

Over the past two decades, significant advances have been achieved in the generation of radiation within the gigahertz (GHz) to terahertz (THz) range, an area often referred to as the "THz gap." This progress reflects both the global trend toward compact, tunable, and efficient THz systems and the growing regional commitment in Latin America to strengthen the fundamental and applied aspects of THz science. Nonlinearities in semiconductors, well understood in the visible and near-infrared regimes, have enabled the development of powerful pulsed sources through nonlinear crystals and photoelectric devices; however, continuous-wave (CW), compact, and tunable emitters in the GHz-THz domain remain a technological challenge. Current CW technologies include electron-beam devices such as gyrotrons, free-electron lasers, and backward wave oscillators, as well as optically pumped far-infrared gas lasers, quantum cascade lasers, solid-state oscillators, frequency multipliers, and photomixers. Among these, solid-state devices such as Schottky diodes, varactors, high-electron-mobility transistors, Gunn diodes, and superlattice electron devices are efficient up to approximately 220 GHz, while InP Gunn diodes can reach near 480 GHz. Quantum cascade lasers offer highly coherent emission in the 2–4 THz range but generally require cryogenic cooling. Meanwhile, photomixers and difference-frequency generators extend spectral coverage, albeit with decreasing power, while mid-infrared frequency combs and semiconductor superlattices continue to promise broader and more efficient access across the GHz-THz spectrum.

Latin American research groups have strategically focused on complementary approaches, combining photonic methods with emerging solid-state and plasmonic technologies, addressing specific THz gap challenges where smaller research teams can achieve competitive results. In this context, Latin American groups—particularly those in Mexico, Brazil, and Argentina—have established multidisciplinary programs combining ultrafast optics, semiconductor physics, and materials engineering to develop efficient THz emitters and detectors. Over roughly the past 15 years, significant progress has been recorded across multiple fronts, from semiconductor superlattices enabling harmonic generation up to 1 THz [96] and nanostructured devices supporting gigahertz-to-terahertz multiplication, to photonic routes involving dual frequency-comb spectrometers [97]. Pioneering studies have explored nonlinear emission in semiconductor microcavities [98], exciton-polariton lasing in the THz regime [99], and coherent phonon generation in distributed Bragg reflector-based resonator structures [100]. More recent advances include graphene plasmonic antennas and graphene-coated cylinders for plasmon-assisted THz lasing [101, 102], as well as the observation of sub-diffractional cavity modes of THz phonon polaritons in oxide nanostructures [103, 104].

Collectively, these developments highlight an increasingly sophisticated regional expertise that spans electronic, photonic, and hybrid polaritonic THz emitters. Several research centers—most notably in Mexico, Brazil, and Argentina—now lead coordinated efforts combining theoretical modeling, materials science, and instrumentation.

In order to place regional developments in a proper global perspective, each source class discussed below is introduced with a brief conceptual description of its operating

principle and key design constraints, followed by a comparison with leading international benchmarks. This structure highlights both the physical mechanisms underlying THz emission and the specific niches in which Latin American efforts align with, complement, or strategically diverge from the current worldwide state of the art.

The following subsections summarize the main lines of progress in THz source development across the region, from photonic and electronic schemes to polaritonic and accelerator-based approaches, illustrating both the scientific depth and growing interconnection of Latin American THz research.

Figure 5 presents original conceptual schematics summarizing the emission mechanisms discussed in this section, illustrating the distinct physical mechanisms underlying photonic, electronic, plasmonic, polaritonic, and accelerator-based emission.

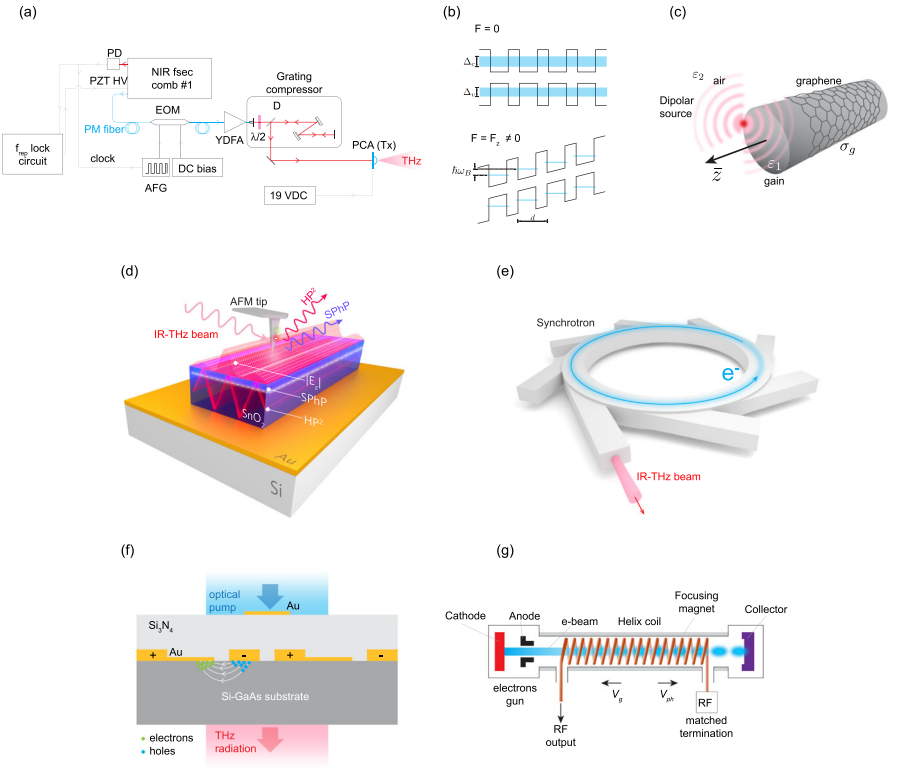

Fig. 5 Schematic overview of the principal terahertz source architectures discussed in Sect. 3. **a** Photonic generation using a femtosecond-driven photoconductive antenna. **b** Biased semiconductor superlattice illustrating miniband formation and Wannier-Stark ladder under applied electric field. **c** Graphene-coated cylindrical structure supporting tunable plasmon modes. **d** Phonon-polariton nanophotonic cavity in SnO_2 ribbons. **e** Large-scale accelerator-based sources: synchrotron storage ring for high-brightness broadband IR-THz generation. **f** Plasmonic-enhanced photoconductive emitter architecture. **g** Vacuum electronic backward-wave oscillator. The schematics are conceptual representations intended to highlight the distinct physical mechanisms underlying terahertz emission across platforms. **d** and **e** were adapted from F. Feres et al., Nature Communications (2021) [103], licensed under CC BY 4.0

Table 2 summarizes the main categories of THz sources currently under development in Latin America, based on representative experimental and theoretical works discussed in this section. The works included were selected according to the following criteria: (i) clear demonstration of a distinct THz emission mechanism, (ii) documented experimental realization or validated theoretical modeling published in peer-reviewed literature, and (iii) relevance to ongoing or emerging research programs within the region. The table highlights the diversity of emission mechanisms—ranging from photonic and electronic schemes to plasmonic, polaritonic, and accelerator-based systems—alongside their operational frequency ranges and distinctive performance characteristics. This compilation illustrates both the technological breadth and the increasing specialization of regional research groups, reflecting the transition from THz applications toward genuine source innovation. The table is intended to be representative rather than exhaustive, and it does not aim to include all existing THz source activities in Latin America.

3.1 Photonic THz generation

Advances in photonic THz generation have introduced innovative fiber- and comb-based approaches that enhance tunability, resolution, and efficiency. Ultrafast optoelectronic switching enabled the first photoconductive THz emitters [114], while coherent electro-optic sampling established the physical detection principle underpinning THz time-domain spectroscopy [115]. Photonic approaches dominate THz source development in Latin America, particularly in Mexico. Research groups at the Universidad Nacional Autónoma de México (UNAM), the Centro de Investigación y de Estudios Avanzados (CINVESTAV), the Centro de Ingeniería y Desarrollo Industrial (CIDESI), the Instituto Nacional de Astrofísica, Óptica y Electrónica (INAOE), and the Centro de Investigaciones en Óptica (CIO) have led advances in photonic THz generation. Their work spans femtosecond laser-driven photoconductive antennas, optical rectification, and difference-frequency generation, producing broadband THz pulses for spectroscopy, metrology, and biomedical imaging. At CIO and UNAM, the groups of Enrique Castro-Camus and Naser Qureshi have demonstrated compact photomixing systems and time-domain THz setups, while at CINVESTAV and CIDESI, Elodie Strupiechonski's team has developed hybrid quantum cascade laser-based sources tailored for integrated THz instrumentation. The CIO group has investigated dual-laser beating and nonlinear crystals for optical-to-THz conversion, with applications in biophotonics.

In Brazil, a notable all-fiber technique enabled tunable THz emission between 2.2 and 3.8 THz with an output power of 0.5 μW [105]. Complementarily, THz dual frequency comb spectroscopy has reached unprecedented resolution by using Mach-Zehnder electro-optic modulators to adaptively tune the effective laser repetition rate (see conceptual schematics of the emission arm in Fig. 5a), improving spectral resolution from 100 to 5 MHz—a 20-fold improvement over conventional Fourier transform based methods without bandwidth reduction [97].

Table 2 Representative THz source developments in Latin America by type, highlighting frequency range, output power, and distinctive features

Source type	Representative group/institution	Frequency range	Output power	Distinctive feature
Photonic (fiber/comb-based)	UNAM, CINVESTAV, CIDESI, INAOE, CIO (Mexico); USP (Brazil)	2.2–3.8 THz	~0.5 μW	Femtosecond-laser-driven photoconductive antennas, optical rectification, dual frequency-comb spectroscopy; high spectral resolution (5 MHz) with adaptive modulation (2015, 2016) [97, 105]
Semiconductor superlattice (harmonic generation)	Collaborations among groups in Colombia, Mexico, and Chile	Up to 1 THz	Not specified	Resonant tunneling and photon-assisted transport in biased SSLs; negative differential conductivity and frequency multiplication effects (2015, 2021, 2017) [96, 106, 107]
Electronic (solid-state and multiplier chains)	USP and UNICAMP (Brazil); CIO, UNAM, INAOE (Mexico)	Sub-THz to ~1 THz	mW-level (est.)	Gunn and HEMT frequency chains; CMOS-compatible on-chip emitters; antenna-based CW difference-frequency THz sources (2013, 2017) [108, 109]
Graphene/CNT plasmonic sources	UBA, CNPEM, USP (Argentina-Brazil collaborations)	4-15 THz	Up to four orders of magnitude enhanced efficiency	Graphene plasmonic antennas and waveguides; tunable chemical potential control; CNT-based Cherenkov-type THz lasing (2010, 2016, 2018, 2022) [99, 101, 102, 110]
Polariton-based (phononic and plasmonic resonators)	CNPEM, UFMG (Brazil)	0.5-20 THz	Efficiency ~3% (predicted)	Phonon polaritons in oxide nanostructures (SnO_2, α-TeO_2); strong coupling regime in semiconductor microcavities; tunable hybrid VED emitters (2021, 2024, 2025)[103, 104, 111]
Accelerator-based (synchrotron)	CNPEM (Brazil, Sirius facility)	3–20 THz (TATU beamline, planned)	High brilliance, CW	Fourth-generation synchrotron providing nanospectroscopy; IMBUIA IR beamline operational (2024) [112], TATU THz line under construction
BWO-based	INAOE, UNAM (Mexico)	Sub-THz to a few THz	Not specified	Compact environmental and spectroscopic systems under development (2021) [113]

3.2 THz Harmonic Generation from Semiconductor Superlattices

Semiconductor superlattices, originally proposed by Esaki and Tsu (1970) [116], provide a platform for nonlinear electron transport and Bloch oscillations, whose theoretical framework is comprehensively described by Wacker (2002) [117]. Collaborative work between groups in Colombia, Mexico, and Chile has led to new modes of THz emission in semiconductor superlattices (see conceptual device's bands structure in Fig. 5b) [106, 107]. In biased semiconductor superlattices, perpendicular charge transport is governed by resonant alignment of energy levels across wells, producing peaks in the current–voltage (I-V) curve associated with negative differential conductivity. When an external GHz-THz field is applied, photon-assisted tunneling occurs, generating resonance replicas at bias shifts equal to integer multiples of the photon energy, in good agreement with theoretical predictions for weakly coupled semiconductor superlattices. Significant theoretical advances in frequency multiplication within the GHz-THz range were reported by M. F. Pereira et al. [96], who employed a hybrid nonequilibrium Green's function combined with a relaxation-rate model to achieve excellent agreement with experimental data across a broad range of input frequencies. Their study also identified critical design limitations in superlattice housings by modeling local electric fields and comparing them with experimentally measured input powers from a backward-wave oscillator. These efforts provide a theoretical and experimental framework for engineering efficient THz harmonic generation in semiconductor nanostructures.

3.3 Electronic THz Sources

Electronic generation of terahertz radiation builds upon fundamental concepts of negative differential conductivity and intervalley electron transfer in III–V semiconductors. The observation of microwave oscillations in GaAs by Gunn [118] demonstrated that charge transport under high electric fields can produce self-sustained oscillations without external resonators, establishing the physical basis for solid-state electronic emitters. The extension of transport engineering into semiconductor superlattices, first proposed by Esaki and Tsu [116], introduced artificial band structures in which miniband formation and Bloch oscillations provide additional nonlinear mechanisms for high-frequency generation. A comprehensive theoretical treatment of nonlinear transport and domain formation in such systems is provided by Wacker [117], clarifying the conditions under which coherent oscillatory behavior may extend toward the terahertz regime.

The realization of direct solid-state emission in the terahertz range was achieved with the demonstration of the terahertz quantum cascade laser [119], where intersubband population inversion in engineered quantum wells enables stimulated emission at frequencies determined by subband spacing rather than by bulk bandgaps. These developments collectively illustrate the transition from microwave oscillators toward engineered semiconductor heterostructures capable of operating intrinsically in the THz domain.

Electronic THz sources form a smaller but rapidly expanding area of research in Brazil. Groups at the Universidade de São Paulo (USP) and the Universidade Estadual de Campinas (UNICAMP) are developing oscillator and multiplier circuits operating in the sub-THz and low-THz range. Research by Nussenzveig, Maia, and collaborators [120] focuses on Gunn and high electron mobility transistor frequency chains and CMOS-compatible on-chip emitters, bridging the gap between microwave and THz domains.

In Mexico, a substantial range of advances in electronic sources has been reported. These activities mark a transition from purely detection-oriented systems toward true THz source engineering. Incremental advances in the engineering of traditional antenna-based sources (see conceptual schematics in Fig. 5f) at CIO [109], UNAM [121], and INAOE [122] have contributed to new time-domain spectrometers and have also contributed to applications in environmental spectroscopy [123]. Continuous-wave laser-based THz sources have also been pursued at both INAOE and UNAM, aiming to realize alternative emitter designs based on difference-frequency generation [108]. Theoretical studies at the universities of Zacatecas and Morelos have made progress toward semiconductor heterostructure-based THz emitters, identifying potential mechanisms for compact solid-state sources [124].

3.4 Graphene and Carbon Nanotubes Plasmonics for THz Emission

Harnessing plasmonics in carbon-based low-dimensional structures has opened promising pathways for the development of compact and tunable terahertz emitters. Graphene plasmonics, characterized by extreme field confinement and electrostatic tunability [125], has emerged as a platform for tunable THz emission and strong light-matter interaction [126]. In Argentina, the groups of Mauro Cuevas, Ricardo Depine, and Raúl Bustos-Marún have provided pioneering theoretical and experimental work on graphene- and plasmon-phonon hybrid emitters, many in collaboration with the Centro Nacional de Pesquisa em Energia e Materiais (CNPEM) and USP in Brazil. Graphene-based systems leverage surface plasmon modes that can be dynamically tuned via the chemical potential, enabling strong field confinement and efficient coupling with nearby emitters. Studies have demonstrated dramatic enhancement of spontaneous and radiative emission—up to four orders of magnitude in radiation efficiency and quantum efficiencies near 0.8—using graphene waveguides and dimer plasmonic antennas operating between 4 and 15 THz [101, 110]. Furthermore, theoretical work on graphene-coated active cylinders revealed tunable lasing conditions for both radiative and nonradiative plasmon modes, with low population inversion thresholds (see conceptual example of this class of sources in Fig. 5c) [102]. Complementarily, carbon nanotube-based systems offer nanoscale Cherenkov-type THz lasing mechanisms, where electron beams in single or bundled carbon nanotubes generate coherent THz radiation [99]. Together, these developments illustrate the growing potential of carbon-based plasmonics for integrated, tunable, and high-efficiency THz sources.

3.5 Polariton-Based THz Sources

Recent progress in polariton-based THz sources has revealed alternative emission mechanisms through hybrid light-matter excitations. In contrast to nonlinear frequency conversion, polaritonic systems rely on strong coupling between electromagnetic fields and collective electronic or lattice excitations, leading to quasi-particles whose dispersion is governed by coupled-mode interactions. In two-dimensional materials such as graphene, collective charge oscillations (plasmons) exhibit extreme field confinement and electrically tunable dispersion relations [125]. The confinement factor $q/k_0 \gg 1$ and the possibility of electrostatic gating enable emission frequencies determined by carrier density and geometric design and not by bulk material resonances. Graphene plasmonics therefore provides a platform for strong light-matter interaction and engineered THz functionality [126].

These concepts have inspired material-engineered THz emitters in which frequency selectivity arises from cavity or resonator design, hybrid plasmonic-electronic interfaces, and nanostructured confinement. At CNPEM and the Universidad Federal de Minas Gerais (UFMG), experiments on phonon-polariton and plasmonic resonators have demonstrated coherent THz emission through nanostructured interfaces, advancing beyond conventional optical rectification into material-engineered polaritonic sources. Phonon polaritons in oxide nanostructures such as SnO_2 nanobelts and α-TeO_2 nanowires have exhibited sub-diffractional confinement, Fabry-Pérot cavity effects, and waveguiding behavior across the mid- to far-IR and THz ranges (see conceptual device in Fig. 5d), verified through synchrotron-based nanospectroscopy and theoretical modeling [103, 104].

In parallel, semiconductor microcavities operating in the strong coupling regime have been theoretically proposed as stimulated THz emitters, in which the emitted frequency corresponds to the polariton mode splitting [99]. These results collectively emphasize the potential of polaritonic coupling and hybrid plasmonic-electronic concepts as future directions for THz emitter miniaturization and tunability.

3.6 Large-Scale Accelerator-Based Sources

Accelerator-based terahertz sources originate from relativistic electron dynamics in periodic magnetic structures. The theoretical basis of free-electron laser emission was established by Madey [127], who demonstrated that stimulated emission can occur when an electron beam traverses an undulator. The resultant electron oscillations produce coherent radiation at a wavelength determined by beam energy and magnetic periodicity. Unlike solid-state emitters, the emission frequency in such systems is not fixed by material band structure, but is tunable via accelerator parameters, enabling broadband and high-brilliance THz generation.

Brazil currently leads the region in high-brilliance THz sources through the Sirius Synchrotron and associated instrumentation at CNPEM. Work by Santos and colleagues [112] explores the use of synchrotron radiation for the development of ultrasensitive nanoscale infrared and THz spectroscopy. These large-scale infrastructures

provide capabilities not yet replicated elsewhere in Latin America and are expected to foster regional collaborations.

Accelerator-based sources, including FELs and synchrotron storage rings, remain among the most powerful and versatile tools for THz and far-IR science. Synchrotron radiation provides continuous-wave emission (Fig. 5d), broadband spectral coverage, and exceptional brightness, enabling experiments otherwise unattainable with laboratory-scale sources. Such facilities host cutting-edge studies ranging from high-resolution gas-phase spectroscopy and vibrational microscopy to the emerging field of spectral nanoscopy, where THz and far-infrared radiation are coupled to scanning probe techniques for nanoscale materials analysis.

In Brazil, the Sirius synchrotron storage ring (Fig. 6)—one of the most advanced fourth-generation storage rings worldwide—has been in operation since 2020, incorporating diffraction-limited X-ray performance and an exceptionally low emittance electron beam. Currently operating 13 beamlines, including IMBUIA—the first infrared station on such a low-emittance accelerator [112]—Sirius is rapidly expanding its capabilities. Responding to the growing needs of the far-infrared and THz communities, the facility will launch TATU in mid-2026, a dedicated THz nanoscopy beamline designed to deliver synchrotron-based nanospectroscopy spanning 3–20 THz. Once commissioned, TATU will provide open access to Latin American researchers, establishing a regional hub for advanced THz science and fostering collaborations with leading facilities across the globe. The open-access model democratizes world-class THz radiation for smaller Latin American institutions, potentially accelerating the region's transition from technology users to developers.

In Mexico, smaller-scale efforts are underway to adapt and develop backward wave oscillator-based sources for environmental and spectroscopic applications [113].

3.7 Regional Outlook and Integration

In summary, Mexico leads in photonic and hybrid THz source development, integrating optics, materials science, and instrumentation. Brazil is diversifying its activities

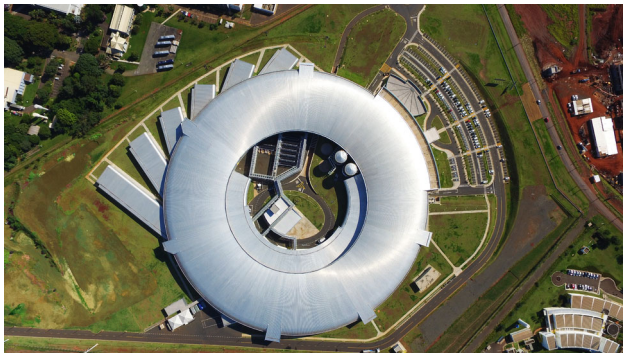

Fig. 6 Aerial view of the Sirius synchrotron light source in Campinas, São Paulo, Brazil—an open-user facility that currently operates the infrared IMBUIA beamline [112] and will soon commission the new THz beamline (TATU), designed to serve the Latin American community with synchrotron-based nanospectroscopy in the 3–20 THz range. Courtesy of CNPEM

with strong efforts in electronic and polaritonic generation, coupled with its mission of providing high-brightness synchrotron THz radiation for an open-user experimental station. Argentina contributes substantially to theoretical modeling and 2D-material emitters, while Chile and Colombia participate mainly through instrumentation and radioastronomy collaborations. Although the number of laboratories remains limited, the cumulative output of these groups over the past decade reflects a coherent regional transition from THz applications toward genuine source technology innovation. The emergence of multi-institutional collaborations, growing access to advanced infrastructure, and the convergence of experimental and theoretical expertise collectively position Latin America as an increasingly relevant actor in global THz source research. A strategic focus on niche innovations, signal processing, material-engineered emission, and hybrid integration has enabled small collaborative teams to achieve an outsized impact.

The development of THz sources in the region has been informed and influenced by challenges specific to the region. Budgetary limitations have led to a focus on more accessible photonic sources by several groups, although a diversity of solid-state and semiconductor sources have also seen significant advances in the region. Such sources are expected to progress from theoretical work to practical applications in the near future.

4 Biological and Medical Applications

by *Jimy Oblitas*[1], *and Monica Ortiz-Martinez*[2],[3]

[1]jimy.oblitas@upn.edu.pe
[2]mortiz@cio.mx
[3]monica.ortiz@secihti.mx

Terahertz (THz) spectroscopy and imaging have emerged as powerful tools in the biomedical and medical fields, offering a unique combination of nonionizing radiation, sensitivity to water content, and capacity to resolve molecular-level interactions [128]. Occupying the electromagnetic spectrum between microwaves and infrared, THz waves interact strongly with polar molecules, particularly water, making them ideal for probing hydration states, tissue composition, and biomolecular structure in a noninvasive manner [129].

Early studies established important experimental and conceptual foundations for biomedical THz applications. Initial demonstrations showed that THz imaging systems could achieve high-contrast visualization of biological tissues and resolve structural features associated with vibrations in water and lipid content [130, 131]. In parallel, THz spectroscopy emerged as a powerful probe of biomolecular hydration dynamics, enabling direct investigation of solvation layers and collective water motions surrounding biomolecules [132]. Subsequent studies further highlighted practical considerations in tissue measurements, particularly the strong influence of hydration on extracted optical properties and the importance of controlled sample preparation protocols [133]. Complementary analyses later emphasized the role of collective

water-biomolecule dynamics and reinforced the potential of THz spectroscopy for monitoring biochemical processes in real time [134].

Building upon these foundational advances, recent years have seen a surge of interest in applying THz technologies across biologycally oriented application domains, including biotechnology, agriculture, and food science. This expansion is driven by the increasing demand for nondestructive and real-time monitoring methods. In these contexts, THz spectroscopy has proven effective in detecting physiological and molecular characteristics such as hydration gradients in plant tissues, the structural behavior of complex carbohydrates such as fructans, and dynamic changes under drought or stress conditions [135]. THz imaging, for example, has been employed to reveal the spatial distribution of water within leaves, helping to explain the remarkable drought resistance at both tissue and molecular scales [135].

In the medical domain, THz imaging has demonstrated diagnostic potential in several areas. One particularly compelling application is in the early detection of diabetic foot syndrome, where THz images can reveal skin dehydration. A recent investigation based on THz imaging showed that peripheral neuropathy seems to be causally related to the hydration deficiency in diabetic patients [136]. Unlike traditional diagnostic methods, THz-based moisture mapping offers a quantitative, objective, and non-contact alternative that could enable earlier intervention and reduce the need for amputations.

Furthermore, THz biophotonics is increasingly being enhanced by computational approaches. The integration of machine learning and deep learning with THz data sets has opened new possibilities for classification, prediction, and automated analysis, improving diagnostic accuracy and allowing the identification of subtle patterns in complex biological systems [137].

This section provides an overview of the current landscape of biological and medical applications of THz spectroscopy and imaging, highlighting both progress and existing gaps to outline a roadmap for broader adoption in diagnostics, physiological monitoring, and biotechnological innovation.

4.1 Medical Diagnosis and Imaging

In the medical domain, the most substantial advances identified originate from Mexico, where THz reflection imaging has been developed to quantify plantar skin hydration as a label-free diagnostic contrast for diabetic foot syndrome (Fig. 7). The approach, termed Moisture Mapping by Terahertz (MMAT), exploits the strong coupling of THz waves to water to differentiate healthy from diseased tissue in a non-contact, non-ionizing manner [136, 138].

Implementation relies on a fiber-laser-driven THz-TDS in reflection geometry with a collinear photoconductive transceiver mounted on a motorized platform. Each examination generates a two-dimensional grid of waveforms acquired through a high-density polyethylene window with scan times under 10 min [136]. Hydration per pixel is retrieved by fitting the complex transfer function of the reflected pulse to a multilayer dielectric model, producing quantitative hydration maps. An associate

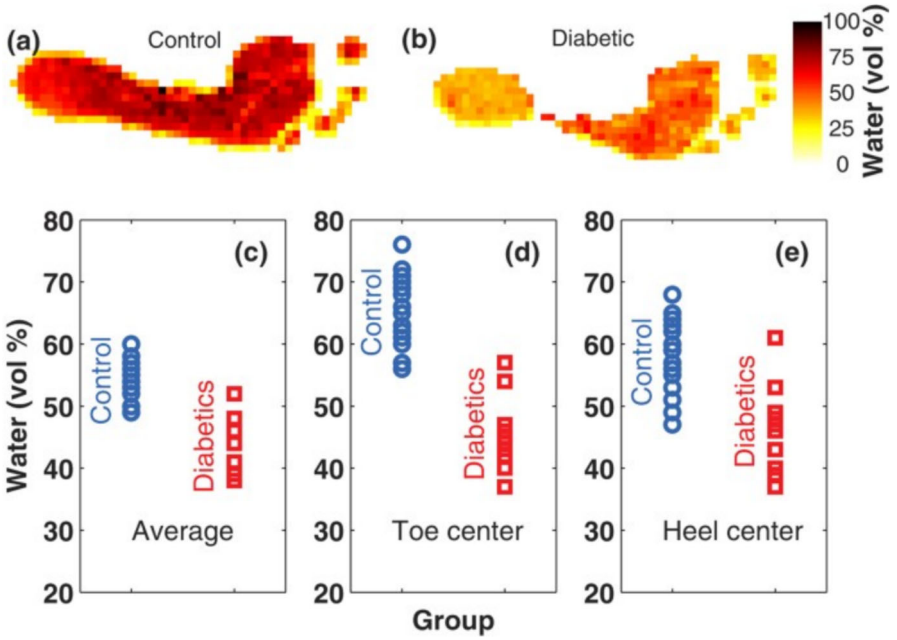

Fig. 7 Representative THz hydration maps for **a** a control subject and **b** a diabetic subject. Volumetric water fraction is shown for **c** the foot-sole average, **d** the center of the greater toe, and **e** the heel region. Reproduced under CC-BY 4.0 from [138]Copyright ©The Authors

red-yellow-green index summarizes the spatial deterioration patterns for clinical interpretation [138].

Clinical validation in Mexico reported diagnostic performance ranging from approximately $76-81\%$ sensitivity and $69-78\%$ specificity based on threshold rules applied to mean hydration and to green-red pixel fractions. Population analyses showed declining hydration with age in non-diabetic controls, lower baseline hydration among diabetic participants, and significant associations between reduced hydration, peripheral neuropathy, and ulcer/amputation history. These findings extend earlier Mexican proof-of-concept work demonstrating the feasibility of noninvasive plantar hydration mapping in living subjects and motivating the standardized MMAT protocol. More generally, operation in the 0.3–1 THz band provides a robust hydration-specific contrast: small changes in tissue water content produce measurable differences in the reflected waveform, enabling quantitative and operator-independent assessment.

From a clinical perspective, MMAT provides complementary information to established diabetic foot assessment methods such as the Semmes-Weinstein monofilament (SWM) test and the ankle-brachial index (ABI). The SWM test evaluates loss of protective sensation but relies on patient perception and examiner technique, introducing an inherent degree of subjectivity, whereas ABI provides an indirect assessment of peripheral arterial disease and does not directly probe tissue condition. In contrast, MMAT offers a quantitative, non-contact measurement of cutaneous hydration, a parameter linked to autonomic dysfunction and skin integrity. Published results

indicate that THz-derived hydration correlates with neuropathy metrics while showing limited association with ABI, suggesting that MMAT is particularly sensitive to neurogenic alterations relative to vascular changes. Accordingly, MMAT is best viewed as a complementary tool that may enhance early risk stratification by providing resolved information on plantar skin condition.

Although MMAT demonstrates promising diagnostic capability, several factors may influence THz-derived hydration measurements and should be considered when interpreting results. Skin hydration can be affected by environmental conditions such as ambient temperature and relative humidity, as well as subject-specific factors. Published MMAT studies have implemented standardized acquisition protocols and participant preparation procedures to mitigate variability; however, residual inter-subject variability and physiological fluctuations cannot be fully excluded. Future investigations incorporating controlled environmental monitoring, larger groups, and multi-center validation will be important to quantify the impact of these potential confounders and to support clinical translation of MMAT-based assessments.

Measurement repeatability is another key consideration for clinical deployment. Existing studies have employed controlled positioning and standardized acquisition workflows that are expected to reduce short-term variability; however, comprehensive intra-session and inter-session repeatability analyses remain limited in the current literature. Longitudinal studies incorporating repeated measurements across visits, operators, and clinical settings will be essential to fully characterize reproducibility, quantify day-to-day variability, and establish the confidence bounds required for routine clinical implementation.

4.2 Biomolecular and Biophysical Characterization

Work in Latin America has leveraged terahertz time-domain spectroscopy (THz-TDS) to interrogate collective modes, hydration structure, and solid-state order in biomolecular and bio-derived materials, spanning experimental measurements and theoretical modeling. In Brazil, THz-TDS has been shown to quantify crystallinity in microcrystalline cellulose by exploiting sharp lattice resonances, most prominently a band near 3.03 THz, allowing rapid prediction of the crystallinity index with relative prediction errors on the order of a few percent; this establishes THz as an ambient, non-ionizing complement to diffraction for polysaccharide solids [139]. In parallel, high-speed Asynchronous Optical Sampling THz-TDS combined with Gaussian peak deconvolution enables qualitative discrimination of neat sugars and binary/ternary mixtures (e.g., glucose, fructose, sucrose, lactose, and sweeteners), resolving partially overlapping absorptions and supporting mixture analysis relevant to food and biochemical contexts rather than full quantitative compositional analysis [140].

Beyond solids, thin-film aqueous measurements remain central to biomolecular sensing. A modified attenuated-total-reflection configuration that forms micrometer-scale water films beneath a top mirror improves signal quality and interpretability for water-rich samples, pointing towards microfluidic THz assays for biochemical detection [141]. This type of measurement addresses the strong and rapidly increasing

absorption of liquid water across the THz band, particularly above $\sim 2-3$ THz, while retaining sensitivity to solute-driven changes in the complex dielectric function.

Linking molecular hydration to tissue-level function, a Mexico-led synthesis demonstrates that agave fructans exhibit unusually large hydration shells (on the order of $\approx$ 320 water molecules), while THz imaging of agave leaves reveals a highly hydrated central core surrounded by less-hydrated outer tissues; together, these observations argue that fructan-water interactions contribute to drought tolerance from the molecular up to the tissue scale [135]. This multiscale perspective connects THz spectral markers of solvation with spatially resolved hydration phenotypes in living plant organs.

The region's contributions also include physics-guided modeling of biomolecular collective motions that fall within the GHz-THz band. Elastic network/finite-element analyses of hen egg-white lysozyme predict families of low-frequency collective modes that provide a theoretical framework for interpreting THz-sensitive protein dynamics, even though the study itself is computational rather than spectroscopic [142]. Such modeling complements experimental efforts by clarifying how structural connectivity and mass distribution shape spectral features accessible to THz probes.

Finally, dielectric-mixture analyses applied to bio-derived matrices illustrate how THz measurements translate into quantitative material parameters. While primarily positioned in agri-food workflows, studies on high-moisture fruit tissues employ Landau-Lifshitz-Looyenga (LLL) inversions (augmented with volatile-component terms) to fit effective dielectric functions across hydration states, providing a template for quantitative THz retrieval in complex organic systems [143]. Representative experimental results for [143] are shown in Fig. 8, where the time-domain waveforms, frequency-domain spectra, and extracted optical constants illustrate the strong sensitivity of THz transmission to water content. These results highlight how effective-medium

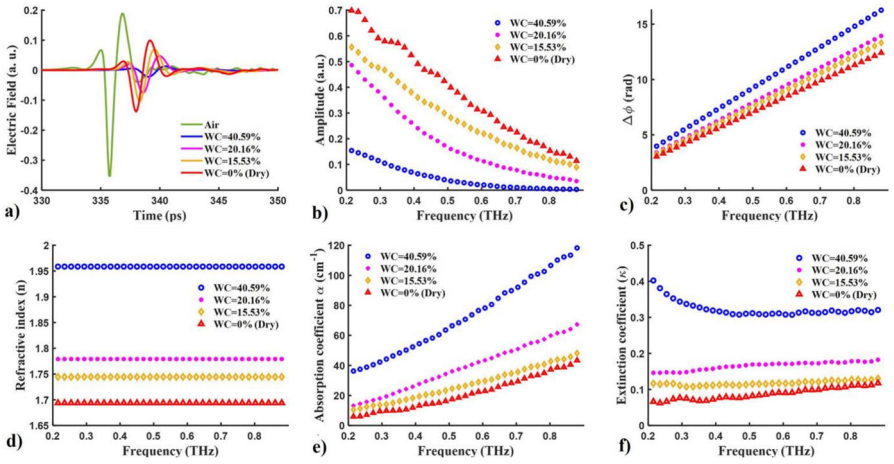

Fig. 8 Representative THz-TDS measurements of Pouteria sapota samples with different water content and extracted optical constants from [143] under the CC-BY-NC-ND 4.0 license. Copyright ©Revista mexicana de física, 2025

modeling enables physically interpretable parameter extraction from broadband THz measurements in food matrices.

Together, these experimental and theoretical efforts from Brazil and Mexico demonstrate how THz spectroscopy and imaging can read out crystalline order, resolve solute-water interactions in aqueous environments, and connect collective modes to biologically relevant structure and function.

4.3 Plant Physiology, Agriculture, and Food Quality

In plant physiology, terahertz methods quantify water dynamics in vivo and map hydration in thick, heterogeneous tissues. In Mexico, time-resolved THz-TDS on living Arabidopsis thaliana retrieves leaf water fraction via effective-medium inversion and tracks changes under light/dark cycles or abscisic-acid perturbation, demonstrating label-free physiological monitoring on biologically relevant timescales [144]. Raster-scanned THz imaging combined with Landau-Lifshitz-Looyenga (LLL) effective-medium modeling provides pixel-wise water content and three-dimensional hydration distributions in succulent leaves (e.g., agaves), revealing a hydrated central core surrounded by less hydrated outer tissues, a phenotype characteristic of drought-adapted plants [145]. It should be noted, however, that the LLL model formally assumes a randomly mixed and isotropic medium; therefore, in thick and structurally heterogeneous lead tissues, it should be interpreted as an effective approximation rather than a strictly exact physical description.

In agricultural production and postharvest quality control, Latin American groups demonstrate non-destructive THz analytics across fresh produce and processed foods. A Peruvian study uses transmission THz-TDS with principal component analysis to classify blueberry (Biloxi) maturity into four stages labeled by CIE Lab* color and total anthocyanins, employing a nitrogen-purged bench (TeraPulse 4000) to stabilize spectral baselines [146]. In Mexico, THz measurements on mamey (Pouteria sapota) slabs show that transmitted FFT amplitude ($\approx 0.2 - 1.4\,\mathrm{THz}$) increases as moisture ratio decreases, supporting calibration curves for non-destructive moisture tracking and enabling retrieval of optical parameters (n, κ, ϵ) [147]. Complementarily, LLL dielectric-mixture inversion augmented with a volatile-components term improves fits to effective dielectric functions of high moisture mamey pulp across hydration states, providing a template for quantitative THz metrology in complex organic matrices [143]. THz pulse attenuation and phase trends also allow thickness/moisture estimation in dried mango slices, illustrating straightforward quality control in processed products [148].

Machine learning (ML) pipelines translate THz features into actionable decisions in agri-food contexts. THz imaging coupled with Random Forest achieves ≈ 91.2 % accuracy for coffee bean authentication using datasets on the order of a few hundred samples [149]. Similarly, THz-based maturity classification of blueberries has employed support vector machine models evaluated using multi-fold cross-validation schemes, reporting accuracies above 80% under controlled conditions [150]. Broader reviews and conference studies further highlight the potential of principal component

analysis, partial least squares, and neural-network-based approaches for tasks such as adulteration detection and freshness assessment [151].

However, most reported THz-ML studies to date rely on single intuition datasets and internally validated models, and external testing on independent cohorts remains limited. Consequently, although the reported performances are encouraging, careful interpretation of generalization capability is warranted. Continued progress will depend on the availability of larger, standardized datasets and multi-center validation efforts to support robust real-world deployment.

Collectively, studies from Mexico, Peru, and Brazil trace a practical path from quantitative water mapping and dielectric modeling to chemometric/machine learning classification and deployable sensors, positioning THz techniques as robust tools for plant phenotyping, postharvest grading, and process line quality control.

4.4 Actual Limitations

In Latin America, the implementation of THz spectroscopy remains limited compared to other well-established spectroscopic techniques, such as near-infrared, Fourier transform infrared, or Raman. This is partly due to the high cost and complexity of THz instrumentation, the scarcity of specialized training programs, and the lack of standardized protocols for sample preparation, measurement, and data interpretation. Moreover, many existing studies rely on proof-of-concept demonstrations, and there is still a gap between laboratory research and industrial or clinical deployment.

Another critical limitation is the strong absorption of THz radiation by water, which, while enabling high sensitivity to hydration changes, also restricts penetration depth in water-rich tissues. This poses challenges for in vivo imaging beyond superficial layers and limits the range of biological targets that can be effectively probed. The absence of methodological standards further complicates the comparison and replication of results across different research groups [137].

Finally, for both biomedical and agroindustrial applications, the interaction between THz waves and bound versus free water remains insufficiently understood. This distinction can significantly affect spectra, and without robust models and reference datasets, interpretation remains challenging. Overcoming these limitations will require coordinated efforts to improve instrumentation accessibility, expand frequency coverage, and develop standardized measurement and analysis protocols.

4.5 Future Perspectives

The future of terahertz spectroscopy and imaging in biomedical and agroindustrial contexts lies in bridging the gap between proof-of-concept studies and large-scale, standardized implementation. On the biomedical side, advances in instrumentation, such as compact, portable THz systems, improved frequency coverage beyond the current $0.1-4.5$ THz range, and higher acquisition speeds, will enable broader clinical adoption. Integration with machine learning algorithms will further enhance diagnostic accuracy, enabling automated analysis of hydration patterns, disease markers, and biomolecular signatures.

In the agroindustrial sector, THz spectroscopy presents opportunities for monitoring structural and compositional changes in biological matrices over time. Since the molecular transport of bioactive compounds in these products occurs through water, and their matrices evolve during storage, THz sensitivity to water-matrix interactions could become a key tool for assessing product shelf life. Phenomena such as glass transitions and crystallization, which have a direct impact on product quality, can be detected with high precision using THz techniques. This opens a new research avenue for quality control and product development, particularly in high-value commodities where early detection of structural changes can prevent economic losses.

Moreover, the ability of THz waves to detect crystalline phases in biological and agroindustrial products creates a novel field for multidisciplinary research, involving food science, materials science, and biophotonics. Future studies could explore the combination of THz spectroscopy with complementary modalities, such as near-infrared, Fourier transform infrared, and hyperspectral imaging, to provide richer datasets for predictive modeling.

5 Cultural Heritage

by *Mariana Alfaro-Gomez*[1], *and Montserrat Gomez*[2]

[1]mariana.alfaro@edu.uaa.mx
[2]res.montserat.gomez@gmail.com

The analysis of cultural heritage with technological advances is a beautiful example in which science can be combined with human social expressions. THz spectroscopy has been shown to be a noninvasive and nondestructive technique for the analysis and conservation of artwork [152, 153]. This technique has unique characteristics that help complement the traditional (or more common) analysis performed in art [154]. It allows for the study of paintings and subsurface structures, stratigraphic analysis, conservation guidance, and identification and authentication of pigments. As this review is intended to highlight contributions made by the Latin American (LA) THz community in this area, we will not focus on the basics of how THz spectroscopy can be used for the analysis of artwork. The reader may refer to previously published work by recognized experts in the field [154].

The LA scientific community has made interesting contributions to cultural heritage using optical and physical techniques. For example, X-ray fluorescence was used to determine the thickness of gold coatings on pre-Colombian objects by a Brazilian group [155]. Another example, reported the use of Fourier transformed infrared spectroscopy (FTIR) for the characterization of a mask from the Lord of Ucupe's tomb in the region of Lambayeque in Peru [156]. FTIR works with far infrared radiation, where the longer wavelengths partially overlap with the THz band. In this reference, a blackish adhesive material found in the eyes of the mask was measured using Attenuated Total Reflection-FTIR, along with other techniques. The results offered insights into the use of materials utilized by the Moche civilization.

The reported applications of THz time-domain image (TDI) or time-domain spectroscopy in LA have been done through collaborations involving multiple institutions such as Western School of Conservation and Restoration (ECRO, Guadalajara, México), National Institute of Anthropology and History (INAH), College of Michoacán (ColMich, Michoacán, México), Center for Research in Optics (CIO, León, México), and Autonomous University of Aguascalientes (UAA). Within this group, scientists have collaborated with art curators and state organizations to bring the benefits of THz technology to the preservation and analysis of cultural heritage. The reported works refer not only to laboratory studies but also to field work. In this review, we highlight the key contributions and methodologies of the research done in this area. A summarizing table of the reviewed reports, as well as a short description of their main contribution, can be found in Table 3.

5.1 Stratigraphic Analysis

THz spectroscopy provides a complementary tool for the non-destructive inspection of paintings. One of the main advantages of using this technique in cultural heritage is its capability to perform noninvasive stratigraphic analysis. THz radiation can penetrate deeper than infrared wavelengths and detect many materials with high transparency to X-ray radiation. Furthermore, the time-domain analysis allows us to *see* underlying structures with depth information by probing subsurface layers. Reflection

Table 3 Summary of THz analysis and contributions made by LA community in the cultural heritage field

Reference	Type of THz analysis	Main contribution
Gomez-Sepulveda et al. (2017) [157]	Stratigraphy	Identification of earlier paint layers and a hidden date (1816) under the surface; detection of the original eighteenth-century free-hand sketches
Reyes-Reyes et al. (2024) [158]	Stratigraphy and material analysis	Internal structural analysis identifying up to six layers; mapping of surface deformations via ToF; detection of mercury sulfide (vermilion) using its THz spectral fingerprint
Koch-Dandolo et al. (2018) [159]	Stratigraphy and structural analysis	Detection of internal defects like canvas detachment; localization of hidden original paint remains and past restoration materials (adhesives) to guide intervention
Koch-Dandolo et al. (2017) [160]	Stratigraphy and structural analysis	Imaging of paint layers opaque to X-rays; identification of pentimenti (compositional changes) and engravings on the metal support
Lambert et al. (2020) [161]	Stratigraphy and structural analysis	Cross-sectional images to determine the state of conservation; identification and quantification of subsurface air gaps caused by paint delamination. Outdoor study

configuration has been used mainly for the analysis of artwork by LA groups not only in easel paintings, but also in ornamental structures, icons, and altarpieces [157–159, 161].

The first LA cultural heritage report using THz-TDI was performed by Gomez-Sepulveda et al [157]. This was an exhaustive study of an Altarpiece, which comprises eight different paintings from Hermenegildo Bustos, a renowned painter in Mexican religious art (Fig. 9). Four of them were analyzed by THz spectroscopy.

This study was carried out using an adapted Menlo spectrometer and a Picometrix system within a frequency range from 0.1 to 1 THz. Two of the paintings were analyzed in a laboratory environment. These paintings were raster scanned to obtain images, as well as time-of-flight (ToF) data. The underlying layers showed differences with respect to the superficial visible images. Three pictorial cycles consistent with historical research were detected and chronologically ordered using ToF information. By isolating a temporal region, a hidden date could be found. The area of interest was enhanced with an equalization method and the hidden date was recognized within the blue square (Fig. 9g). This result was cross-checked with X-ray and infrared images, also shown in Fig. 9.

From the underlying layers, the intermediate one could be attributed to another author dating from 1816. The results suggested that the paintings were intentionally modified throughout time, possibly for aesthetic or liturgical reasons. Through

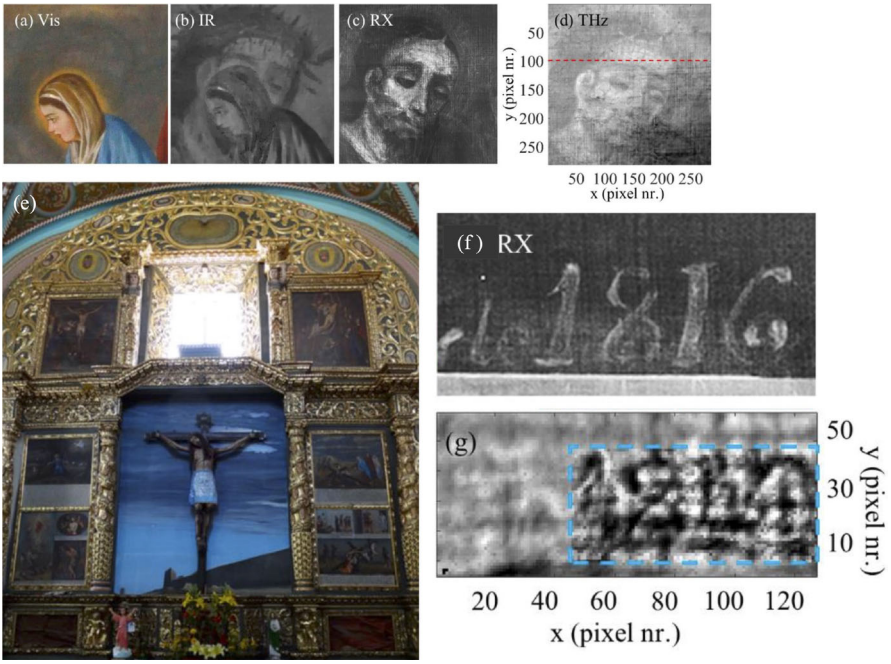

Fig. 9 **a** Visible, **b** infrared, **c** X-ray, and **d** THz images of one of the studied paintings. **e** Altarpiece studied with TDI. Four different paintings were studied by the THz team. **f** X-ray and **g** THz image of a hidden date, the region of interest was isolated by a windowing function in the THz range. Adapted with permission from [157]. Copyright ©Springer Nature, 2016

this work, the authors demonstrated the importance of characterizing the pigments to ensure consistency with the temporal stratigraphy and to better understand previous restorations. The importance of determining adequate frequency intervals to show better contrast was also demonstrated. This study was the first documented application in this context and showed the capability of THz spectroscopy to reveal hidden layers and images.

5.2 Structural Analysis

Besides stratigraphic analysis, THz spectroscopy allows the study of hidden subsurface features such as layer interfaces, internal air gaps, and structural deformations. A stratified easel painting with a complex structure was studied by Dandolo et al. [159]. In this study, a heavily retouched and restored painting was analyzed with TDI, providing information about its structure. The painting presented a lining intervention from a conservation treatment which gave extremely uneven layers that resulted in a very challenging multilayer analysis. The authors resolved this challenge by implementing a signal separation method [162] that worked satisfactorily. Images with a high level of clarity of single regions could be obtained. This case positioned THz technology in the Latin American context, as the understanding and visualization of the different retouching layers allowed restorers to make informed decisions during the critical cleaning process and the removal of overpaint.

One of the few *on-site* studies of THz-TDI performed on three-dimensional irregularly shaped heritage objects was reported in [161]. Interestingly enough, this study was also performed under uncontrolled climate conditions at a kiosk in Guadalajara, Mexico. Figure 10 shows the analyzed kiosk and surface, as well as the members of the group taking measurements.

The study reports measurements of accumulated layers on curved structures using a hand-held point gauge (API Teragauge). The irregular surfaces were scanned in reflection mode. In the optimal state, the surfaces should be uniform and smooth; however, air gaps were detected in deteriorated zones. A deconvolution method was implemented for the analysis. Separation gaps were about 240 μm or more. Regardless of the difficulties due to outdoor conditions and the challenge of performing measurements over an irregular surface, the spectra obtained were conclusively useful in determining the deterioration state of the paint layers present on the kiosk. Figure 10d shows a scheme of the THz hand-held gauge, as well as the deconvolution process (Fig. 10e to g). The implementation of the THz technique in the study of the Guadalajara Kiosk was of great significance as multiple layers of painting were applied throughout time as part of maintenance efforts. The image obtained allowed to identify that this excessive accumulation of layers posed a risk for the conservation of the kiosk, as they were delaminated and showing separations between them. The findings of the study were key to understanding the real state of preservation and to making informed decisions during the restoration process.

Another recent analysis reported by the LA community in art was the analysis of a glided wooden artifact [158]. In this work, stratigraphic analysis of an icon with gold details over a wooden support was reported (Fig. 11). The state of conservation

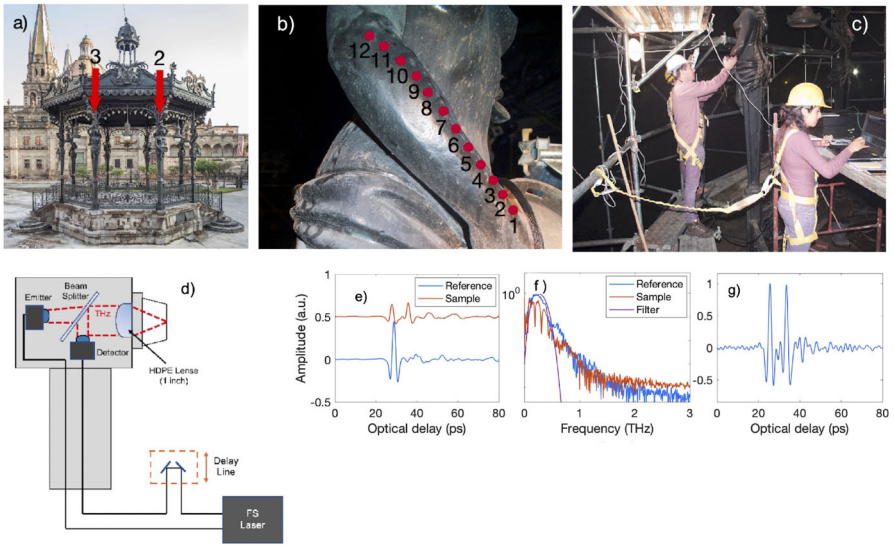

Fig. 10 **a** Guadalajara Kiosk analyzed with THz technology, red arrows point to some of the analyzed zones. **b** Example of a scanned area. **c** Group members taking measurements. **d** schematics of the API THz gauge. **e** to **g** Deconvolution process with Gaussian filter. Adapted with permission from [161]. Copyright ©Springer Nature, 2019

was observed with this analysis, as restoration areas could be seen as contrasting reflections with respect to the background. The ToF data of the first reflected echo provided topographic information and showed an irregular surface due to a convex shape along the wooden structure. B-scans, which are cross-sectional images created by graphing time-domain waveforms versus linear position on the painting, revealed the internal structure of the icon and confirmed the application of gold leaf only in

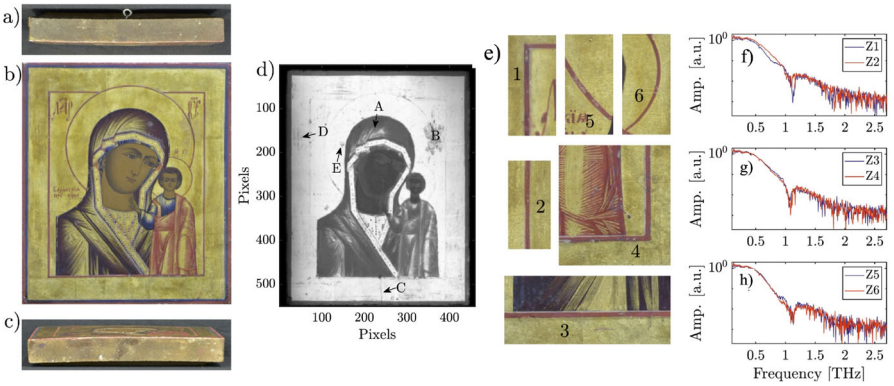

Fig. 11 **a** Upper, **b** frontal, and **c** lower view of the glided wooden artifact analyzed with THz technique by Castro-Camus Group. **d** Peak-to-peak THz image, **e** zones of the artifact where vermillion was detected, and **f** to **g** spectra of the marked zones in **e**, presenting the characteristic absorption band of the pigment. Adapted from [158] under the CC-BY 4.0 license. Copyright ©The Authors, 2024

specific areas. The study of this complex object, which presented not only multiple painting layers, but also gold leaf over its surface, was successfully carried out with THz spectroscopy. This research provided a clearer understanding of the sophisticated craftsmanship technique employed by the artist, in particular the original application of the gold leaf, and made it possible to distinguish it from later interventions, which appeared golden to the naked eye, but were not part of the original manufacture. Thanks to the ability of TDI to reveal the internal structure of the layers, it was possible to accurately differentiate between authentic elements and those added during restorations performed in later periods.

The capabilities of TDS for the analysis of metal-based art were tested by Dandolo et al. in [160]. This is an important feature, given that X-ray analysis does not perform well on metals. The analysis of the data was done with deconvolution and filtering in frequency domain techniques. The results presented B- and C-scans and integration of the electric field amplitude. C-scans specifically show a frontal view of the painting features. Each pixel of a C-scan presents information about the magnitude of a specific THz parameter. The signals were studied even with the high reflection of the back metal surface. Different types of pigments also presented changes in THz reflectivity, allowing the authors to detect differences not distinguishable under visible light. Figure 12 shows an image of one of the analyzed metal pieces, as well as the X-ray and

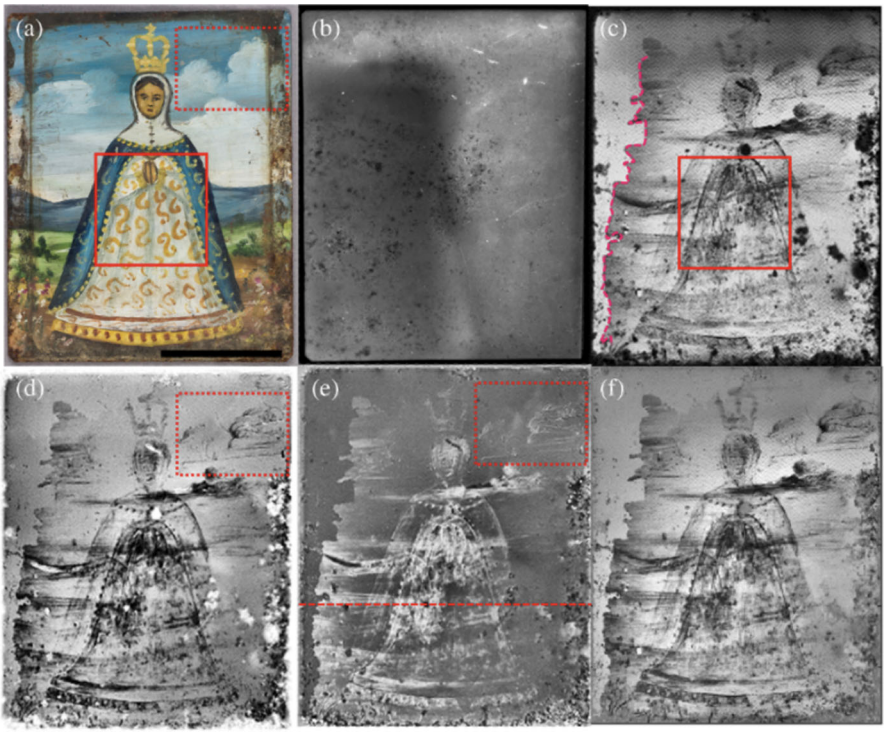

Fig. 12 **a** Painting over metal analyzed with TDI. **b** X-ray image of the piece and **c** to **f** THz images obtained with different elements of the THz data. Different features can be observed in each processing. Reproduced with permission from [160]. Copyright ©Springer Nature, 2017

THz images at different frequencies. This study represented a significant contribution to the field of restoration-conservation because until then, it was not possible to assess the state of conservation of metallic sheet as support for pictorial layers due its high reflectivity to X-rays. The THz images obtained demonstrated a sufficient sensitivity to distinguish between areas in good condition and zones with advanced corrosion of the underlying metal. Moreover, THz images allowed to identify pigments and pictorial stages that were added during previous interventions, which had likely been applied with the purpose of hiding or repairing damage caused by such corrosion.

5.3 Material Identification

Besides the analysis of stratigraphy and layers, another important feature of THz-TDS in cultural heritage is the identification and authentication of pigments. In this matter, another Latin American contribution was presented by Reyes-Reyes et al. [158]. In this reference, the identification of mercury sulfide (or *vermilion*), a red pigment, over the icon was performed using THz spectroscopy. This pigment presents a characteristic absorption peak centered at 1.14 THz. An identification algorithm based on the ratio between the area under the sample spectrum and an interpolation of the spectrum between 1.0 and 1.27 THz was developed. Given that the signal-to-noise ratio below 1.45 THz hindered the analysis in some areas of the icon, a visual inspection had to be performed to validate the absorption peak within the noise. The results were validated with X-ray fluorescence. Some areas with visually red pigments showed inconsistent results between THz and X-ray fluorescence results. These areas were visually red, as well as the vermilion areas, which indicated that the analysis helped to differentiate between visually similar pigments. This may be related to different restorations of the piece. Figure 11 e to h show the analysis of the vermillion signature on the icon.

5.4 Final Remarks: Impact of THz Technology in Art in Latin America

In the cultural heritage study, terahertz technology is becoming a popular and powerful tool for non-invasive exploration of artwork, particularly in cases such as paintings on canvas, metal, wood, and metallic structures. In paintings with multiple interventions, such as overpainting or previous restorations, the use of THz images has allowed to reconstruct the stratigraphic sequence of layers, which is essential to understand the modifications of a piece of art through time and to identify the changes and interventions made by different artists or restaurateurs. Although THz imaging does not allow to observe color, particle morphology, or microscopic details, like conventional stratigraphy, it provides non-invasive information from a complete painting and not only from a small segment. With this, its potential is highly significant, as it enables a first non-invasive stratigraphic mapping of the artwork. This facilitates a better understanding of its structure prior to any intervention and, if sampling is required, allows it to be carried out in a much more selective and well-informed manner. In the case study over metallic sheet, THz technology has not only facilitated the detection of overpaintings and surface modifications, but also has contributed to identifying corrosion

processes being active below pictorial layers. This represents a significant diagnostic capability that other techniques, such as X-ray imaging, cannot provide.

THz imaging has been presented to art conservators and restorers as a key technique for the study of the craftsmanship of patrimonial objects, making visible the internal structure of the work without direct interventions. This particular capability allows the precise evaluation of the conservation state of an artwork, the study of its material evolution, and even guidance to the restoration process with deeply founded and localized information. Pigment identification is especially relevant for the authentication and dating of artwork. Although THz spectroscopy does not give definitive dating or authentication, its data, along with historical records and knowledge of the time period and artist, can give a trustworthy analysis from the restaurateurs. A representative example of this is the vermilion, which was widely used until the early twentieth century, when it began to be replaced by other pigments, such as cadmium red. Therefore, detecting one pigment or the other not only allows for a more precise chronological framing of the creation of the piece, as many pigments were used in specific historic periods and replaced over time for more modern versions, but also helps identify later interventions that may have altered or replaced the original paint layer.

Although the exploration and advancement of the capabilities of this technique are still needed, its advantages are especially notable in contexts where other techniques, such as X-ray imaging, do not give effective results given the intrinsic nature of the materials, or where institutional restrictions do not allow sample taking or direct contact with the work. Moreover, its application could be extended for the restoration processes, such as the detection of mural or sculpture fillings, opening new possibilities for its integration into diagnosis and conservation protocols. Without a doubt, the Latin American community has contributed, as highlighted in this section, with important and relevant results in this meaningful THz application.

6 Terahertz Materials Research

by *Felix G. G. Hernandez* [1], *and Federico Sanjuan* [2]

[1] felixggh@if.usp.br
[2] federico.sanjuan@univ-pau.fr

The terahertz spectral window corresponds to photon energies of only a few millielectronvolts (1 THz $\simeq$ 4.14 meV), making it ideally suited for probing low-energy excitations that are often inaccessible to conventional optical or microwave techniques. In this regime, THz radiation is particularly sensitive to collective and quasiparticle phenomena such as optical phonons in crystalline lattices [163, 164], plasmons in conducting and nanostructured materials [165], magnons and spin excitations [166], and rotational and vibrational modes in molecular systems and inter- or intraband transitions in semiconductors.

Among the most versatile techniques in this field is THz-TDS [167], which employs broadband pulses with phase-sensitive detection of the transmitted or reflected electric

field. This approach provides direct access to the complex optical response functions of materials—including refractive index, dielectric permittivity, and optical conductivity—without the need for parametric fitting or Kramers-Kronig transformations [168]. Its ability to resolve both amplitude and phase enables the unambiguous determination of intrinsic material parameters, even in systems where electronic, vibrational, and spin-related processes are strongly coupled.

Because THz photons carry low energies, they can probe these processes without causing ionization or structural damage, offering a powerful and non-destructive means of investigating carrier dynamics, conductivity mechanisms, phase transitions, and molecular conformational changes. Moreover, the technique is compatible with extreme experimental conditions such as cryogenic temperatures and high magnetic fields, enabling the exploration of quantum materials and correlated electron systems under controlled environments [169].

A broad range of materials has been explored using THz spectroscopy [170], from conventional semiconductors and insulators to emerging systems such as organic conductors, polymers, biomolecules, metamaterials, graphene, and topological insulators. Each of these exhibits distinct behavior in the THz range that provides insights into their microscopic structure and macroscopic functionality. Consequently, THz has become an essential tool of modern condensed-matter research, underpinning advances in optoelectronics, quantum technologies, and ultrafast spectroscopy.

From a spectroscopic perspective, the effective probing depth of THz radiation in dielectric materials such as polymers, ceramics, and semiconductors typically ranges from several hundred micrometers to a few millimeters, depending on absorption coefficient and frequency [170]. Conductive or metallic layers strongly attenuate the electric field, often requiring reflection geometries rather than transmission measurements. The minimum lateral sample dimensions are generally constrained by the diffraction-limited beam waist (typically a few millimeters in conventional THz-TDS systems), while sample thickness must be compatible with both penetration depth and Fabry-Pérot interference considerations. Scattering-type near-field optical microscopy has been used to overcome the diffraction limit and investigate materials at the nanoscale [171]. In standard THz-TDS experiments, acquisition times for a single spectrum are on the order of seconds, with averaging extending measurements to several minutes when higher signal-to-noise ratios are required. These practical constraints define the accessible material thicknesses and electronic or vibrational features that can be reliably resolved [172].

This section focuses specifically on the progress achieved in Latin America, highlighting the emergence of regional expertise and infrastructure that are driving forward materials research in the terahertz domain.

6.1 Regional Developments

Across Latin America, from Mexico to Argentina, numerous research groups—initially rooted in photonics and optical spectroscopy—have since the early 2000s undertaken investigations in the terahertz domain, particularly for materials-related applications.

In Mexico, several groups have made pioneering contributions to terahertz device development, imaging, and metamaterials, illustrating the early and sustained engagement of the region in THz materials science. Early reports on the creation of polaritonic metamaterials [173] demonstrated their broad potential for developing optical components such as lenses, beam splitters, polarizers, filters, and collimators at the Instituto de Física, Benemérita Universidad Autónoma de Puebla (BUAP).

More recent studies on semi-insulating GaAs substrates have revealed critical insights into the behavior of photoconductive antennas (PCAs) used in THz-TDS. Work from the Instituto Nacional de Astrofísica, Óptica y Electrónica (INAOE) in Puebla showed that the parameters of the pump laser strongly affect the electrical response of photoconductive antennas [122]. In addition, surface modifications and their influence on THz emission spectra were investigated in collaboration with groups at the Universidad Nacional Autónoma de México (UNAM) [174].

Beyond device engineering, the Puebla group advanced THz imaging in collaboration with the Instituto de Ciencias Aplicadas y Tecnología (ICAT) at UNAM. They developed a continuous-wave sub-wavelength THz imaging system that combined solid-immersion microscopy with interferometric detection, achieving spatial resolution beyond the diffraction limit at 703 GHz using low-cost pyroelectric detectors [175]. They also studied the transmission properties of photonic crystals immersed in different oils using THz-TDS, demonstrating that the effective refractive index is highly sensitive to the surrounding dielectric environment [123]. These results highlight the potential of THz photonic crystals for chemical sensing and for precise control of optical properties in metamaterial design. Additional research at ICAT-UNAM has focused on the application of THz spectroscopy for detecting pollutant dyes in aqueous environments [176]. Likewise, the Laboratorio Nacional de Ciencia y Tecnologia de Terahertz at the Centro de Investigaciones en óptica (CIO) in León has developed applications of terahertz scattering to study water absorption in porous rock samples [177].

Significant advances have also been achieved in Chile; the research teams at the ANID laboratory and the Departments of Physics of the Pontificia Universidad Católica de Chile (UC) and Universidad de Santiago de Chile (USACH) have proposed metal-organic framework (MOF) crystals as promising candidates for nonlinear THz photonics [178].

In Argentina, related research has been undertaken at the Centro de Investigaciones Ópticas (CIOp) [179]. New methods have been proposed to determine the optical properties of materials from a single measurement, eliminating the need for a conventional reference measurement in THz-TDS [180]. This simplification addresses a key practical limitation, as performing two separate measurements can be time-consuming or impractical for industrial applications. This was demonstrated specifically for a pulsed THz signal. In this case, the average refractive index is obtained through the following processing steps: the main pulse and at least one echo are measured in the time domain. The absolute value of the discrete Fourier transform is then applied, producing a frequency-domain modulation, whose period depends on the phase shift between the transmitted and reflected signals. A second discrete Fourier transform (absolute value) is applied to this modulation, yielding a time signal, where a peak appears at a delay related to the optical path inside the sample. Assuming a constant refractive

index and constant incident electromagnetic field magnitude in the frequency domain, the resulting signal can be expressed as a Dirac delta distribution located at a time shift proportional to the refractive index. Extensions of this method were later proposed for birefringent and multilayer materials [181, 182], enabling the determination of refractive indices and optical-axis orientation in birefringent systems, as well as thickness and average refractive indices in multilayer dielectrics, all from minimal measurement sets. These approaches significantly streamline industrial THz characterization workflows.

Signal processing has also been a focus of Argentine research. At the Centro de Simulación Computacional (CSC) in Buenos Aires, parametric methods have been proposed to enhance the extraction of optical parameters from THz time-domain signals [183]. In particular, the autoregressive (AR) model has been applied to estimate the THz power spectral density. Compared to conventional fast Fourier transform (FFT) analysis, AR spectral estimation does not assume signal periodicity and can provide improved frequency resolution compared to FFT for a given signal length when the signal is well described by the AR model. The achievable resolution is not determined solely by signal length, as in the FFT case, but also depends on other factors such as signal-to-noise ratio and model order selection. Another advantage of the AR model is that it yields a consistent estimator whose variance decreases with an increasing number of measurements. The results showed that applying this model to terahertz signals led to a reduction in spectral variance exceeding 10 dB compared to FFT-based results, thereby improving the signal-to-noise ratio and frequency resolution without experimental modification, an advance that enhances the precision and reliability of THz spectral analysis.

In Brazil, early THz work at the Instituto de Física Gleb Wataghin (IFGW) da Universidade Estadual de Campinas (UNICAMP) focused on terahertz generation between 2007 and 2008 [184, 185] and on imaging systems using monochromatic sources in 2013 [186]. Since 2016, this group has developed terahertz dual-frequency comb spectroscopy, achieving high spectral resolution without compromising bandwidth [97], as discussed in the first section of this review. Brazilian groups have also reported numerous THz-TDS applications. At the IFGW and at the Instituto de Química da UNICAMP, THz-TDS has been extensively used as an analytical tool [187–192]. Technological developments at IFGW proposed the fabrication of a plasmon-induced tunable metasurface for multiband superabsorption and terahertz sensing [193]. The group also investigated the development of optical fibers, for applications such as terahertz waveguides, that are essential for developing the full potential of complex terahertz systems [194]. Furthermore, engineering-oriented studies have explored terahertz imaging for applications such as analyzing dental tissues and detecting structural anomalies at the Universidade Federal de Pernambuco (UFPE) [195].

THz nano-imaging and nanospectroscopy have been established at the Brazilian Synchrotron in the Centro Nacional de Pesquisa em Energia e Materiais (CNPEM) in Campinas. Recent facility papers and beamline reports describe nanospectroscopy stations with broadband coverage from the mid-IR to the far-IR/THz region, validating this approach for nanoscale THz experiments. Notable results include the demonstration of sub-diffractional cavity modes and phonon-polaritons in nanobelts [103] and several studies on hyperbolic phonon-polaritons [196] and nanocavities in anisotropic

crystals [197, 198], collectively showcasing the leadership in THz nanospectroscopy of the laboratory in the region.

At the Instituto de Física da Universidade de São Paulo (USP), recent implementation of several terahertz-related facilities reflects the global expansion of terahertz science, driven by technological breakthroughs and increasing interdisciplinary demand. THz-TDS forms the basis of the experimental infrastructure at the Terahertz Science, Technology, and Innovation Research Group (GCTI-THz/USP). The first setup developed by this group employs a transmission-based THz-TDS system using PCAs, achieving an excellent signal-to-noise ratio across 0.1–2 THz. The setup includes an optical cryostat enabling measurements between 10 and 300 K with millimeter-scale spatial resolution [199]. Polarization-resolved components allow for high-precision THz polarimetry [200], as shown in Fig. 13. The group has recently established a second multi-user facility, extending its spectral range to 0.1–6 THz and enabling THz imaging in both transmission and reflection geometries. Complemented

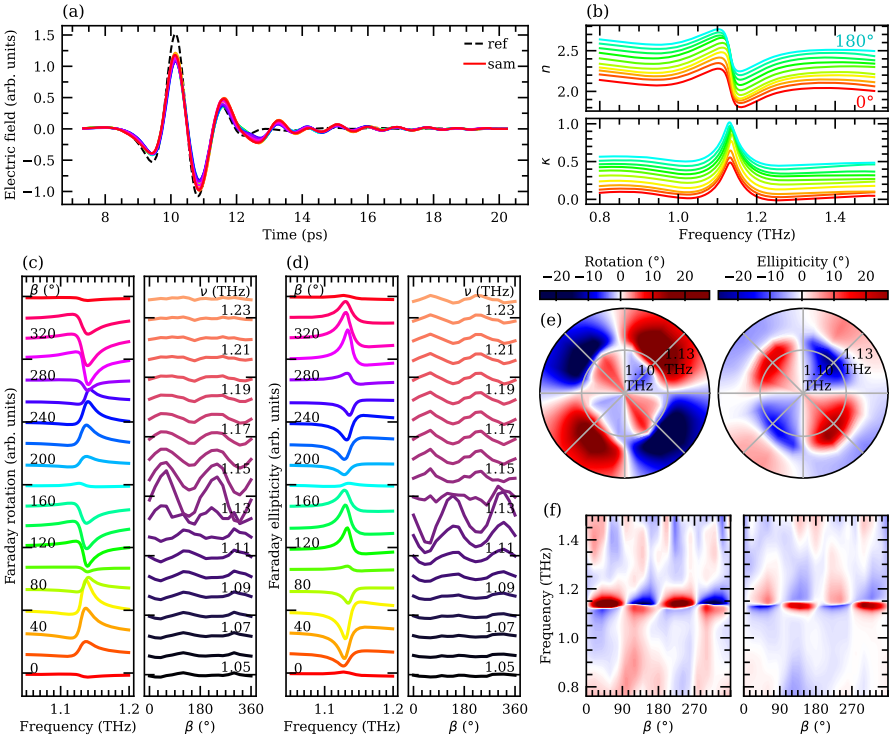

Fig. 13 Example of THz-TDS measurement in clinoclore using the GCTI-THz/USP setup. The system supports low-temperature measurements (down to 10 K) and high-precision terahertz polarimetry, with spatial resolution approaching the diffraction limit across 0.1–2 THz. **a** Time-domain signals for different sample orientations β (solid) and a reference (dashed). **b** Extracted refractive index n and extinction coefficient κ for β between 0° and 180°. **c** Faraday rotation and **d** ellipticity versus β and frequency ν. **e** Polar and **f** Cartesian projections of rotation (left) and ellipticity (right) maps, highlighting the polarization-dependent symmetries. Data in **b**–**d** are vertically offset for clarity. Reproduced under the CC-BY-NC-ND 4.0 from [205]. Copyright ©The Authors

by a high-energy amplified laser (2 mJ pulses at 1 kHz) for optical pump-THz probe studies, this system supports time-resolved investigations of ultrafast processes. The researchers are now integrating a 7 T superconducting magnet operating down to 1.5 K, which will enable exploration of magneto-optical effects, field-induced phase transitions, and emergent topological phenomena in the THz regime. Implementation details are documented in recent theses [199–202] and technical reports [203, 204].

Initial studies characterized the terahertz permittivity of epitaxial lead telluride (PbTe) thin films—thermoelectric materials with complex phonon dynamics [199, 206]. THz-TDS measurements across a broad temperature range provided direct access to low-frequency optical phonon modes and free-carrier dynamics, revealing temperature-dependent softening of the transverse optical phonon consistent with incipient ferroelectricity. Modeling with a Lorentz-Drude approach enabled the extraction of plasma frequencies, damping constants, and phonon coupling strengths, thereby disentangling electronic and lattice contributions to the dielectric function and revealing strong anharmonicity and dynamic lattice instabilities in PbTe thin films.

More recent work has focused on PbTe-SnTe alloys, which exhibit both topological and structural phase transitions [201, 207]. In $Pb_{(1-x)}Sn_xTe$ crystals, substitution of Pb by Sn induces a continuous evolution from a trivial semiconductor to a topological crystalline insulator, accompanied by a ferroelectric-like (polar) distortion. THz-TDS measurements revealed strong coupling between free carriers and soft transverse optical phonons, with marked changes across composition- and temperature-driven phase boundaries. This coupling is particularly sensitive to inversion-symmetry breaking, manifesting as mode splitting and circular dichroism under magnetic fields [163, 164], as well as the formation of phonon-polaritons in THz resonant cavities [208].

In collaboration with the CNPEM and the Universidade Federal de Lavras (UFLA), another research focus of the group at USP has been THz polarimetry of layered minerals exhibiting strong anisotropic interactions. A notable case is clinoclore, a naturally occurring van der Waals crystal that hosts low-energy shear modes with remarkable potential for THz polarization control [200, 205]. By employing polarization-resolved THz-TDS, these vibrational modes were shown to induce distinct birefringent responses, which were quantitatively modeled using Jones matrix analysis. These results establish natural layered minerals as versatile model systems for investigating and engineering THz polarization phenomena.

A researcher from the Instituto Nacional de Telecomunicações (Inatel), now affiliated with the Universidade Federal do ABC (UFABC), has made extensive contributions to establishing 3D printing as a viable route for scalable, low-cost THz components. In particular, focusing grating couplers [209], prisms with tunable dispersion [210], and rectangular waveguides [211] have been fabricated using this approach. He has also investigated the accurate determination of liquid material parameters using THz-TDS [212]. In parallel, the USP group developed 3D-printed polymer photonic crystals functioning as narrowband THz wave plates [202, 213]. Designed for operation around 0.5 THz, these structures exploit artificial birefringence enabled by subwavelength geometries, demonstrating additive manufacturing as a viable approach for polarization control in the sub-terahertz regime.

To provide a structured overview of the chronological evolution and institutional breadth of terahertz materials research in Latin America, the key milestones discussed

above are summarized in Table 4. The table highlights the progression from early THz generation and spectroscopy developments to advanced nanospectroscopy, additive manufacturing, and quantum materials investigations.

6.2 Conclusions and Outlook

Terahertz research in Latin America has progressed from foundational instrumentation efforts to sophisticated investigations of materials and light-matter interactions. Regional groups now operate advanced THz-TDS under extreme conditions and nano-THz platforms to study phonons, polaritons, and collective excitations in semiconductors, quantum materials, layered minerals, and photonic structures.

With expanding facilities and increasing international collaborations, the region demonstrates growing scientific maturity and global visibility. Continued integration

Table 4 Chronological milestones in terahertz materials research in Latin America

Years	Institution	Research theme	Reference
2007–2008	UNICAMP (Brazil)	THz laser sources and generation	[184, 185]
2011–2015	CIOp, CSC (Argentina)	THz-TDS methodology and signal processing	[179–183]
2012	BUAP (Mexico)	THz polaritonic metamaterials	[173]
2013–2016	UNICAMP (Brazil)	THz imaging and dual-frequency comb spectroscopy	[97, 186]
2017	UFPE (Brazil)	THz imaging systems and engineering applications	[195]
2014–2024	UNICAMP (Brazil)	Analytical THz spectroscopy (oxides, polymers, sugars, gases)	[187, 189–192]
2017	CIO (Mexico)	THz scattering and porosimetry	[177]
2017–2019	INATEL (Brazil)	3D-printed THz components and waveguides	[209–211]
2020	UNICAMP (Brazil)	Graphene metasurfaces and THz optical fibers	[193, 194]
2020–2026	CNPEM (Brazil)	THz nanospectroscopy and phonon–polaritons	[104, 196–198]
2021	INAOE, UNAM (Mexico)	GaAs-based THz photoconductive devices	[122, 174]
2022	BUAP, UNAM (Mexico)	THz photonic crystal sensing	[123]
2022–2026	USP (Brazil)	Magneto-THz infrastructure, polarimetry, and quantum materials	[163, 203, 205–207, 213]
	UNAM (Mexico)	Environmental THz sensing	[176]
2025	UC, USACH (Chile)	Nonlinear THz photonics	[178]

of materials design, modeling, and experimental innovation will be essential to consolidate Latin America's position in the global THz research landscape.

7 Final Remarks

In this article, we provided an overview of research activities involving terahertz and millimeter waves in Latin America. We aimed to offer a broad perspective on the most recurrent topics investigated and published in the region, although an exhaustive review is beyond the scope of a compact article. The authors of this review encourage other researchers from the region to get in touch to collaborate, share facilities and experiences, and perhaps organize a regional meeting in the future. We also sought to provide perspectives on future research directions that could see significant contributions from the region.

No doubt, the most productive research topic in Latin America is radio astronomy, partly due to the presence of multiple radio telescopes in the region, including two of the largest instruments of this type in the world, and it is foreseeable that this area of research will remain extremely productive in the future. Furthermore, the rich cultural heritage of the region calls for much more active involvement of terahertz groups in artifact inspection and restoration guidance, which can also benefit the conservation community. Additionally, applications in industrial and agronomical non-destructive testing represent a clear area of opportunity, as a growing industrial sector increasingly demands more sophisticated quality-control technologies. Finally, basic research on sources, detectors, and new materials may also become a major growth area, given the number of groups now capable of fabricating advanced materials and structures, as well as a broad theoretical community that can support such research.

We note that, although still modest, the number of groups interested in this field in Latin America has grown considerably over the last decade and is expected to accelerate further over the next few years. We look forward to the consolidation of a strong research community in this part of the world.

Author Contribution E. C. wrote the introductory section. Other authors contributed equally to this review.

Funding R.O.F. acknowledges the Brazilian Ministry of Science, Technology, and Innovation (MCTI) for supporting the construction and operation of the Sirius accelerator, an open-access user facility of the Brazilian Synchrotron Light Laboratory (LNLS) at the Brazilian Center for Research in Energy and Materials (CNPEM). The São Paulo Research Foundation (FAPESP) is also acknowledged for its partial support toward the construction of the TATU endstation (grants 2019/14017-9 and 2024/09159-7), as well as the National Council for Scientific and Technological Development (CNPq) for additional funding (grant 300197/2025-0).
F.G.G.H acknowledges financial support from FAPESP, Grants Nos. 2021/12470-8, 2023/04245-0, and 2023/16742-8, from Grant Nos. 409245/2022-4 and 306550/2023-7 of the CNPq, scholarships for graduate students and posdoctoral researchers from FAPESP, CNPq, and from the Brazilian Federal Agency for Support and Evaluation of Graduate Education (CAPES), and scholarships for undergraduate students from the iniciação científica programs of the Universidade de São Paulo.
N.Q. acknowledges funding from DGAPA-UNAM: PAPIIT 101424.

Data Availability No datasets were generated or analysed during the current study.

Declarations

Ethical Approval No ethics committee was required for the preparation of this manuscript.

Conflict of Interest The authors declare no competing interests.

References

1. Moulton, P.F.: Spectroscopic and laser characteristics of ti: Al2o3. Journal of the Optical Society of America B **3**(1), 125–133 (1986)
2. Auston, D.H., Cheung, K.: Coherent time-domain far-infrared spectroscopy. Journal of the Optical Society of America B **2**(4), 606–612 (1985)
3. Faist, J., Capasso, F., Sivco, D.L., Sirtori, C., Hutchinson, A.L., Cho, A.Y.: Quantum cascade laser. Science **264**(5158), 553–556 (1994)
4. Tonouchi, M.: Cutting-edge terahertz technology. Nature photonics **1**(2), 97–105 (2007)
5. Wikipedia contributors: List of countries by GDP (nominal). https://en.wikipedia.org/wiki/List_of_countries_by_GDP_(nominal). Accessed: February 25, 2026 (2026)
6. Wikipedia contributors: List of sovereign states by research and development spending. https://en.wikipedia.org/wiki/List_of_sovereign_states_by_research_and_development_spending. Accessed: February 25, 2026 (2026)
7. Event Horizon Telescope Collaboration, Akiyama, K., Alberdi, A., Alef, W., Asada, K., Azulay, R., Baczko, A.-K., Ball, D., Baloković, M., Barrett, J., Bintley, D., Blackburn, L., Boland, W., Bouman, K.L., Bower, G.C., Bremer, M., Brinkerink, C.D., Brissenden, R., Britzen, S., Broderick, A.E., Broguiere, D., Bronzwaer, T., Byun, D.-Y., Carlstrom, J.E., Chael, A., Chan, C.-k., Chatterjee, S., Chatterjee, K., Chen, M.-T., Chen, Y., Cho, I., Christian, P., Conway, J.E., Cordes, J.M., Crew, G.B., Cui, Y., Davelaar, J., De Laurentis, M., Deane, R., Dempsey, J., Desvignes, G., Dexter, J., Doeleman, S.S., Eatough, R.P., Falcke, H., Fish, V.L., Fomalont, E., Fraga-Encinas, R., Freeman, W.T., Friberg, P., Fromm, C.M., Gómez, J.L., Galison, P., Gammie, C.F., García, R., Gentaz, O., Georgiev, B., Goddi, C., Gold, R., Gu, M., Gurwell, M., Hada, K., Hecht, M.H., Hesper, R., Ho, L.C., Ho, P., Honma, M., Huang, C.-W.L., Huang, L., Hughes, D.H., Ikeda, S., Inoue, M., Issaoun, S., James, D.J., Jannuzi, B.T., Janssen, M., Jeter, B., Jiang, W., Johnson, M.D., Jorstad, S., Jung, T., Karami, M., Karuppusamy, R., Kawashima, T., Keating, G.K., Kettenis, M., Kim, J.-Y., Kim, J., Kim, J., Kino, M., Koay, J.Y., Koch, P.M., Koyama, S., Kramer, M., Kramer, C., Krichbaum, T.P., Kuo, C.-Y., Lauer, T.R., Lee, S.-S., Li, Y.-R., Li, Z., Lindqvist, M., Liu, K., Liuzzo, E., Lo, W.-P., Lobanov, A.P., Loinard, L., Lonsdale, C., Lu, R.-S., MacDonald, N.R., Mao, J., Markoff, S., Marrone, D.P., Marscher, A.P., Martí-Vidal, I., Matsushita, S., Matthews, L.D., Medeiros, L., Menten, K.M., Mizuno, Y., Mizuno, I., Moran, J.M., Moriyama, K., Moscibrodzka, M., Müller, C., Nagai, H., Nagar, N.M., Nakamura, M., Narayan, R., Narayanan, G., Natarajan, I., Neri, R., Ni, C., Noutsos, A., Okino, H., Olivares, H., Ortiz-León, G.N., Oyama, T., Özel, F., Palumbo, D.C.M., Patel, N., Pen, U.-L., Pesce, D.W., Piétu, V., Plambeck, R., PopStefanija, A., Porth, O., Prather, B., Preciado-López, J.A., Psaltis, D., Pu, H.-Y., Ramakrishnan, V., Rao, R., Rawlings, M.G., Raymond, A.W., Rezzolla, L., Ripperda, B., Roelofs, F., Rogers, A., Ros, E., Rose, M., Roshanineshat, A., Rottmann, H., Roy, A.L., Ruszczyk, C., Ryan, B.R., Rygl, K.L.J., Sánchez, S., Sánchez-Arguelles, D., Sasada, M., Savolainen, T., Schloerb, F.P., Schuster, K.-

F., Shao, L., Shen, Z., Small, D., Sohn, B.W., SooHoo, J., Tazaki, F., Tiede, P., Tilanus, R.P.J., Titus, M., Toma, K., Torne, P., Trent, T., Trippe, S., Tsuda, S., van Bemmel, I., van Langevelde, H.J., van Rossum, D.R., Wagner, J., Wardle, J., Weintroub, J., Wex, N., Wharton, R., Wielgus, M., Wong, G.N., Wu, Q., Young, K., Young, A.: First M87 Event Horizon Telescope Results. I. The Shadow of the Supermassive Black Hole. ApJL **875**(1), 1 (2019). https://doi.org/10.3847/2041-8213/ab0ec7 arXiv:1906.11238 [astro-ph.GA]

8. Event Horizon Telescope Collaboration, Akiyama, K., Alberdi, A., Alef, W., Algaba, J.C., Anantua, R., Asada, K., Azulay, R., Bach, U., Baczko, A.-K., Ball, D., Baloković, M., Barrett, J., Bauböck, M., Benson, B.A., Bintley, D., Blackburn, L., Blundell, R., Bouman, K.L., Bower, G.C., Boyce, H., Bremer, M., Brinkerink, C.D., Brissenden, R., Britzen, S., Broderick, A.E., Broguiere, D., Bronzwaer, T., Bustamante, S., Byun, D.-Y., Carlstrom, J.E., Ceccobello, C., Chael, A., Chan, C.-k., Chatterjee, K., Chatterjee, S., Chen, M.-T., Chen, Y., Cheng, X., Cho, I., Christian, P., Conroy, N.S., Conway, J.E., Cordes, J.M., Crawford, T.M., Crew, G.B., Cruz-Osorio, A., Cui, Y., Davelaar, J., De Laurentis, M., Deane, R., Dempsey, J., Desvignes, G., Dexter, J., Dhruv, V., Doeleman, S.S., Dougal, S., Dzib, S.A., Eatough, R.P., Emami, R., Falcke, H., Farah, J., Fish, V.L., Fomalont, E., Ford, H.A., Fraga-Encinas, R., Freeman, W.T., Friberg, P., Fromm, C.M., Fuentes, A., Galison, P., Gammie, C.F., García, R., Gentaz, O., Georgiev, B., Goddi, C., Gold, R., Gómez-Ruiz, A.I., Gómez, J.L., Gu, M., Gurwell, M., Hada, K., Haggard, D., Haworth, K., Hecht, M.H., Hesper, R., Heumann, D., Ho, L.C., Ho, P., Honma, M., Huang, C.-W.L., Huang, L., Hughes, D.H., Ikeda, S., Impellizzeri, C.M.V., Inoue, M., Issaoun, S., James, D.J., Jannuzi, B.T., Janssen, M., Jeter, B., Jiang, W., Jiménez-Rosales, A., Johnson, M.D., Jorstad, S., Joshi, A.V., Jung, T., Karami, M., Karuppusamy, R., Kawashima, T., Keating, G.K., Kettenis, M., Kim, D.-J., Kim, J.-Y., Kim, J., Kim, J., Kino, M., Koay, J.Y., Kocherlakota, P., Kofuji, Y., Koch, P.M., Koyama, S., Kramer, C., Kramer, M., Krichbaum, T.P., Kuo, C.-Y., La Bella, N., Lauer, T.R., Lee, D., Lee, S.-S., Leung, P.K., Levis, A., Li, Z., Lico, R., Lindahl, G., Lindqvist, M., Lisakov, M., Liu, J., Liu, K., Liuzzo, E., Lo, W.-P., Lobanov, A.P., Loinard, L., Lonsdale, C.J., Lu, R.-S., Mao, J., Marchili, N., Markoff, S., Marrone, D.P., Marscher, A.P., Martí-Vidal, I., Matsushita, S., Matthews, L.D., Medeiros, L., Menten, K.M., Michalik, D., Mizuno, I., Mizuno, Y., Moran, J.M., Moriyama, K., Moscibrodzka, M., Müller, C., Mus, A., Musoke, G., Myserlis, I., Nadolski, A., Nagai, H., Nagar, N.M., Nakamura, M., Narayan, R., Narayanan, G., Natarajan, I., Nathanail, A., Fuentes, S.N., Neilsen, J., Neri, R., Ni, C., Noutsos, A., Nowak, M.A., Oh, J., Okino, H., Olivares, H., Ortiz-León, G.N., Oyama, T., Özel, F., Palumbo, D.C.M., Paraschos, G.F., Park, J., Parsons, H., Patel, N., Pen, U.-L., Pesce, D.W., Piétu, V., Plambeck, R., PopStefanija, A., Porth, O., Pötzl, F.M., Prather, B., Preciado-López, J.A., Psaltis, D.: First Sagittarius A* Event Horizon Telescope Results. I. The Shadow of the Supermassive Black Hole in the Center of the Milky Way. ApJL **930**(2), 12 (2022). https://doi.org/10.3847/2041-8213/ac6674
9. Breakthrough Prize: Winners Of The 2020 Breakthrough Prize In Life Sciences, Fundamental Physics And Mathematics Announced. https://breakthroughprize.org/News/54. Accessed: March 5, 2026 (2019)
10. European Southern Observatory: Breakthrough Prize in Fundamental Physics awarded to the Event Horizon Telescope Collaboration. https://www.eso.org/public/czechrepublic/announcements/ann19043/?lang. Accessed: March 5, 2026 (2019)
11. Large Millimeter Telescope: September 5th, 2019: the EHT has been awarded the 2020 Breakthrough Prize in Fundamental Physics. https://lmtgtm.org/september-5th-2019-the-eht-has-been-awarded-the-2020-breakthrough-prize-in-fundamental-physics. Accessed: March 5, 2026 (2019)
12. Wilson, G.W., *et al.*: The AzTEC mm-wavelength camera. Monthly Notices of the Royal Astronomical Society **386**, 807–818 (2008). https://doi.org/10.1111/j.1365-2966.2008.12980
13. Hughes, D., Schloerb, F.P., Aretxaga, I., et al.: The Large Millimeter Telescope (LMT) Alfonso Serrano: current status and telescope performance. Proceedings Volume 11445, Ground-based and Airborne Telescopes VIII **1144522** (2020). https://doi.org/10.1117/12.2561893
14. Schwan, D., *et al.*: Millimeter-wave bolometer array receiver for the Atacama Pathfinder Experiment Sunyaev-Zeldovich (APEX-SZ) instrument. Rev. Sci. Instrum. **82**, 091301 (2011). https://doi.org/10.1063/1.3637460
15. Tapia, M.B., Ade, P.A.R., Pérez, E.A., *et al.*: Mexico-UK Submillimeter Camera for AsTronomy focal plane performance at the Large Millimeter Telescope. Journal of Astronomical Telescopes, Instruments, and Systems **10**, 045003 (2024). https://doi.org/10.1117/1.JATIS.10.4.045003
16. Gómez Rivera, V.H.: Estudio de Detectores de Inductancia Cinética para Medición de Radiación Milimétrica. Instituto Nacional de Astrofísica, Óptica y Electrónica (INAOE). Ph.D. Thesis (2020)

17. Gómez-Rivera, V., et al.: Design and characterization of the MUSCAT detectors. Proc. SPIE 11453, Millimeter, Submillimeter, and Far-Infrared Detectors and Instrumentation for Astronomy X **114531Q** (2020). https://doi.org/10.1117/12.2576334
18. Wilson, G.W., Abi-Saad, S., Ade, P., et al.: The TolTEC camera: an overview of the instrument and in-lab testing results. Proc. SPIE 11453, Millimeter, Submillimeter, and Far-Infrared Detectors and Instrumentation for Astronomy X **1145302** (2020). https://doi.org/10.1117/12.2562331
19. Huang, Y.-D., Hwang, Y.-J., Chiong, C.-C., Yen, H.-W., Koch, P.M., Huang, C.-D., Liu, B., Chen, C.L., Tsai, J.J., Hsiung, W.-L., Chi, L.-P., Ho, C.-T., Wang, C.-C., Chien, C., Chu, Y.-H., Ho, P., Kemper, F., Morata, O., Gonzalez, A., Iguchi, S., Uzawa, Y., Iono, D., Nagai, H., Effland, J., Saini, K., Pospieszalski, M., Henke, D., Yeung, K., Finger, R., Tapia, V., Reyes, N., Siringo, G., Marconi, G., Cabezas, R.: ALMA Band-1 (35-50GHz) receiver: first light, performance, and road to completion. Millimeter, Submillimeter, and Far-Infrared Detectors and Instrumentation for Astronomy XI, SPIE **12190** (2022). https://doi.org/10.1117/12.2629766
20. Yagoubov, P., Mroczkowski, T., Belitsky, V., Cuadrado-Calle, D., Cuttaia, F., Fuller, G.A., Gallego, J.-D., Gonzalez, A., Kaneko, K., Mena, P., Molina, R., Nesti, R., Tapia, V., Villa, F., Beltrán, M., Cavaliere, F., Ceru, J., Chesmore, G.E., Coughlin, K., De Breuck, C., Fredrixon, M., George, D., Gibson, H., Golec, J., Josaitis, A., Kemper, F., Kotiranta, M., Lapkin, I., López-Fernández, I., Marconi, G., Mariotti, S., McGenn, W., McMahon, J., Murk, A., Pezzotta, F., Phillips, N., Reyes, N., Ricciardi, S., Sandri, M., Strandberg, M., Terenzi, L., Testi, L., Thomas, B., Uzawa, Y., Viganò, D., Wadefalk, N.: Wideband 67-116 GHz receiver development for ALMA Band 2. Astronomy & Astrophysics **634**, 46 (2020). https://doi.org/10.1051/0004-6361/201936777 arXiv:1912.10841 [astro-ph.IM]
21. Claude, S., Jiang, F., Niranjanan, P., Dindo, P., Erickson, D., Yeung, K., Derdall, D., Duncan, D., Garcia, D., Leckie, B., Pfleger, M., Rodrigues, G., Szeto, K., Welle, P., Wood, I., Caputa, K., Lichtenberger, A., Pan, S.-K.: Performance of the pre-production band 3 (84-116 GHz) receivers for ALMA. Millimeter and Submillimeter Detectors and Instrumentation for Astronomy IV, SPIE **7020** (2008). https://doi.org/10.1117/12.788128
22. Arnal, E.M., Abraham, Z., Cappa, C., Castro, G., Pino, E.M., Larrarte, J.J., Lepine, J., Viramonte, J.: LLAMA: A new mm and submm observing facility. Revista Mexicana de Astronomía y Astrofísica (Serie de Conferencias) **49** (2017)
23. Romero, G.E.: Large Latin American Millimeter Array. Science Reviews from the end of the world. **1** (2020). https://doi.org/10.48550/arXiv.2010.00738
24. Swetz, D.S., Ade, P.A.R., Amiri, M., et al.: Overview of the Atacama Cosmology Telescope: Receiver, Instrumentation, and Telescope System. The Astrophysical Journal Supplement Series **194-2** (2011). https://doi.org/10.1088/0067-0049/194/2/41
25. Ade, P., Aguirre, J., Ahmed, Z., et al.: The Simons Observatory: science goals and forecasts. Journal of Cosmology and Astroparticle Physics **2019** (2019). https://doi.org/10.1088/1475-7516/2019/02/056
26. Selina, R.J., Murphy, E.J., McKinnon, M., et al.: The Next-Generation Very Large Array: a technical overview. Proc. SPIE 10700, Ground-based and Airborne Telescopes VII **107001O** (2018). https://doi.org/10.1117/12.2312089
27. Richards, P.L.: Bolometers for infrared and millimeter waves. J. Appl. Phys. **76** (1994). https://doi.org/10.1063/1.357128
28. Lee, A.T., Richards, P.L., Nam, S.W., Cabrera, B., Irwin, K.D.: A superconducting bolometer with strong electrothermal feedback. Appl. Phys. Lett. **69** (1996). https://doi.org/10.1063/1.117491
29. Irwin, K.D., Hilton, G.C.: Transition-edge sensors. https://doi.org/10.1007/10933596_3 (2005)
30. Mazin, B.A.: Microwave Kinetic Inductance Detectors: The First Decade. AIP Conf. Proc. **1185** (2009). https://doi.org/10.1063/1.3292300
31. Doyle, S., Mauskopf, P., Naylon, J., Porch, A., Duncomb, C.: Lumped Element Kinetic Inductance Detectors. Journal of Low Temperature Physics **151** (2008). https://doi.org/10.1007/s10909-007-9685-2
32. Holland, W., Duncan, W., Kelly, B., *et al.*: SCUBA-2: a large-format submillimeter camera on the James Clerk Maxwell Telescope. Proceedings Volume 4855, Millimeter and Submillimeter Detectors for Astronomy (2003). https://doi.org/10.1117/12.459152
33. Swetz, D., Ade, P.A.R., Allen, C., et al.: Instrument design and characterization of the Millimeter Bolometer Array Camera on the Atacama Cosmology Telescope. Proceedings Volume 7020, Millimeter and Submillimeter Detectors and Instrumentation for Astronomy IV **702008** (2008). https://doi.org/10.1117/12.789876

34. Benson, B., Ade, P.A., Ahmed, Z., et al.: SPT-3G: a next-generation cosmic microwave background polarization experiment on the South Pole telescope. Proceedings Volume 9153, Millimeter, Submillimeter, and Far-Infrared Detectors and Instrumentation for Astronomy VII **91531P** (2014). https://doi.org/10.1117/12.2057305
35. Irwin, K.D.: SQUID multiplexers for transition-edge sensors. Physica C: Superconductivity**368** (2002). https://doi.org/10.1016/S0921-4534(01)01167-4
36. Irwin, K.D.: Microwave SQUID multiplexer. Appl. Phys. Lett. **85** (2004). https://doi.org/10.1063/1.1791733
37. Calvo, M., Benoît, A., Catalano, A., et al.: The NIKA2 Instrument, A Dual-Band Kilopixel KID Array for Millimetric Astronomy. J Low Temp Phys **184** (2016). https://doi.org/10.1007/s10909-016-1582-0
38. Galitzki, N., Ade, P., Angilè, F., et al.: Instrumental performance and results from testing of the BLAST-TNG receiver, submillimeter optics, and MKID detector arrays. Proceedings Volume 9914, Millimeter, Submillimeter, and Far-Infrared Detectors and Instrumentation for Astronomy VIII **99140J** (2016). https://doi.org/10.1117/12.2231167
39. Carr, T.D., Lynch, M.A., Paul, M.P., Brown, G.W., May, J., Six, N.F., Robinson, V.M., Block, W.F.: Very long baseline interferometry of Jupiter at 18 MHz. Radio Sci **5** (1970). https://doi.org/10.1029/RS005i010p01223
40. Guzmán, A.E., May, J., Alvarez, H., Maeda, K.: All-sky Galactic radiation at 45 MHz and spectral index between 45 and 408 MHz. Astronomy and Astrophysics **525** (2011). https://doi.org/10.1051/0004-6361/200913628
41. Dame, T.M., Hartmann, D., Thaddeus, P.: The Milky Way in Molecular Clouds: A New Complete CO Survey. The Astrophysical Journal **547** (2001). https://doi.org/10.1086/31838823
42. May, J., Bronfman, L., Alvarez, H., Murphy, D.C., Thaddeus, P.: A deep CO survey of the third galactic quadrant. Astronomy and Astrophysics, Suppl. Ser. **99** (1993)
43. Bronfman, L., Alvarez, H., Cohen, R.S., Thaddeus, P.: A Deep CO Survey of Molecular Clouds in the Southern Milky Way. Astrophysical Journal Supplement **71** (1989). https://doi.org/10.1086/191384
44. Bitran, M., Alvarez, H., Bronfman, L., May, J., Thaddeus, P.: A large scale CO survey of the Galactic center region. A & A Supplement series **125** (1997). https://doi.org/10.1051/aas:1997214
45. Max-Moerbeck Astudillo, W.K.: Implementación de un oscilador Gunn en un receptor a 115 GHz, para fines radioastronoómicos. Tesis (ingeniero civil electricista) (2005). https://bibliotecadigital.uchile.cl/permalink/56UDC_INST/1fulsad/alma991004283899703936
46. Ramos Oliver, N.E.: Automatización de un Radiómetro para Medir la Opacidad Atmosférica a 115 GHZ. Tesis Pregrado (2009). https://repositorio.uchile.cl/handle/2250/103388
47. Reyes Guzmaán, N.A.: Integración física de un amplificador de bajo ruido a un receptor en 100 GHZ. Tesis (ingeniero civil electricista) (2006). https://bibliotecadigital.uchile.cl/permalink/56UDC_INST/1fulsad/alma991004619269703936
48. Vásquez Rosati, P.F.: Instalación y Puesta en Marcha del Radiotelescopio Mini. Tesis (ingeniero civil electricista) (2011). https://repositorio.uchile.cl/handle/2250/104334
49. Astudillo Alvarado, P.J.: Medición del patrón de radiacion del Telescopio Mini. Tesis Ingeniero Civil Eléctrico (2014). https://repositorio.uchile.cl/handle/2250/116317
50. Reyes, N., Zorzi, P., Mena, F.P., Granet, C., Michael, E., Bronfman, L., May, J.: Design of a Heterodyne Receiver for Band 1 of ALMA. Proceedings of the 20th International Symposium on Space Terahertz Technology. (2009)
51. Reyes, N., Zorzi, P., Jarufe, C., Altamirano, P., Mena, F.P., Pizarro, J., Bronfman, L., May, J., Granet, C., Michael, E.: Construction of a Heterodyne Receiver for Band 1 of ALMA. Twenty-First International Symposium on Space Terahertz Technology (2010)
52. Cubillos Jara, D.J.: Desarrollo de un receptor en configuración 2SB para banda W extendida (67-116 GHZ) con aplicaciones en el telescopio. Tesis para optar al grado de Doctora en Ingeniería Eléctrica (2023). https://doi.org/10.58011/7k3p-0470
53. Finger, R., Mena, P., Reyes, N., Rodriguez, R., Bronfman, L.: A Calibrated Digital Sideband Separating Spectrometer for Radio Astronomy Applications. Publications of the Astronomical Society of the Pacific **125** (2013). https://doi.org/10.1086/670175
54. Rodríguez, R., Finger, R., Mena, F.P., Reyes, N., Michael, E., Bronfman, L.: A Sideband-separating Receiver with a Calibrated Digital If-Hybrid Spectrometer for the Millimeter Band. Publications of the Astronomical Society of the Pacific **126** (2014). https://doi.org/10.1086/676307

55. Finger, R., Mena, F.P., Baryshev, A., Khudchenko, A., Rodriguez, R., Huaracan, E., Alvear, A., Barkhof, J., Hesper, R., Bronfman, L.: Ultra-pure digital sideband separation at sub-millimeter wavelengths. Astronomy & Astrophysics **584** (2015). https://doi.org/10.1051/0004-6361/201526503
56. Curotto, F., Finger, R., Kojima, T., Uemizu, K., González, Uzawa, Y., Bronfman, L.: Digital calibration test results for Atacama Large Millimeter/submillimeter Array band 7+8 sideband separating receiver. Journal of Astronomical Telescopes, Instruments, and Systems **8** (2022). https://doi.org/10.1117/1.JATIS.8.2.024004
57. Monasterio Lagos, D.A.: Diseño de un triplicador de frecuencia de 35 a 105 GHz basado en diodos Schottky. Tesis Ingeniero Civil Electricista (2012). https://repositorio.uchile.cl/handle/2250/112346
58. Montofre, D., Khudchenko, A., Mena, F.P., Hesper, R., Baryshev, A.M.: Single-Layer Dichroic Filters for Multifrequency Receivers at THz Frequencies. IEEE Transactions on Terahertz Science and Technology **10** (2020). https://doi.org/10.1109/TTHZ.2020.3025692
59. Jarufe, C., Rodriguez, R., Tapia, V., Astudillo, P., Monasterio, D., Molina, R., Mena, F.P., Reyes, L. Nicolas and; Bronfman: Optimized Corrugated Tapered Slot Antenna for mm-Wave Applications. IEEE Transactions on Antennas and Propagation **66** (2018). https://doi.org/10.1109/TAP.2018.2797534
60. Montofré, D.A., Molina, R., Khudchenko, A., Hesper, R., Baryshev, A.M., Reyes, N.: High-Performance Smooth-Walled Horn Antennas for THz Frequency Range: Design and Evaluation. IEEE Transactions on Terahertz Science and Technology **9** (2019). https://doi.org/10.1109/TTHZ.2019.2938985
61. Medina Porcile, C.: CCAT-prime telescope holography simulations and surface error analysis. Universidad de Chile. https://repositorio.uchile.cl/handle/2250/170183 (2019)
62. Monasterio, D., Jarufe, C., Gallardo, D., Reyes, N., Mena, F.P., Bronfman, L.: A Compact Sideband Separating Downconverter With Excellent Return Loss and Good Conversion Gain for the W Band. IEEE Transactions on Terahertz Science and Technology **9** (2019). https://doi.org/10.1109/TTHZ.2019.2937955
63. Monasterio, D., Jorquera, S., Curotto, F., Espinoza, C., Finger, R., Bronfman, L.: A Proof of Concept Balanced Mixer with the use of a Digital IF Power Combiner to Improve LO Noise Rejection. Publications of the Astronomical Society of the Pacific **135** (2023). https://doi.org/10.1088/1538-3873/ad0789
64. Gallardo, D., Finger, R., Solis, F., Monasterio, D., Jorquera, S., Pizarro, J., Riquelme, J., Curotto, F., Pizarro, F., Bronfman, L.: An Ultra-Wideband Dual Polarization Antenna Array for the Detection and Localization of Bright Fast Radio Transients in the Milky Way. eprint arXiv:2501.08764 (2025). https://doi.org/10.48550/arXiv.2501.08764
65. Vives, G., Manuel, D.S.J.: Development and characterization of a 2D, 700–2600 MHz receiver array, for the estimation of direction of arrival (DoA) in the frequency domain. https://repositorio.uchile.cl/handle/2250/205047 (2024)
66. Solís Garrido, F.A.: Assembly, integration and verification of an astronomy experiment for galactic fast radio burst detection. Universidad de Chile. Tesis (2024)
67. Morales Cabrera, Á.I.: Diseño, implementación y pruebas de un sistema de oscilador local y su sistema de control. Universidad de Chile. Tesis (2024)
68. Yun, M., Schloerb, F.P., Hughes, D., et al.: Scientific operation of the Large Millimeter Telescope. Proceedings Volume 13098, Observatory Operations: Strategies, Processes, and Systems X **130982I** (2024). https://doi.org/10.1117/12.3020561
69. Tamura, Y., Sakai, T., Kawabe, R., et al.: FINER: Far-Infrared Nebular Emission Receiver for the large millimeter telescope. Proc. SPIE 13102, Millimeter, Submillimeter, and Far-Infrared Detectors and Instrumentation for Astronomy XII **131020G** (2024). https://doi.org/10.1117/12.3017788
70. Redford, J., Barry, P.S., Bradford, C.M., *et al.*: SuperSpec: On-Chip Spectrometer Design, Characterization, and Performance. J. Low Temperature Physics **209**, 548–555 (2022). https://doi.org/10.1007/s10909-022-02866-x
71. Schouws, S., Bouwens, R.J., Ormerod, K., Smit, R., Algera, H., Sommovigo, L., Hodge, J., Ferrara, A., Oesch, P.A., Rowland, L.E., van Leeuwen, I., Stefanon, M., Herard-Demanche, T., Fudamoto, Y., Röttgering, H., van der Werf, P.: Detection of $[O\ III]_{88\mu m}$ in JADES-GS-z14-0 at z = 14.1793. ApJ **988**(1), 19 (2025). https://doi.org/10.3847/1538-4357/adbf1b arXiv:2409.20549 [astro-ph.GA]
72. Carniani, S., D'Eugenio, F., Ji, X., Parlanti, E., Scholtz, J., Sun, F., Venturi, G., Bakx, T.J.L.C., Curti, M., Maiolino, R., Tacchella, S., Zavala, J.A., Hainline, K., Witstok, J., Johnson, B.D., Alberts, S., Bunker, A.J., Charlot, S., Eisenstein, D.J., Helton, J.M., Jakobsen, P., Kumari, N., Robertson, B.,

Saxena, A., Übler, H., Williams, C.C., Willmer, C.N.A., Willott, C.: The eventful life of a luminous galaxy at z = 14: metal enrichment, feedback, and low gas fraction? A& A **696**, 87 (2025). https://doi.org/10.1051/0004-6361/202452451 arXiv:2409.20533 [astro-ph.GA]

73. ...Leroy, A.K., Schinnerer, E., Hughes, A., Rosolowsky, E., Pety, J., Schruba, A., Usero, A., Blanc, G.A., Chevance, M., Emsellem, E., Faesi, C.M., Herrera, C.N., Liu, D., Meidt, S.E., Querejeta, M., Saito, T., Sandstrom, K.M., Sun, J., Williams, T.G., Anand, G.S., Barnes, A.T., Behrens, E.A., Belfiore, F., Benincasa, S.M., Bešlić, I., Bigiel, F., Bolatto, A.D., den Brok, J.S., Cao, Y., Chandar, R., Chastenet, J., Chiang, I.-D., Congiu, E., Dale, D.A., Deger, S., Eibensteiner, C., Egorov, O.V., García-Rodríguez, A., Glover, S.C.O., Grasha, K., Henshaw, J.D., Ho, I.-T., Kepley, A.A., Kim, J., Klessen, R.S., Kreckel, K., Koch, E.W., Kruijssen, J.M.D., Larson, K.L., Lee, J.C., Lopez, L.A., Machado, J., Mayker, N., McElroy, R., Murphy, E.J., Ostriker, E.C., Pan, H.-A., Pessa, I., Puschnig, J., Razza, A., Sánchez-Blázquez, P., Santoro, F., Sardone, A., Scheuermann, F., Sliwa, K., Sormani, M.C., Stuber, S.K., Thilker, D.A., Turner, J.A., Utomo, D., Watkins, E.J., Whitmore, B.: PHANGS-ALMA: Arcsecond CO(2-1) Imaging of Nearby Star-forming Galaxies. ApJ Supp **257**(2), 43 (2021). https://doi.org/10.3847/1538-4365/ac17f3 arXiv:2104.07739 [astro-ph.GA]
74. Hacar, A., Tafalla, M., Forbrich, J., Alves, J., Meingast, S., Grossschedl, J., Teixeira, P.S.: An ALMA study of the Orion Integral Filament. I. Evidence for narrow fibers in a massive cloud. A& A **610**, 77 (2018). https://doi.org/10.1051/0004-6361/201731894 arXiv:1801.01500 [astro-ph.GA]
75. Tobin, J.J., Kratter, K.M., Persson, M.V., Looney, L.W., Dunham, M.M., Segura-Cox, D., Li, Z.-Y., Chandler, C.J., Sadavoy, S.I., Harris, R.J., Melis, C., Pérez, L.M.: A triple protostar system formed via fragmentation of a gravitationally unstable disk. Nature. **538**(7626), 483–486 (2016). https://doi.org/10.1038/nature20094 arXiv:1610.08524 [astro-ph.SR]
76. ALMA Partnership, Brogan, C.L., Pérez, L.M., Hunter, T.R., Dent, W.R.F., Hales, A.S., Hills, R.E., Corder, S., Fomalont, E.B., Vlahakis, C., Asaki, Y., Barkats, D., Hirota, A., Hodge, J.A., Impellizzeri, C.M.V., Kneissl, R., Liuzzo, E., Lucas, R., Marcelino, N., Matsushita, S., Nakanishi, K., Phillips, N., Richards, A.M.S., Toledo, I., Aladro, R., Broguiere, D., Cortes, J.R., Cortes, P.C., Espada, D., Galarza, F., Garcia-Appadoo, D., Guzman-Ramirez, L., Humphreys, E.M., Jung, T., Kameno, S., Laing, R.A., Leon, S., Marconi, G., Mignano, A., Nikolic, B., Nyman, L.-A., Radiszcz, M., Remijan, A., Rodón, J.A., Sawada, T., Takahashi, S., Tilanus, R.P.J., Vila Vilaro, B., Watson, L.C., Wiklind, T., Akiyama, E., Chapillon, E., de Gregorio-Monsalvo, I., Di Francesco, J., Gueth, F., Kawamura, A., Lee, C.-F., Nguyen Luong, Q., Mangum, J., Pietu, V., Sanhueza, P., Saigo, K., Takakuwa, S., Ubach, C., van Kempen, T., Wootten, A., Castro-Carrizo, A., Francke, H., Gallardo, J., Garcia, J., Gonzalez, S., Hill, T., Kaminski, T., Kurono, Y., Liu, H.-Y., Lopez, C., Morales, F., Plarre, K., Schieven, G., Testi, L., Videla, L., Villard, E., Andreani, P., Hibbard, J.E., Tatematsu, K.: The 2014 ALMA Long Baseline Campaign: First Results from High Angular Resolution Observations toward the HL Tau Region. ApJL **808**(1), 3 (2015). https://doi.org/10.1088/2041-8205/808/1/L3 arXiv:1503.02649 [astro-ph.SR]
77. Kim, H., Trejo, A., Liu, S.-Y., Sahai, R., Taam, R.E., Morris, M.R., Hirano, N., Hsieh, I.-T.: The large-scale nebular pattern of a superwind binary in an eccentric orbit. Nature Astronomy **1**, 0060 (2017). https://doi.org/10.1038/s41550-017-0060 arXiv:1704.00449 [astro-ph.SR]
78. Jørgensen, J.K., Müller, H.S.P., Calcutt, H., Coutens, A., Drozdovskaya, M.N., Öberg, K.I., Persson, M.V., Taquet, V., van Dishoeck, E.F., Wampfler, S.F.: The ALMA-PILS survey: isotopic composition of oxygen-containing complex organic molecules toward IRAS 16293-2422B. A& A **620**, 170 (2018). https://doi.org/10.1051/0004-6361/201731667 arXiv:1808.08753 [astro-ph.SR]
79. Öberg, K.I., Guzmán, V.V., Walsh, C., Aikawa, Y., Bergin, E.A., Law, C.J., Loomis, R.A., Alarcón, F., Andrews, S.M., Bae, J., Bergner, J.B., Boehler, Y., Booth, A.S., Bosman, A.D., Calahan, J.K., Cataldi, G., Cleeves, L.I., Czekala, I., Furuya, K., Huang, J., Ilee, J.D., Kurtovic, N.T., Le Gal, R., Liu, Y., Long, F., Ménard, F., Nomura, H., Pérez, L.M., Qi, C., Schwarz, K.R., Sierra, A., Teague, R., Tsukagoshi, T., Yamato, Y., van't Hoff, M.L.R., Waggoner, A.R., Wilner, D.J., Zhang, K.: Molecules with ALMA at Planet-forming Scales (MAPS). I. Program Overview and Highlights. ApJ Supp. **257**(1), 1 (2021). https://doi.org/10.3847/1538-4365/ac1432 arXiv:2109.06268 [astro-ph.EP]
80. Laskar, T., Alexander, K.D., Berger, E., Guidorzi, C., Margutti, R., Fong, W.-f., Kilpatrick, C.D., Milne, P., Drout, M.R., Mundell, C.G., Kobayashi, S., Lunnan, R., Barniol Duran, R., Menten, K.M., Ioka, K., Williams, P.K.G.: First ALMA Light Curve Constrains Refreshed Reverse Shocks and Jet Magnetization in GRB 161219B. ApJ **862**(2), 94 (2018). https://doi.org/10.3847/1538-4357/aacbcc arXiv:1808.09476 [astro-ph.HE]

81. Maeda, K., Michiyama, T., Chandra, P., Ryder, S., Kuncarayakti, H., Hiramatsu, D., Imanishi, M.: Resurrection of Type IIL Supernova 2018ivc: Implications for a Binary Evolution Sequence Connecting Hydrogen-rich and Hydrogen-poor Progenitors. ApJL **945**(1), 3 (2023). https://doi.org/10.3847/2041-8213/acb25e arXiv:2301.07357 [astro-ph.HE]
82. Cendes, Y., Alexander, K.D., Berger, E., Eftekhari, T., Williams, P.K.G., Chornock, R.: Radio Observations of an Ordinary Outflow from the Tidal Disruption Event AT2019dsg. ApJL **919**(2), 127 (2021). https://doi.org/10.3847/1538-4357/ac110a arXiv:2103.06299 [astro-ph.HE]
83. de Pater, I., Sault, R.J., Moeckel, C., Moullet, A., Wong, M.H., Goullaud, C., DeBoer, D., Butler, B.J., Bjoraker, G., Ádámkovics, M., Cosentino, R., Donnelly, P.T., Fletcher, L.N., Kasaba, Y., Orton, G.S., Rogers, J.H., Sinclair, J.A., Villard, E.: First ALMA Millimeter-wavelength Maps of Jupiter, with a Multiwavelength Study of Convection. AJ **158**(4), 139 (2019). https://doi.org/10.3847/1538-3881/ab3643 arXiv:1907.11820 [astro-ph.EP]
84. Palmer, M.Y., Cordiner, M.A., Nixon, C.A., Charnley, S.B., Teanby, N.A., Kisiel, Z., Irwin, P.G.J., Mumma, M.J.: ALMA detection and astrobiological potential of vinyl cyanide on Titan. Science Advances **3**(7), 1700022 (2017). https://doi.org/10.1126/sciadv.1700022
85. ALMA Partnership, Hunter, T.R., Kneissl, R., Moullet, A., Brogan, C.L., Fomalont, E.B., Vlahakis, C., Asaki, Y., Barkats, D., Dent, W.R.F., Hills, R.E., Hirota, A., Hodge, J.A., Impellizzeri, C.M.V., Liuzzo, E., Lucas, R., Marcelino, N., Matsushita, S., Nakanishi, K., Pérez, L.M., Phillips, N., Richards, A.M.S., Toledo, I., Aladro, R., Broguiere, D., Cortes, J.R., Cortes, P.C., Espada, D., Galarza, F., Garcia-Appadoo, D., Guzman-Ramirez, L., Hales, A.S., Humphreys, E.M., Jung, T., Kameno, S., Laing, R.A., Leon, S., Marconi, G., Mignano, A., Nikolic, B., Nyman, L.-A., Radiszcz, M., Remijan, A., Rodón, J.A., Sawada, T., Takahashi, S., Tilanus, R.P.J., Vila Vilaro, B., Watson, L.C., Wiklind, T., De Gregorio-Monsalvo, I., Di Francesco, J., Mangum, J., Francke, H., Gallardo, J., Garcia, J., Gonzalez, S., Hill, T., Kaminski, T., Kurono, Y., Lopez, C., Morales, F., Plarre, K., Randall, S., van kempen, T., Videla, L., Villard, E., Andreani, P., Hibbard, J.E., Tatematsu, K.: The 2014 ALMA Long Baseline Campaign: Observations of Asteroid 3 Juno at 60 Kilometer Resolution. ApJL **808**(1), 2 (2015). https://doi.org/10.1088/2041-8205/808/1/L2 arXiv:1503.02650 [astro-ph.EP]
86. Cordiner, M.A., Gibb, E.L., Kisiel, Z., Roth, N.X., Biver, N., Bockelée-Morvan, D., Boissier, J., Bonev, B.P., Charnley, S.B., Coulson, I.M., Crovisier, J., Drozdovskaya, M.N., Furuya, K., Jin, M., Kuan, Y.-J., Lippi, M., Lis, D.C., Milam, S.N., Opitom, C., Qi, C., Remijan, A.J.: A D/H ratio consistent with Earth's water in Halley-type comet 12P from ALMA HDO mapping. Nature Astronomy (2025). https://doi.org/10.1038/s41550-025-02614-7 arXiv:2508.05925 [astro-ph.EP]
87. Shimojo, M., Bastian, T.S., Hales, A.S., White, S.M., Iwai, K., Hills, R.E., Hirota, A., Phillips, N.M., Sawada, T., Yagoubov, P., Siringo, G., Asayama, S., Sugimoto, M., Brajša, R., Skokić, I., Bárta, M., Kim, S., de Gregorio-Monsalvo, I., Corder, S.A., Hudson, H.S., Wedemeyer, S., Gary, D.E., De Pontieu, B., Loukitcheva, M., Fleishman, G.D., Chen, B., Kobelski, A., Yan, Y.: Observing the Sun with the Atacama Large Millimeter/submillimeter Array (ALMA): High-Resolution Interferometric Imaging. Solar Physics **292**(7), 87 (2017). https://doi.org/10.1007/s11207-017-1095-2 arXiv:1704.03236 [astro-ph.SR]
88. Padin, S., Shepherd, M.C., Cartwright, J.K., et al.: The Cosmic Background Imager. Publications of the Astronomical Society of the Pacific **114** (2001). https://doi.org/10.1086/324786
89. Puchalla, J.L., R. Caldwell and, K.L.C., et al.: Millimeter-Wavelength Galactic Observations with the Mobile Anisotropy Telescope. The Astronomical Journal **123** (2002). https://doi.org/10.1086/339302
90. Essinger-Hileman, T., Appel, J.W., Beal, J.A., et al.: The Atacama B-Mode Search: CMB Polarimetry with Transition-Edge-Sensor Bolometers. AIP Conf. Proc **1185** (2009). https://doi.org/10.1063/1.3292387
91. Kermish, Z., Ade, P., Anthony, A., et al.: The POLARBEAR experiment. Proceedings Volume 8452, Millimeter, Submillimeter, and Far-Infrared Detectors and Instrumentation for Astronomy VI **84521C** (2012). https://doi.org/10.1117/12.926354
92. Essinger-Hileman, T., Ali, A., Amiri, M., et al.: CLASS: the cosmology large angular scale surveyor. Proceedings Volume 9153, Millimeter, Submillimeter, and Far-Infrared Detectors and Instrumentation for Astronomy VII **91531I** (2014). https://doi.org/10.1117/12.2056701
93. Güsten, R., Booth, R.S., Cesarsky, C., et al.: APEX: the Atacama Pathfinder EXperiment. Proc. SPIE 6267, Ground-based and Airborne Telescopes **626714** (2006). https://doi.org/10.1117/12.670798

94. Klaassen, P.D., Mroczkowski, T.K., Cicone, C., et al.: The Atacama Large Aperture Submillimeter Telescope (AtLAST). Proceedings Volume 11445, Ground-based and Airborne Telescopes VIII **114452F** (2020). https://doi.org/10.1117/12.2561315
95. Ramasawmy, J., Klaassen, P.D., Cicone, C., et al.: The Atacama Large Aperture Submillimetre Telescope: key science drivers. Proceedings Volume 12190, Millimeter, Submillimeter, and Far-Infrared Detectors and Instrumentation for Astronomy XI **1219007** (2022). https://doi.org/10.1117/12.2627505
96. Pereira, M.F., Zubelli, J.P., Winge, D., Wacker, A., Rodrigues, A.S., Anfertev, V., Vaks, V.: Theory and measurements of harmonic generation in semiconductor superlattices with applications in the 100 GHz to 1 THz range. Physical Review B **96**(4), 1–5 (2017). https://doi.org/10.1103/PhysRevB.96.045306
97. Vieira, F.S., Cruz, F.C., Plusquellic, D.F., Diddams, S.A.: Tunable resolution terahertz dual frequency comb spectrometer. Optics Express **24**(26), 30100 (2016). https://doi.org/10.1364/oe.24.030100
98. Savenko, I.G., Shelykh, I.A., Kaliteevski, M.A.: Nonlinear terahertz emission in semiconductor microcavities. Physical Review Letters **107**(2), 8–11 (2011). https://doi.org/10.1103/PhysRevLett.107.027401 arXiv:1103.1336
99. Kavokin, K.V., Kaliteevski, M.A., Abram, R.A., Kavokin, A.V., Sharkova, S., Shelykh, I.A.: Stimulated emission of terahertz radiation by exciton-polariton lasers. Applied Physics Letters **97**(20), 1–4 (2010). https://doi.org/10.1063/1.3519978
100. Lanzillotti-Kimura, N.D., Fainstein, A., Jusserand, B.: Towards GHz-THz cavity optomechanics in DBR-based semiconductor resonators. Ultrasonics **56**, 80–89 (2015). https://doi.org/10.1016/j.ultras.2014.05.017
101. Cuevas, M.: Theoretical investigation of the spontaneous emission on graphene plasmonic antenna in THz regime. Superlattices and Microstructures **122**(August), 216–227 (2018). https://doi.org/10.1016/j.spmi.2018.08.006 arXiv:1808.03135
102. Prelat, L., Passarelli, N., Bustos-Marún, R., Depine, R.A.: Terahertz lasing conditions of radiative and nonradiative propagating plasmon modes in graphene-coated cylinders. Journal of the Optical Society of America B **39**(9), 2547 (2022). https://doi.org/10.1364/JOSAB.463846 arXiv:2208.06694
103. Feres, F.H., Mayer, R.A., Wehmeier, L., Maia, F.C.B., Viana, E.R., Malachias, A., Bechtel, H.A., Klopf, J.M., Eng, L.M., Kehr, S.C., González, J.C., Freitas, R.O., Barcelos, I.D.: Sub-diffractional cavity modes of terahertz hyperbolic phonon polaritons in tin oxide. Nature Communications **12**(1), 1995 (2021). https://doi.org/10.1038/s41467-021-22209-w
104. Mayer, R.A., Wehmeier, L., Torquato, M., Chen, X., Feres, F.H., Maia, F.C.B., Obst, M., Kaps, F.G., Luferau, A., Klopf, J.M., Gilbert Corder, S.N., Bechtel, H.A., González, J.C., Viana, E.R., Eng, L.M., Kehr, S.C., Freitas, R.O., Barcelos, I.D.: Paratellurite Nanowires as a Versatile Material for THz Phonon Polaritons. ACS Photonics (2024). https://doi.org/10.1021/acsphotonics.4c01249
105. Liu, W., Zhang, J., Rioux, M., Viens, J., Messaddeq, Y., Yao, J.: Frequency tunable continuous THz wave generation in a periodically poled fiber. IEEE Transactions on Terahertz Science and Technology **5**(3), 470–477 (2015). https://doi.org/10.1109/TTHZ.2015.2412381
106. Cárdenas, J.R., Ferreira, R., Bastard, G.: Enhanced terahertz emission by landau quantization in semiconductor superlattices. Superlattices and Microstructures **87**, 97–102 (2015) https://doi.org/10.1016/j.spmi.2015.04.042 . Proceedings of the 16th International Conference on the Physics of Light–Matter Coupling in Nanostructures, PLMCN 2015 (Medellín, Colombia), 3-8 February, 2015
107. Martínez-Orozco, J.C., Rojas-Briseño, J.G., Rodríguez-Magdaleno, K.A., Rodríguez-Vargas, I., Mora-Ramos, M.E., Restrepo, R.L., Ungan, F., Kasapoglu, E., Duque, C.A.: Effect of the magnetic field on the nonlinear optical rectification and second and third harmonic generation in double δ-doped GaAs quantum wells. Physica B: Condensed Matter **525**, 30–35 (2017). https://doi.org/10.1016/j.physb.2017.08.082
108. Treviño-Palacios, C. G., Zapata-Nava, O. J., Mejía-Uriarte, E. V., Qureshi, N., Paz-Martínez, G., Kolokolstev, O.: Dual wavelength continuous wave laser using a birefringent filter. J. Eur. Opt. Soc.-Rapid Publ. **8**, 13021 (2013). https://doi.org/10.2971/jeos.2013.13021
109. Turan, D., Corzo-Garcia, S.C., Yardimci, N.T., Castro-Camus, E., Jarrahi, M.: Impact of the metal adhesion layer on the radiation power of plasmonic photoconductive terahertz sources. Journal of Infrared, Millimeter, and Terahertz Waves **38**, 1448–1456 (2017). https://doi.org/10.1007/s10762-017-0431-9
110. Olivo, J.: Surface plasmon enhancement of spontaneous emission in graphene waveguides. Journal of Optics (United Kingdom) **18**(10) (2016). https://doi.org/10.1364/JOSAB.496787 arXiv:1609.04073

111. Khutoryan, E., Kuleshov, A., Ponomarenko, S., Lukin, K., Melezhik, P., Vlasenko, S., Tatematsu, Y., Tani, M.: Coupling of Spoof Surface Plasmon Polariton With Multiple-Order Smith–Purcell Radiation in THz Cherenkov Oscillator. IEEE Transactions on Electron Devices **72**(3), 1383–1389 (2025). https://doi.org/10.1109/TED.2024.3524206
112. Santos, T.M., Lordano, S., Mayer, R.A., Volpe, L., Rodrigues, G.M., Meyer, B., Westfahl, H., Freitas, R.O.: Synchrotron infrared nanospectroscopy in fourth-generation storage rings. Journal of Synchrotron Radiation **31**(Pt 3), 547–556 (2024). https://doi.org/10.1107/S1600577524002364
113. García-Jomaso, Y.A., Hernández-Roa, D.L., no-Mejía, J.G., no-Palacios, C.G.T., Kolokoltsev, O.V., Qureshi, N.: Sub-wavelength continuous thz imaging system based on interferometric detection. Opt. Express **29**(12), 19120–19125 (2021). https://doi.org/10.1364/OE.424163
114. Auston, D.H.: Picosecond optoelectronic switching and gating in silicon. Applied Physics Letters **26**(3), 101–103 (1975). https://doi.org/10.1063/1.88079
115. Wu, Q., Zhang, X.-C.: Free-space electro-optic sampling of terahertz beams. Applied Physics Letters **67**(24), 3523–3525 (1995). https://doi.org/10.1063/1.114909
116. Esaki, L., Tsu, R.: Superlattice and negative differential conductivity in semiconductors. IBM Journal of Research and Development **14**(1), 61–65 (1970). https://doi.org/10.1147/rd.141.0061
117. Wacker, A.: Semiconductor superlattices: a model system for nonlinear transport. Physics Reports **357**(1–3), 1–111 (2002). https://doi.org/10.1016/S0370-1573(01)00029-1
118. Gunn, J.B.: Microwave oscillations of current in iii–v semiconductors. Solid State Communications **1**(4), 88–91 (1963). https://doi.org/10.1016/0038-1098(63)90041-3
119. Köhler, R., Tredicucci, A., Beltram, F., Beere, H.E., Linfield, E.H., Davies, A.G., Ritchie, D.A., Iotti, R.C., Rossi, F.: Terahertz semiconductor-heterostructure laser. Nature **417**, 156–159 (2002). https://doi.org/10.1038/417156a
120. Dutt, B.A., Luke, K., Gaeta, A.L., Nussenzveig, P., Lipson, M.: On-chip optical squeezing and quantum correlations. In: Latin America Optics and Photonics Conference. OSA, Cancun, Mexico (2014). https://doi.org/10.1364/LAOP.2014.LTu3B.1 . OSA
121. Paz-Martínez, G., Garduño-Mejía, J., Kolokoltsev, O.V., Treviño-Palacios, C.G., Qureshi, N.: Focus and alignment tolerance in a photoconductive terahertz source. Journal of Infrared, Millimeter, and Terahertz Waves **36**, 830–837 (2015). https://doi.org/10.1007/s10762-015-0185-1
122. Paz-Martínez, G., Treviño-Palacios, C.G., Molina-Reyes, J., Romero-Morán, A., Cervantes-García, E., Mateos, J., González, T.: Influence of Laser Modulation Frequency on the Performance of Terahertz Photoconductive Switches on Semi-Insulating GaAs Exhibiting Negative Differential Conductance. IEEE Transactions on Terahertz Science and Technology **11**(5), 591–597 (2021). https://doi.org/10.1109/TTHZ.2021.3083926
123. Hernández-Roa, D.L., García-Jomaso, Y.A., Bruce, N.C., no-Mejía, J.G., Pilloni, O., Oropeza-Ramos, L., no-Palacios, C.G.T., nez-Romero, C.L.O., Velázquez-Benítez, A.M., Qureshi, N.: Effect of oils on the transmission properties of a terahertz photonic crystal. Appl. Opt. **61**(1), 135–140 (2022). https://doi.org/10.1364/AO.441042
124. Rodríguez-Magdaleno, K.A., Turkoglu, A., Ungan, F., Mora-Ramos, M.E., Martínez-Orozco, J.C.: Donor impurity atom effect on the inter-subband absorption coefficient for symmetric double n-type δ-doped GaAs quantum well. Superlattices and Microstructures **156**, 106988 (2021). https://doi.org/10.1016/j.spmi.2021.106988
125. Jablan, M., Buljan, H., Soljačić, M.: Plasmonics in graphene at infrared frequencies. Physical Review B **80**(24), 245435 (2009). https://doi.org/10.1103/PhysRevB.80.245435
126. Koppens, F.H.L., Chang, D.E., Abajo, F.J.: Graphene plasmonics: A platform for strong light–matter interactions. Nano Letters **11**(8), 3370–3377 (2011). https://doi.org/10.1021/nl201771h
127. Madey, J.M.J.: Stimulated emission of bremsstrahlung in a periodic magnetic field. Journal of Applied Physics **42**(5), 1906–1913 (1971). https://doi.org/10.1063/1.1660466
128. Malhotra, I., Singh, G.: Terahertz technology for biomedical application. In: Terahertz Antenna Technology for Imaging and Sensing Applications, pp. 235–264. Springer, ??? (2021)
129. Penkov, N.V.: Terahertz spectroscopy as a method for investigation of hydration shells of biomolecules. Biophysical Reviews **15**(5), 833–849 (2023)
130. Darmo, J., Tamosiunas, V., Fasching, G., Kröll, J., Unterrainer, K., Beck, M., Giovannini, M., Faist, J., Kremser, C., Debbage, P.: Imaging with a terahertz quantum cascade laser. Optics express **12**(9), 1879–1884 (2004)
131. Lu, J.-Y., Chang, H.-H., Chen, L.-J., Tien, M.-C., Sun, C.-K.: Optoelectronic-based high-efficiency quasi-cw terahertz imaging. IEEE Photonics technology letters **17**(11), 2406–2408 (2005)

132. Heugen, U., Schwaab, G., Bründermann, E., Heyden, M., Yu, X., Leitner, D., Havenith, M.: Solute-induced retardation of water dynamics probed directly by terahertz spectroscopy. Proceedings of the National Academy of Sciences **103**(33), 12301–12306 (2006)
133. Png, G., Choi, J., Ng, B.W., Mickan, S., Abbott, D., Zhang, X.: The impact of hydration changes in fresh bio-tissue on thz spectroscopic measurements. Physics in Medicine & Biology **53**(13), 3501–3517 (2008)
134. Born, B., Havenith, M.: Terahertz dance of proteins and sugars with water. Journal of Infrared, Millimeter, and Terahertz Waves **30**(12), 1245–1254 (2009)
135. Castro-Camus, E., Singh, A.K., Perez-Lopez, A.V., Morales-Hernandez, J.A., Simpson, J., Villanueva-Rodriguez, S.J., Ortiz-Martinez, M.: Terahertz spectroscopy and imaging as a tool to unlock physiological and molecular mechanisms for drought resistance of agaves. Applied Optics **64**(8), 2057–2062 (2025)
136. Hernandez-Cardoso, G.G., Amador-Medina, L.F., Gutierrez-Torres, G., Reyes-Reyes, E.S., Benavides Martínez, C.A., Cardona Espinoza, C., Arce Cruz, J., Salas-Gutierrez, I., Murillo-Ortíz, B.O., Castro-Camus, E.: Terahertz imaging demonstrates its diagnostic potential and reveals a relationship between cutaneous dehydration and neuropathy for diabetic foot syndrome patients. Scientific Reports **12**(1), 3110 (2022)
137. Chen, X., Lindley-Hatcher, H., Stantchev, R.I., Wang, J., Li, K., Hernandez Serrano, A., Taylor, Z.D., Castro-Camus, E., Pickwell-MacPherson, E.: Terahertz (thz) biophotonics technology: Instrumentation, techniques, and biomedical applications. Chemical Physics Reviews **3**(1) (2022)
138. Hernandez-Cardoso, G., Rojas-Landeros, S., Alfaro-Gomez, M., Hernandez-Serrano, A., Salas-Gutierrez, I., Lemus-Bedolla, E., Castillo-Guzman, A., Lopez-Lemus, H., Castro-Camus, E.: Terahertz imaging for early screening of diabetic foot syndrome: A proof of concept. Scientific reports **7**(1), 42124 (2017)
139. Vieira, F.S., Pasquini, C.: Determination of cellulose crystallinity by terahertz-time domain spectroscopy. Analytical chemistry **86**(8), 3780–3786 (2014)
140. Silva, I.J., Raimundo, I.M., Mizaikoff, B.: Analysis of sugars and sweeteners via terahertz time-domain spectroscopy. Analytical Methods **14**(27), 2657–2664 (2022)
141. Guerrero, M.A.J., Mendoza-Galván, A., Strupiechonski, E.: Electromagnetic analysis of water spectra in bulk and film forms at terahertz frequencies in a modified attenuated total reflection configuration. IEEE Transactions on Terahertz Science and Technology **13**(3), 262–269 (2023)
142. Giordani, G., Scaramozzino, D., Iturrioz, I., Lacidogna, G., Carpinteri, A.: Modal analysis of the lysozyme protein considering all-atom and coarse-grained finite element models. Applied Sciences **11**(2), 547 (2021)
143. Vilchis, H., López-Páez, M.F., Conde, J., Briones, E., Morales, G.L.: Dielectric properties of pouteria sapota compounds in terahertz frequency range. Revista Mexicana de Física **70**(5 Sep-Oct), 051303–1 (2024)
144. Castro-Camus, E., Palomar, M., Covarrubias, A.: Leaf water dynamics of arabidopsis thaliana monitored in-vivo using terahertz time-domain spectroscopy. Scientific reports **3**(1), 2910 (2013)
145. Singh, A.K., Pérez-López, A.V., Simpson, J., Castro-Camus, E.: Three-dimensional water mapping of succulent agave victoriae-reginae leaves by terahertz imaging. Scientific Reports **10**(1), 1404 (2020)
146. Cruz, J.O.: Terahertz time-domain spectroscopy (thz-tds) for classification of blueberries according to their maturity. In: 2020 IEEE Engineering International Research Conference (EIRCON), pp. 1–4 (2020). IEEE
147. López-Morales, G., López-Páez, M.F., López, P., Carriles, R., Vilchis, H.: Detection of moisture ratio and carotenoid compounds in mamey (pouteria sapota) fruit during dehydration process using spectroscopic techniques. Journal of Food Science and Technology **60**(7), 1952–1959 (2023)
148. H-Domínguez, E., Cruz-Lopez, E., Reyes-Nava, J., Conde, J., Briones, E., Vilchis, H.: First principles for evaluation of the moisture content in mango slice by tera-hertz pulses. In: 2018 15th International Conference on Electrical Engineering, Computing Science and Automatic Control (CCE), pp. 1–4 (2018). IEEE
149. Uceda, P., Yoshida, H., Castillo, P.: Terahertz imaging and machine learning in the classification of coffee beans. In: Brazilian Technology Symposium, pp. 854–861 (2020). Springer
150. Arteaga, H., León-Roque, N., Oblitas, J.: The frequency range in thz spectroscopy and its relationship to the water content in food: A first approach. Scientia Agropecuaria **12**(4), 625–634 (2021)

151. Oblitas-Cruz, J., Miano, A.C., Terrones, G.: Terahertz time-domain spectroscopy for the classification of mature cheese [espectroscopía de terahercios en el dominio del tiempo para la clasificación de queso madurado]. (2021)
152. Jackson, J.B., Bowen, J., Walker, G., Labaune, J., Mourou, G., Menu, M., Fukunaga, K.: A survey of terahertz applications in cultural heritage conservation science. IEEE Transactions on Terahertz Science and Technology **1**(1), 220–231 (2011). https://doi.org/10.1109/TTHZ.2011.2159538
153. Fukunaga, K., Hosako, I.: Innovative non-invasive analysis techniques for cultural heritage using terahertz technology. Comptes Rendus. Physique **11**(7-8), 519–526 (2010)
154. Fukunaga, K.: THz Technology Applied to Cultural Heritage in Practice vol. 10. Springer, ??? (2016)
155. Lopes, F., Melquiades, F.L., Appoloni, C.R., Cesareo, R., Rizzutto, M., Silva, T.F.: Thickness determination of gold layer on pre-columbian objects and a gilding frame, combining pxrf and pls regression. X-Ray Spectrometry **45**(6), 344–351 (2016). https://doi.org/10.1002/xrs.2711 https://analyticalsciencejournals.onlinelibrary.wiley.com/doi/pdf/10.1002/xrs.2711
156. Iannaccone, R., Ribechini, E., Lucejko, J.J., Bertelli, I., Marceddu, S., Aldana, J., Colombini, M.P., Brunetti, A.: The lord of ucupe mask from moche culture (peru). a multianalytical study of the materials from the metals to the adhesive. Journal of Cultural Heritage **66**, 407–414 (2024). https://doi.org/10.1016/j.culher.2023.12.011
157. Gomez-Sepulveda, A.M., Hernandez-Serrano, A.I., Radpour, R., Koch-Dandolo, C.L., Rojas-Landeros, S.C., Ascencio-Rojas, L.F., Zarate, A., Hernandez, G., Gonzalez-Tirado, R.C., Insaurralde-Caballero, M., Castro-Camus, E.: History of mexican easel paintings from an altarpiece revealed by non-invasive terahertz time-domain imaging. Journal of Infrared, Millimeter, and Terahertz Waves **38**(4), 403–412 (2016). https://doi.org/10.1007/s10762-016-0346-x
158. Reyes-Reyes, E.S., Carriles-Jaimes, R., D'Angelo, E., Nazir, S., Koch-Dandolo, C.L., Kuester, F., Jepsen, P.U., Castro-Camus, E.: Terahertz time-domain imaging for the examination of gilded wooden artifacts. Scientific Reports **14**(1), 6261 (2024). https://doi.org/10.1038/s41598-024-56913-6 . https://www.nature.com/articles/s41598-024-56913-6.pdf
159. Koch Dandolo, C.L., Pasco Saldaña, G.M., Insaurralde Caballero, M.A., Gómez Sepúlveda, M.A., Hernández-Serrano, A.I., Mesa Orozco, A., Alvarado Calderón, J., Calderón Zárate, M.S., González, K.L., Dios, E.C., Hernández Rosales, G., Castro-Camus, E.: Terahertz time-domain imaging to guide a conservation intervention on a stratified easel painting. Journal of Infrared, Millimeter, and Terahertz Waves **39**(8), 773–784 (2018). https://doi.org/10.1007/s10762-018-0505-3
160. Koch Dandolo, C.L., Gomez-Sepulveda, A.M., Hernandez-Serrano, A.I., Castro-Camus, E.: Examination of painting on metal support by terahertz time-domain imaging. Journal of Infrared, Millimeter, and Terahertz Waves **38**(10), 1278–1287 (2017). https://doi.org/10.1007/s10762-017-0409-7
161. Lambert, F.E.M., Reyes-Reyes, E.S., Hernandez-Cardoso, G.G., Gomez-Sepulveda, A.M., Castro-Camus, E.: In situ determination of the state of conservation of paint coatings on the kiosk of guadalajara using terahertz time-domain spectroscopy. Journal of Infrared, Millimeter, and Terahertz Waves **41**(4), 355–364 (2019). https://doi.org/10.1007/s10762-019-00645-6
162. Koch-Dandolo, C.L., Filtenborg, T., Fukunaga, K., Skou-Hansen, J., Jepsen, P.U.: Reflection terahertz time-domain imaging for analysis of an 18th century neoclassical easel painting. Applied Optics **54**(16), 5123–5129 (2015). https://doi.org/10.1364/AO.54.005123
163. Baydin, A., Hernandez, F.G.G., Rodriguez-Vega, M., Okazaki, A.K., Tay, F., Noe, G.T., Katayama, I., Takeda, J., Nojiri, H., Rappl, P.H.O., Abramof, E., Fiete, G.A., Kono, J.: Magnetic control of soft chiral phonons in PbTe. Phys. Rev. Lett. **128**, 075901 (2022). https://doi.org/10.1103/PhysRevLett.128.075901
164. Hernandez, F.G.G., Baydin, A., Chaudhary, S., Tay, F., Katayama, I., Takeda, J., Nojiri, H., Okazaki, A.K., Rappl, P.H.O., Abramof, E., Rodriguez-Vega, M., Fiete, G.A., Kono, J.: Observation of interplay between phonon chirality and electronic band topology. Science Advances **9**(50), 4074 (2023). https://doi.org/10.1126/sciadv.adj4074
165. Singh, A., Němec, H., Kunc, J., Kužel, P.: Nanoscale terahertz conductivity and ultrafast dynamics of terahertz plasmons in periodic arrays of epitaxial graphene nanoribbons. Physical Review Research **6**(3), 033063 (2024). https://doi.org/10.1103/PhysRevResearch.6.033063
166. Zhang, Z., Gao, F.Y., Chien, Y.-C., Liu, Z.-J., Curtis, J.B., Sung, E.R., Ma, X., Ren, W., Cao, S., Narang, P., Hoegen, A., Baldini, E., Nelson, K.A.: Terahertz-field-driven magnon upconversion in an antiferromagnet. Nature Physics **20**(5), 788–793 (2024). https://doi.org/10.1038/s41567-023-02350-7

167. Koch, M., Mittleman, D.M., Ornik, J., Castro-Camus, E.: Terahertz time-domain spectroscopy. Nature Reviews Methods Primers **3**(1), 1–14 (2023). https://doi.org/10.1038/s43586-023-00232-z
168. Schmuttenmaer, C.A.: Exploring Dynamics in the Far-Infrared with Terahertz Spectroscopy. Chemical Reviews **104**(4), 1759–1780 (2004). https://doi.org/10.1021/cr020685g
169. Leitenstorfer, A., Moskalenko, A.S., Kampfrath, T., Kono, J., Castro-Camus, E., Peng, K., Qureshi, N., Turchinovich, D., Tanaka, K., Markelz, A.G., Havenith, M., Hough, C., Joyce, H.J., Padilla, W.J., Zhou, B., Kim, K.-Y., Zhang, X.-C., Jepsen, P.U., Dhillon, S., Vitiello, M., Linfield, E., Davies, A.G., Hoffmann, M.C., Lewis, R., Tonouchi, M., Klarskov, P., Seifert, T.S., Gerasimenko, Y.A., Mihailovic, D., Huber, R., Boland, J.L., Mitrofanov, O., Dean, P., Ellison, B.N., Huggard, P.G., Rea, S.P., Walker, C., Leisawitz, D.T., Gao, J.R., Li, C., Chen, Q., Valušis, G., Wallace, V.P., Pickwell-MacPherson, E., Shang, X., Hesler, J., Ridler, N., Renaud, C.C., Kallfass, I., Nagatsuma, T., Zeitler, J.A., Arnone, D., Johnston, M.B., Cunningham, J.: The 2023 terahertz science and technology roadmap. Journal of Physics D: Applied Physics **56**(22), 223001 (2023). https://doi.org/10.1088/1361-6463/acbe4c
170. Neu, J., Schmuttenmaer, C.A.: Tutorial: An introduction to terahertz time domain spectroscopy (THz-TDS). Journal of Applied Physics **124**(23), 231101 (2018). https://doi.org/10.1063/1.5047659
171. Hillenbrand, R., Abate, Y., Liu, M., Chen, X., Basov, D.N.: Visible-to-thz near-field nanoscopy. Nature Reviews Materials **10**, 285–310 (2025). https://doi.org/10.1038/s41578-024-00761-3
172. Dutra, M., Marulanda, E., Vasques, G.G., Oliveira, J.F., Sabino, P.C., Delgado, R.B., Mendonça-Fereira, L., Benvenho, A.R.V., Baggio-Saitovitch, E., Machado, R.K., Kawahala, N.M., Munevar, J., Avila, M.A., Hernandez, F.G.G.: Engineering a Correlated Narrow-Gap Semiconductor: Effects of Ga Substitution in $EuZn_2P_2$. (2025). arXiv:2512.17123 [cond-mat.mtrl-sci]
173. Reyes-Coronado, A., Acosta, M.F., Merino, R.I., Orera, V.M., Kenanakis, G., Katsarakis, N., Soukoulis, C.M.: Self-organization approach for THz polaritonic metamaterials. Optics Express **20**, 14663–14682 (2012). https://doi.org/10.1364/OE.20.014663
174. Muñoz-Rosas, A.L., Qureshi, N., Paz-Martínez, G., Treviño-Palacios, C.G., Alonso-Huitrón, J.C., Rodríguez-Gómez, A.: Semi-insulating GaAs surface modifications and their influence in the response of THz devices. Results in Physics **24**, 104095 (2021). https://doi.org/10.1016/j.rinp.2021.104095
175. García-Jomaso, Y.A., Hernández-Roa, D.L., no-Mejía, J.G., no-Palacios, C.G.T., Kolokoltsev, O.V., Qureshi, N.: Sub-wavelength continuous THz imaging system based on interferometric detection. Opt. Express **29**(12), 19120–19125 (2021). https://doi.org/10.1364/OE.424163
176. Garnica-Palafox, I.M., Velázquez-Benítez, A.M., Sánchez-Arévalo, F., Qureshi, N.: Terahertz detection of acid blue 113 dye using hybrid hydrogels. Journal of Infrared, Millimeter, and Terahertz Waves **45**, 300–321 (2024). https://doi.org/10.1007/s10762-024-00968-z
177. Heshmat, B., Andrews, G.M., Naranjo-Montoya, O.A., Castro-Camus, E., Ciceri, D., Sanchez, A.R., Raskar, R.: Terahertz scattering and water absorption for porosimetry. Optics express **25**, 27370–27385 (2017). https://doi.org/10.1364/OE.25.027370
178. Wahaia, F., Kašalynas, I., Pashnev, D., Valušis, G., Urbanowicz, A., Karaliunas, M., Seifert, B.: Optical properties of millimeter-size metal-organic framework single crystals using THz techniques. Journal of Molecular Structure **1322**, 140612 (2025). https://doi.org/10.1016/j.molstruc.2024.140612
179. Sanjuan, F., Tocho, J.O.: Optical properties of silicon, sapphire, silica and glass in the terahertz range. In: Latin America Optics and Photonics Conference (LAOP) (2012). https://doi.org/10.1364/LAOP.2012.LT4C.1
180. Sanjuan, F., Vidal, B.: Refractive index calculation from echo interference in pulsed terahertz spectroscopy. Electronics Letters **50**, 308–309 (2014). https://doi.org/10.1049/el.2013.3937
181. Sanjuan, F., Bockelt, A., Vidal, B.: Birefringence measurement in the terahertz range based on double fourier analysis. Optics Letters **39**, 809–8012 (2014). https://doi.org/10.1364/OL.39.000809
182. Sanjuan, F., Bockelt, A., Vidal, B.: Determination of refractive index and thickness of a multilayer structure with a single thz time domain spectroscopy measurement. Applied Optics **53**, 4910–4913 (2014). https://doi.org/10.1364/AO.53.004910
183. Sanjuan, F., Galarza, C.: Spectral estimation of terahertz time-domain signals using a simple parametric method. Electronics Letters **25**, 2130–2132 (2015). https://doi.org/10.1049/el.2015.2955
184. Costa, L.F.L., Moraes, J.C.S., Cruz, F.C., Viscovini, R.C., Pereira, D.: Infrared and far-infrared spectroscopy of 13CH3OH: TeraHertz laser lines and assignments. Journal of Molecular Spectroscopy **241**(2), 151–154 (2007). https://doi.org/10.1016/j.jms.2006.12.002
185. Viscovini, R.C., Moraes, J.C.S., Costa, L.F.L., Cruz, F.C., Pereira, D.: DCOOD optically pumped by a 13CO2 laser: new terahertz laser lines. Applied Physics B **91**(3), 517–520 (2008). https://doi.org/10.1007/s00340-008-3018-2

186. Melo, A.M., Toledo, M.A.P., Maia, F.C.B., Rocha, A., Plotegher, M.B., Pereira, D., Cruz, F.C.: Imaging at 0.2 and 2.5 terahertz. Proceedings SPIE 8624, Terahertz, RF, Millimeter, and Submillimeter-Wave Technology and Applications VI, 86240E (2013). https://doi.org/10.1117/12.2002108
187. Netto, G.B.: Espectroscopia em terahertz de óxidos magnéticos. Master's thesis, Instituto de Física Gleb Wataghin, Universidade Estadual de Campinas (UNICAMP) (September 2023). https://doi.org/10.47749/T/UNICAMP.2023.1374671
188. Vieira, F.S., Pasquini, C.: Determination of cellulose crystallinity by terahertz-time domain spectroscopy. Analytical Chemistry **86**(8), 3780–3786 (2014). https://doi.org/10.1021/ac4035746 . PMID: 24654843
189. Silva, I.J.G.d.: Aplicações analíticas da espectroscopia vibracional: estudo de sacarídeos por espectroscopia terahertz e aplicação de laser de cascata interbanda para metano por infravermelho médio. Tese (doutorado), Universidade Estadual de Campinas, Instituto de Química (2017). https://repositorio.unicamp.br/acervo/detalhe/981119
190. Silva, I.J.G., Raimundo, I.M., Mizaikoff, B.: Analysis of sugars and sweeteners via terahertz time-domain spectroscopy. Anal. Methods **14**, 2657–2664 (2022). https://doi.org/10.1039/D2AY00377E
191. Ribessi, R.L.: Aplicação de espectroscopias vibracionais na análise de espécies gasosas. Tese (doutorado), Universidade Estadual de Campinas, Instituto de Química (2023). https://www.repositorio.unicamp.br/acervo/detalhe/1397159
192. Silva, H.O., Rohwedder, J.J.R., Nome, R.A.: Femtosecond terahertz pulse propagation measurements and simulations of dewetting kinetics in real time. ACS Omega **9**(36), 38107–38115 (2024). https://doi.org/10.1021/acsomega.4c05275
193. Islam, M.S., Sultana, J., Biabanifard, M., Vafapour, Z., Nine, M.J., Dinovitser, A., Cordeiro, C.M.B., Ng, B.W.-H., Abbott, D.: Tunable localized surface plasmon graphene metasurface for multiband superabsorption and terahertz sensing. Carbon **158**, 559–567 (2020). https://doi.org/10.1016/j.carbon.2019.11.026
194. Islam, M.S., Cordeiro, C.M.B., Franco, M.A.R., Sultana, J., Cruz, A.L.S., Abbott, D.: Terahertz optical fibers. Opt. Express **28**(11), 16089–16117 (2020). https://doi.org/10.1364/OE.389999
195. Souza, W.d.S.: Desenvolvimento e aplicações de sistemas espectroscópicos de imagem explorando telefones móveis e radiação terahertz. Master's thesis, Universidade Federal de Pernambuco (July 2018). https://repositorio.ufpe.br/handle/123456789/32617
196. Santos, C.N., Feres, F.H., Hannotte, T., Peretti, R., Vanwolleghem, M., Eliet, S., Walter, B., Faucher, M., Cernescu, A., Freitas, R.O., Lampin, J.-F.: High quality-factor terahertz phonon-polaritons in layered lead iodide. Nature Communications (2026). https://doi.org/10.1038/s41467-026-69027-6
197. Barcelos, I.D., Bechtel, H.A., Matos, C.J.S., Bahamon, D.A., Kaestner, B., Maia, F.C.B., Freitas, R.O.: Probing Polaritons in 2D Materials with Synchrotron Infrared Nanospectroscopy. Advanced Optical Materials **8**(5), 1901091 (2020). https://doi.org/10.1002/adom.201901091
198. Barcelos, I.D., Canassa, T.A., Mayer, R.A., Feres, F.H., Oliveira, E.G., Goncalves, A.-M.B., Bechtel, H.A., Freitas, R.O., Maia, F.C.B., Alves, D.C.B.: Ultrabroadband Nanocavity of Hyperbolic Phonon–Polaritons in 1D-Like α-MoO3. ACS Photonics **8**(10), 3017–3026 (2021). https://doi.org/10.1021/acsphotonics.1c00955
199. Kawahala, N.M.: Espectroscopia de terahertz no domínio do tempo: implementação, caracterização e aplicações. PhD thesis, Universidade de São Paulo (2023). https://doi.org/10.11606/T.43.2023.tde-25052023-103743
200. Matos, D.A.: Absorção e efeitos da polarização de ondas terahertz no clinocloro. Master's thesis, Universidade de São Paulo (2023). https://doi.org/10.11606/D.43.2023.tde-04092023-143205
201. Stefanato, E.D.: Estudo da transição polar dependente da concentração de portadores de carga em filmes finos de Pb0.5Sn0.5Te dopados com bismuto. Master's thesis, Universidade de São Paulo (2025). https://doi.org/10.11606/D.43.2025.tde-03052025-160145
202. Freitas, G.F.: Cristais fotônicos impressos em 3D para manipulação da polarização de ondas terahertz. Master's thesis, Universidade de São Paulo (2025). https://doi.org/10.11606/D.43.2025.tde-29042025-161842
203. Marulanda, E., Costa, F.L., Kawahala, N.M., Hernandez, F.G.G.: Windowing in terahertz time-domain spectroscopy: resolving resonances in thin-film samples. Journal of Infrared, Millimeter, and Terahertz Waves **46**(10), 75 (2025). https://doi.org/10.1007/s10762-025-01092-2
204. Dias, L.O., Stefanato, E.D., Kawahala, N.M., Hernandez, F.G.G.: Optimizing Aperture Geometry in THz-TDS for Accurate Spectroscopy of Quantum Materials. Brazilian Journal of Physics **56**(1), 35 (2026). https://doi.org/10.1007/s13538-025-01973-w

205. Kawahala, N.M., Matos, D.A., Oliveira, R., Longuinhos, R., Ribeiro-Soares, J., Barcelos, I.D., Hernandez, F.G.G.: Shaping terahertz waves using anisotropic shear modes in a van der Waals mineral. npj 2D Materials and Applications **9**(1), 16 (2025). https://doi.org/10.1038/s41699-025-00540-w
206. Kawahala, N.M., Matos, D.A., Rappl, P.H.O., Abramof, E., Baydin, A., Kono, J., Hernandez, F.G.G.: Thickness-Dependent Terahertz Permittivity of Epitaxially Grown PbTe Thin Films. Coatings **13**(11), 1855 (2023). https://doi.org/10.3390/coatings13111855
207. Stefanato, E.D., Kawahala, N.M., Kawata, B.A., Rappl, P.H.O., Abramof, E., Hernandez, F.G.G.: Metallicity-driven polar transitions in topological epilayers. Communications Physics **8**, 419 (2025). https://doi.org/10.1038/s42005-025-02330-8
208. Baydin, A., Manjappa, M., Mishra, S.S., Xu, H., Doumani, J., Tay, F., Kim, D., Rappl, P.H.O., Abramof, E., Singh, R., Hernandez, F.G.G., Kono, J.: Terahertz cavity phonon polaritons in lead telluride in the deep-strong coupling regime (2025). arXiv:2501.10856 [physics.optics]
209. Jahn, D., Weidenbach, M., Lehr, J., Scheller, M., Koch, M.: 3D Printed Terahertz Focusing Grating Couplers. Journal of Infrared, Millimeter, and Terahertz Waves **38**(6), 708–716 (2017). https://doi.org/10.1007/s10762-017-0370-5
210. Busch, S.F., Castro-Camus, E., Beltran-Mejia, F., Koch, M.: 3D Printed Prisms with Tunable Dispersion for the THz Frequency Range. Journal of Infrared, Millimeter, and Terahertz Waves **39**(6), 553–560 (2018). https://doi.org/10.1007/s10762-018-0488-0
211. Guo, R., Stuebling, E.M., Beltran-Mejia, F., Koch, M.: 3D Printed Terahertz Rectangular Waveguides of Polystyrene and TOPAS: A Comparison. Journal of Infrared, Millimeter, and Terahertz Waves **40**(1), 1–4 (2019). https://doi.org/10.1007/s10762-018-0552-9
212. Ornik, J., Lehr, J., Reuter, M., Jahn, D., Beltran-Mejia, F., Balzer, J.C., Kleine-Ostmann, T., Koch, M.: Repeatability of material parameter extraction of liquids from transmission terahertz time-domain measurements. Opt. Express **28**(19), 28178–28189 (2020). https://doi.org/10.1364/OE.403159
213. Freitas, G.F., Roque, L.T., Kawahala, N.M., Hernandez, F.G.G.: Optical analysis of 3d-printed terahertz waveplates from common thermoplastics. Scientific Reports **16**, 2532 (2026). https://doi.org/10.1038/s41598-025-32267-5

Authors and Affiliations

Enrique Castro-Camus[1] · Daniel Ferrusca[2] · John Carpenter[3] · David Hughes[2] · Naser Qureshi[4] · Raul O. Freitas[5] · Elodie Strupiechonski[6] · Jimy Oblitas[7] · Mariana Alfaro-Gomez[8] · Alma Montserrat Gomez-Sepulveda[9] · Felix G. G. Hernandez[10] · Federico Sanjuan[11] · Monica Ortiz-Martinez[1,12]

✉ Enrique Castro-Camus
enrique@cio.mx

✉ Naser Qureshi
naser.qureshi@icat.unam.mx

Monica Ortiz-Martinez
mortiz@cio.mx

1 Centro de Investigaciones en Optica A.C., Loma del Bosque 115, Lomas del Campestre, Leon 37150, Guanajuato, Mexico

2 Instituto Nacional de Astrofísica, Óptica y Electrónica, Luis Enrique Erro #1, Sta María Tonanzintla, San Andrés Cholula 72840, Puebla, Mexico

3 Joint ALMA Observatory, Avenida Alonso de Cordova 3107, Vitacura, Santiago, Chile

4 Instituto de Ciencias Aplicadas y Tecnologia, Universidad Nacional Autónoma de Mexico, Mexico City 04510, Mexico

5 Brazilian Synchrotron Light Laboratory (LNLS), Brazilian Center for Research in Energy and Materials (CNPEM), 13083-100 Campinas, Brazil

6 Centro de Ingenieria y Desarrollo Industrial, Avenida Pie de la Cuesta #702, Santiago de Queretaro 76125, Queretaro, Mexico

7 Universidad Privada del Norte, Via de Evitamiento s/n cuadra 15, Cajamarca 06002, Peru

8 Departamento de Matematicas y Fisica, Universidad Autonoma de Aguascalientes, Av. Universidad 940, Cd. Universitaria, Aguascalientes 20100, Aguascalientes, Mexico

9 Escuela de Conservacion y Restauracion de Occidente, Analco No. 285, Barrio de Analco, Guadalajara 44450, Jalisco, Mexico

10 Instituto de Física, Universidade de São Paulo, São Paulo 05508-090, SP, Brazil

11 Laboratoire des Fluides Complexes et leurs Reservoirs, Université de Pau et des Pays de l'Adour, E2S UPPA, CNRS, Avenue de l'université, Pau 64000, Nouvelle Aquitaine, France

12 Secretaria de Ciencia, Humanidades, Tecnologia e Innovacion, Av. Insurgentes Sur 1582, Col. Credito Constructor, Benito Juarez, Mexico City 03940, Mexico